



National Library
of Canada

Bibliothèque nationale
du Canada

Canadian Theses Service

Services des thèses canadiennes

Ottawa, Canada
K1A 0N4

CANADIAN THESES

THÈSES CANADIENNES

NOTICE

The quality of this microfiche is heavily dependent upon the quality of the original thesis submitted for microfilming. Every effort has been made to ensure the highest quality of reproduction possible.

If pages are missing, contact the university which granted the degree.

Some pages may have indistinct print especially if the original pages were typed with a poor typewriter ribbon or if the university sent us an inferior photocopy.

Previously copyrighted materials (journal articles, published tests, etc.) are not filmed.

Reproduction in full or in part of this film is governed by the Canadian Copyright Act, R.S.C. 1970, c. C-30.

**THIS DISSERTATION
HAS BEEN MICROFILMED
EXACTLY AS RECEIVED**

AVIS

La qualité de cette microfiche dépend grandement de la qualité de la thèse soumise au microfilmage. Nous avons tout fait pour assurer une qualité supérieure de reproduction.

S'il manque des pages, veuillez communiquer avec l'université qui a conféré le grade.

La qualité d'impression de certaines pages peut laisser à désirer, surtout si les pages originales ont été dactylographiées à l'aide d'un ruban usé ou si l'université nous a fait parvenir une photocopie de qualité inférieure.

Les documents qui font déjà l'objet d'un droit d'auteur (articles de revue, examens publiés, etc.) ne sont pas microfilmés.

La reproduction, même partielle, de ce microfilm est soumise à la Loi canadienne sur le droit d'auteur, SRC 1970, c. C-30.

**LA THÈSE A ÉTÉ
MICROFILMÉE TELLE QUE
NOUS L'AVONS REÇUE**

EFFECTS OF AMPLIFIER NONLINEARITIES ON MULTILEVEL PAM
SCHEMES.

by

HATZINAKOS DIMITRIOS

A thesis
presented to the University of Ottawa
in fulfillment of the
thesis requirement for the degree of
M.A.Sc.
in
ELECTRICAL ENGINEERING

© Dimitrios Hatzinakos, Ottawa, Canada, 1986.

Permission has been granted to the National Library of Canada to microfilm this thesis and to lend or sell copies of the film.

The author (copyright owner) has reserved other publication rights, and neither the thesis nor extensive extracts from it may be printed or otherwise reproduced without his/her written permission.

L'autorisation a été accordée à la Bibliothèque nationale du Canada de microfilmer cette thèse et de prêter ou de vendre des exemplaires du film.

L'auteur (titulaire du droit d'auteur) se réserve les autres droits de publication; ni la thèse ni de longs extraits de celle-ci ne doivent être imprimés ou autrement reproduits sans son autorisation écrite.

ISBN 0-315-36487-4



UNIVERSITÉ D'OTTAWA
UNIVERSITY OF OTTAWA

The University of Ottawa requires the signatures of all persons using or photocopying this thesis. Please sign below, and give address and date.

ABSTRACT

The effects of amplitude and phase nonlinearities on the transmission of multilevel Pulse-Amplitude-Modulated (PAM) signals are investigated. Specific AM-AM and AM-PM characteristics have been chosen and used for 2,4,8,16 and 32 level PAM schemes. Computer simulation methods and baseband measurements have been used to calculate the degradation in the error performance, when the operation point is changed from the linear region of the characteristics towards saturation. The results obtained for the spectral regrowth due to the nonlinear amplification and adjacent channel interference problems have been explained.

The experimental and the computer simulation results match very closely. For the measurements a 4-PAM encoder-decoder has been designed and the generated signal has been applied to a low frequency power amplifier, which exhibits AM-AM nonlinearity.

Methods for reducing the nonlinear distortion have also been investigated. Predistortion linearization techniques have been used and suboptimum baseband linearizers have been proposed. A baseband AM-AM linearizer has been designed in order to compare simulation results with measurements. Improvements in the performance have been obtained by adjusting the conventional thresholds during the decoding. In combination with the linearization process, led to significant improvements.

ACKNOWLEDGEMENTS

I would like to express my gratitude to my supervisor Dr. K.Feher for his helpful guidance and valuable comments to my work.

I wish to thank all the members of the Digital Communications Research Group at the University of Ottawa, for the help and friendship given to me the last two years. Their advices and willingness to discuss my work was a great advantage. They are Mrs K.Sreenath, K.T.Wu, I.Sasase, D.Makrakis, J.S.Seo, A.Yongacoglu, A.Kucar, J.Mathiopoulos, R.V.Scott, D.Prendergast, H.Ohnishi.

Special thanks must also go to Mr T.Tzakis for his friendship and the many forms of support provided to me.

Finally I wish to thank my family for encouraging and inspiring my career.

LIST OF FIGURES

Fig. 2.1. Measurement set-up for the AM-AM characteristic.

Fig. 2.2. (a) The single tone measured AM-AM power characteristic of the LM-380 power amplifier. (b) Instantaneous amplitude characteristic derived from the measured curve of Fig. 2.2 (a) using the equation 2.1.

Fig. 2.3. (a) The normalized power characteristics with respect to the saturation power of the LM-380 power amplifier. (b) Instantaneous amplitude characteristics derived from the curves of Fig. 2.3 (a) using the equation 2.2.

Fig. 2.4. The Quadrature Model

Fig. 2.5. Amplitude characteristics of the Quadrature model derived from the characteristics of Fig. 2.3 using the equations 2.6 and 2.7.

Fig. 3.1. Computer simulation set-up.

Fig. 3.2. Measurement set-up.

Fig. 3.3. Measured Eye diagram of a 4-PAM signal with the LM-380 amplifier. Linear region. Nyquist filter with $\alpha = 0.2$ is used. The signal rate is 413.3 kb/s.

Fig. 3.4. Measured Eye diagram of a 4-PAM signal with the LM-380 amplifier (3 dB Output Backoff).

Fig. 3.5. Measured Eye diagram of a 4-PAM signal with the LM-380 amplifier (2 dB Output Backoff).

Fig. 3.6. Space diagram of a 4-PAM scheme with the LM-380 characteristic (4 dB Output Backoff). Computer simulation results with $\alpha = 0.2$ Nyquist filter.

Fig. 3.7. Space diagram of a 16-PAM scheme with the H-261 AM-PM characteristic. Computer simulation results with $\alpha = 0.2$ Nyquist filter (10 dB Output Backoff).

Fig. 3.8. Eye diagram of an 8-PAM scheme with the LM-380, H-261 characteristics (6 dB Output Backoff). Computer simulation results with $\alpha = 0.2$ Nyquist filter.

- Fig. 3.9. Space diagram of an 8-PAM scheme with the LM-380, H-261 characteristics (6 dB Output Backoff). Computer simulation results with $\alpha = 0.2$ Nyquist filter.

Fig. 3.10. Performance of a 4-PAM signal with the LM-380 AM-AM characteristic. Computer simulation results with $\alpha = 0.2$ Nyquist filters.

Fig. 3.11. Performance of a 4-PAM signal with the H-261 AM-PM characteristic. Computer simulation results with $\alpha = 0.2$ Nyquist filters.

Fig 3.12: Performance of a 4-PAM signal with the LM-380 and H-261 characteristics. Computer simulation results with $\alpha = 0.2$ Nyquist filters.

Fig 3.13. Performance of a 4-PAM signal with the LM-380 AM-AM characteristic. Measured results with $\alpha = 0.2$ filters.

Fig 3.14. C/N Degradation of a 4-PAM signal with the LM-380 AM-AM characteristic. Computer simulation and Measured results with $\alpha = 0.2$ Nyquist filters.

Fig. 3.15. Degradation due to Amplitude conversion (LM-380 characteristic). Computer simulation results for 2, 4, 8, 16 and 32 PAM schemes with $\alpha = 0.2$ and $\alpha = 0.5$ Nyquist filters.

Fig. 3.16. Degradation due to AM-PM conversion (H-261 characteristic). Computer simulation results for 2, 4, 8, 16 and 32 PAM schemes with $\alpha = 0.2$ Nyquist filters.

Fig. 3.17. Impact of channel nonlinearities on 2, 4, 8, 16 and 32 PAM signals. Computer simulation results.

Fig. 3.18. Measured spectrum diagrams of a 4-PAM signal with the LM-380 amplifier. (a) 4 dB, 8 dB Output Backoff, (b) 2 dB, 8 dB Output Backoff. The signal rate is 413.3 kb/s. Nyquist filters with $\alpha = 0.2$ were used.

Fig. 3.19. Spectral regrowth of a 4-PAM due to the LM-380 and H-261 nonlinearities. Computer simulation results with $\alpha = 0.2$ Nyquist filters (a) In Phase component spectrum. (b) Quadrature component spectrum.

Fig. 4.1. Predistortion linearization.

Fig. 4.2. (a) Predistortion linearization of AM-AM nonlinearity. (b) Required overall characteristic.

Fig. 4.3. Linearization of the LM-380 AM-AM characteristic.

Fig. 4.4. Implemented piece-wise linear approximation of the LM-380 predistorter characteristic.

Fig. 4.5. Predistortion compensation (linearization) for AM-AM and AM-PM nonlinearities.

Fig. 4.6. Compensation of the normalized LM-380,H-261 characteristics.

Fig. 4.7. Baseband predistorter for AM-AM,AM-PM nonlinearities.

Fig. 4.8. AM-AM predistortion compensation for AM-AM,AM-PM nonlinearities.

Fig. 4.9. AM-AM compensation of the LM-380,H-261 characteristics.

Fig. 5.1. Improvement in the error performance of a 4-PAM signal obtained by linearizing the LM-380 characteristic. Computer simulation results with $\alpha = 0.2$ Nyquist filters.

Fig. 5.2. Improvement in the error performance of a 4-PAM signal,obtained by linearizing the LM-380 characteristic and by adjusting the decoding thresholds.

Fig. 5.3. Improvements in the S/N ratio degradation of a 4-PAM signal, obtained by linearizing the LM-380 characteristic and by adjusting the decoding thresholds.

Fig. 5.4. Eye diagram of a 4-PAM signal with the LM-380 amplifier (4 dB Output Backoff). Computer simulation result with $\alpha = 0.2$ Nyquist filter. The conventional and adjusted thresholds are shown.

Fig 5.5. Measured eye diagram of a 4-PAM signal with (a) the LM-380 amplifier, (b) the linearized LM-380 amplifier (4 dB Output Backoff). Filters with $\alpha = 0.2$ are used.

Fig. 5.6. Reduction of the spectral regrowth of a 4-PAM signal by linearizing the LM-380 AM-AM characteristic. The signal rate is 413.3 kb/s.

Fig. 5.7. Improvements in the performance of 8 and 16 PAM signals obtained by linearizing the LM-380,H-261 characteristics and by adjusting the decoding thresholds. Computer simulation results with $\alpha = 0.2$ Nyquist filters.

Fig. 5.8. Improvements in the performance of 4 and 32 PAM signals obtained by linearizing the LM-380,H-261 characteristics and by adjusting the decoding thresholds. Computer simulation results with $\alpha = 0.2$ Nyquist filters.

Fig. 5.9. Reduction in the spectral regrowth of a 4-PAM signal obtained by linearizing the LM-380 and H-261 characteristics. Computer simulation results with $\alpha = 0.2$ Nyquist filters. (a) In Phase component spectrum, (b) Quadrature component spectrum.

Fig. 5.10. Improvements in the S/N degradation of a 4-PAM signal obtained by linearizing the LM-380 and H-261 characteristics. Computer simulation results with $Q = 0.2$ Nyquist filters.

Fig. A.1. Photograph of the implemented 4-PAM Encoder - Decoder.

Fig. A.2. Implemented 4-PAM Encoder circuit.

Fig. A.3. Implemented 4-PAM Decoder circuit.

Fig. A.4. Measured eye and spectrum diagrams of the wideband 4-PAM signal generated by the circuit of Fig. A.2. The signal rate is 206.66 kBaud.

Fig. A.5. Measured eye and spectrum diagrams of the 4-PAM signal generated by the circuit of Figure A.2. Nyquist filters with $Q = 0.2$ were used.

Fig. A.6. Error performance of the 4-PAM signal generated by the implemented circuit.

Fig. A.7. Photograph of the Experimental set-up in the Digital Communications Laboratory, Department of Electrical Engineering, University of Ottawa.

Fig. B.1. Amplification stage circuit diagram.

Fig. B.2. Output power gain versus Frequency of the LM-380 amplification stage.

Fig. B.3. Error performance of the 4-PAM signal of Appendix A with the LM-380 amplification stage.

Fig. C.1. Photograph of the implemented Predistorter for the LM-380 Amplification stage.

Fig. C.2. Circuit of the Predistorter linearizer for the LM-380 Amplification stage.

Fig. C.3. Measured eye diagrams of a 4-PAM signal at the Input and Output of the predistorter (4 dB Output Backoff).

LIST OF TABLES

Table 2.1. The coefficients of the Normalized LM-380 AM-AM characteristic of Figure 2.3 (b)

Table 2.2. The coefficients of the LM-380 AM-AM characteristic of Figure 2.2 (b).

Table 2.3. The coefficients of the normalized H-261 AM-PM characteristic of Figure 2.3 (b).

Table 2.4. The coefficients of the In-Phase nonlinearity $G(R)$ derived from the LM-380 and H-261 characteristics (Figure 2.5).

Table 2.5. The coefficients of the Quadrature nonlinearity $G(R)$ derived from the LM-380 and H-261 characteristics (Figure 2.5).

Table 2.6. The coefficients of the In-Phase nonlinearity $G(R)$ derived from the LM-380 and Intelsat-V characteristics (Figure 2.5).

Table 2.7. The coefficients of the Quadrature nonlinearity $G(R)$ derived from the LM-380 and Intelsat-V characteristics (Figure 2.5).

Table 3.1. Amplitude margin of PAM schemes.

Table 3.2. Phase margin of PAM schemes.

Table 3.3. Bandwidth efficiency of PAM signals.

Table 3.4. Optimum operating points of various PAM schemes with the nonlinearities of Chapter II.

Table 4.1. Coefficients of the LM-380 predistorter.

Table 4.2. Coefficients of the LM-380, H-261 predistorter.

Table 4.3. Coefficients of the Amplitude Predistorter for the LM-380 and H-261 characteristics

Table A.1. Encoding table with reference to Figure A.2.

Table A.2. Decoding table with reference to Figure A.3.

Table C.1. Gain of the implemented predistorter.

LIST OF ABBREVIATIONS

- BER - bit error rate.
- C/N - signal to noise power ratio.
- D/A - digital to analog conversion.
- FFT - fast Fourier transform
- IF - intermediate Frequency
- ISI - intersymbol interference
- MSK - minimum shift keying.
- OBE - out of band emission
- OBO - output Backoff
- PAM - pulse amplitude modulation.
- QAM - quadrature amplitude modulation.
- QPRS - quadrature partial response signalling.
- QPSK - quadrature phase shift keying.
- RF - radio Frequency.
- S/N - signal to noise power ratio
- TWT - travelling wave tube

LIST OF SYMBOLS

$$\operatorname{erfc}(x) = \frac{2}{\sqrt{\pi}} \int_x^{\infty} e^{-t^2} dt$$

f_b - bit rate.

f_s - symbol rate.

$P_s(e)$ - symbol error probability.

$P(e)$ - bit error probability.

T_s - symbol interval.

CONTENTS

ABSTRACT	iv
ACKNOWLEDGEMENTS	v
LIST OF FIGURES	vi
LIST OF TABLES	x
LIST OF ABBREVIATIONS	xi
LIST OF SYMBOLS	xii
<u>Chapter</u>	<u>page</u>
I. INTRODUCTION	1
II. MODELS AND CHARACTERISTICS USED	6
2.1 Measurement of the AM-AM characteristic	6
2.2 Normalized AM-AM and AM-PM characteristics	9
2.3 The Quadrature model	11
2.4 Models for characteristic representation	16
2.4.1 The polynomial model	16
2.4.2 Hetrakul and Taylor model	17
2.4.3 Saleh model	18
2.4.4 Representation of the used characteristics	19
III. EFFECTS OF AMPLITUDE AND PHASE NONLINEARITIES ON PAM SIGNALS	24
3.1 Computer simulation set-up.	24
3.2 Measurement set-up.	27
3.3 Effects on the signal performance.	30
3.3.1 Analysis of the effects.	30
3.3.2 Calculation of the error performance.	41
3.3.3 Spectral regrowth	54
IV. LINEARIZATION OF THE AMPLIFIER CHARACTERISTICS	58
4.1 General	58
4.2 Linerization of the LM-380 AM-AM characteristic	60
4.3 Compensation of the LM-380 and H-261 characteristics.	66

4.4	Amplitude compensation for the LM-380 and H-261 characteristics	72
V.	LINEARIZATION RESULTS.-IMPROVEMENTS IN THE ERROR PERFORMANCE BY ADJUSTING THE DECODING THRESHOLDS.	76
5.1	Performance with the linearized LM-380 characteristic and threshold adjustment.	76
5.2	Performance with the compensated LM-380 , H-261 characteristics and threshold adjustment.	85
5.2.1	Error performance	85
5.2.2	Spectral regrowth reduction	86
5.3	Performance when only Amplitude or phase compensation for AM-AM and AM-PM nonlinearities is considered.	90
VI.	CONCLUSION	92
	REFERENCES	94
 <u>Appendix</u>		<u>page</u>
A.	IMPLEMENTATION AND PERFORMANCE EVALUATION OF A 4-PAM SYSTEM	96
A.1	Description of the Hardware implementation.	96
A.1.1	Description of the Encoder circuit.	96
A.1.2	Description of the Decoder circuit.	99
A.2	Experimental results and discussions.	101
B.	AMPLIFICATION STAGE CIRCUIT DESCRIPTION	107
C.	IMPLEMENTATION AND PERFORMANCE EVALUATION OF A PREDISTORTER LINEARIZER FOR THE LM-380 AMPLIFICATION STAGE.	112
B.1	Description of the circuit.	112
B.2	Performance of the predistorter.	115
D.	COMPUTER SIMULATION PROGRAMS.	117

Chapter I

INTRODUCTION

A bandlimited signal when transmitted via radio channels is distorted due to the presence of nonlinear elements such as power amplifiers (TWT or GaAs FET). These exhibit nonlinear distortions in both amplitude (AM-AM conversion) and phase (AM-PM conversion). [10,11]

For efficient use the power amplifiers must be operated close to the saturation. On the other hand the need for more efficient use of the available spectrum, suggest use of spectrally efficient signals such as multilevel schemes. However the sensitivity of these schemes to the impairments of the nonlinear channel increases rapidly with the number of levels.

The amount of distortion and the degradation in the system performance are dependent upon the nature of the amplifier characteristics and the shape of the transmit filter. Due to the significant envelope fluctuation of the filtered multilevel signals, spectral regrowth effects are also observed at the output of the amplifier.

Significant work has been made so far on the study of the nonlinear channel effects and methods to compensate for them. First, various models for representation of the channel nonlinearities have been proposed and techniques for their study have been developed. Thus a nonlinear element can be classified as memoryless, effectively memoryless

or with memory [12]. The Volterra series, Heiter's model or the simplified Quadrature model can be used to represent a nonlinear system [4,9,13]. Bessel functions, odd and even order polynomials and two or three parameter formulas have been proposed to express the characteristics of the nonlinear elements [1,3,9,14].

The probability of error performance and spectral properties of various constant envelope modulation schemes like QPSK or MSK in a nonlinear environment, have been investigated by many authors in depth. These schemes are not so sensitive to the channel nonlinearities. Methods to reduce the nonlinear distortion by predistorting or postdistorting the transmitted signal, so that the overall system response becomes more linear have been investigated and applied [3 to 9].

Recently, the performance and sensitivity of non-constant envelope multilevel schemes have attracted the attention. This is due to the high spectral efficiency of these schemes. PAM, QAM or QPRS schemes are involved in the investigation [2,13,15,16, 17,18]. However, the effects of the nonlinear channel on these schemes have not been studied in great detail. Most of the research has been limited to low level schemes and only a few publications have been available on the study of the high level schemes. The increasing need for more efficient use of the available spectrum, makes the investigation of the behaviour of higher schemes in a nonlinear environment indispensable.

Among the most popular investigated systems are the QAM systems. A QAM signal consists of two phase-quadrature carriers, each modulated by a PAM signal [11,22]. This means that a PAM system is the equiva-

lent baseband of a linearly modulated QAM system. In our investigation 2,4,8,16 and 32 level PAM schemes were chosen, for reasons of simplicity. These are the baseband equivalent schemes of 4,16,64,256 and 1024 QAM modulated systems.

The objectives of this study are:

i) To examine the effects of amplitude and phase nonlinearities on multilevel PAM schemes by computing their probability of error performance and their spectral properties.

ii) To apply methods in order to reduce the nonlinear distortion and improve the system performance.

iii) To compare the sensitivity and behaviour of different PAM schemes to the nonlinear channel impairments.

Specific AM-AM and AM-PM characteristics have been chosen for this purpose. These are assumed to be frequency independent, effectively memoryless nonlinearities. Computer simulation methods and baseband measurements have been used. The organization of the Thesis is as follows.

In Chapter II the amplitude and phase characteristics used in our study are given and various models for their representation are described. The representation is needed for the calculation of the computer simulation results. A comparison between the different models is made. According to the nature of the application, in later Chapters a different model is chosen.

The computer simulation and measurement set ups are described in Chapter III. Computer simulation results on the probability of error performance and spectral regrowth of 2,4,8,16 and 32 PAM schemes, distorted by the nonlinearities of Chapter II are presented. The measurements made for a 4-PAM signal justify the simulated results. The dependence of the distortion on the nature of the nonlinearities, the filter shape and the number of signal levels is shown.

In Chapter IV a brief analysis of the predistortion linearization techniques applied in our study is made. The characteristics of suboptimum linearizers are drawn and their coefficients for the different representation models are computed. The overall predistorter-amplifier characteristics are much more linear and exhibit low phase rotation. According to them baseband linearizers are proposed. An amplitude linearizer for the LM-380 characteristic is designed and implemented.

The improvement in the performance obtained by the linearization, is calculated in Chapter V again for 2,4,8,16 and 32 PAM schemes. Experimental results for a 4-PAM signal, using the implemented linearizer justify the simulated ones. Comparisons with the performance of the conventional system are made. The reduction of the spectral regrowth and thus of the adjacent and cochannel channel interference is explained. Improvements in the performance are obtained by adjusting the conventional thresholds during the decoding. The total improvement in the system performance is very significant.

The summary of our conclusions based on the obtained results is given in Chapter VI.

The designed circuits diagrams as well as the used computer programs are given analytically in Appendix A to D.

Chapter II

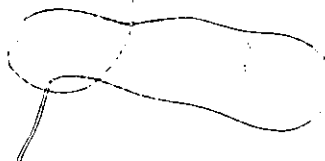
MODELS AND CHARACTERISTICS USED

In this chapter the amplitude and phase characteristics used in our study are given. A brief description of various existing models for the representation of the characteristics is presented. The coefficients required for the representation are calculated. A comparison between the different models is made.

2.1 MEASUREMENT OF THE AM-AM CHARACTERISTIC

The set up for the measurement of the AM-AM characteristic used in our study is given in Figure 2.1. The amplification stage consists of the LM-380 audio power amplifier, impedance matching and DC offset components (see Appendix B). The measured AM-AM characteristic is that of the amplification stage. Since the source of the nonlinear distortions is the LM-380 amplifier, in the next chapters we refer to it as the LM-380 characteristic for simplicity.

For the measurements, a sinusoidal signal was used as input to the amplification stage. The input and output power were measured with a spectrum analyzer. The measured characteristic is drawn in Figure 2.2 (a). We note the nonlinear nature of the characteristic near saturation.



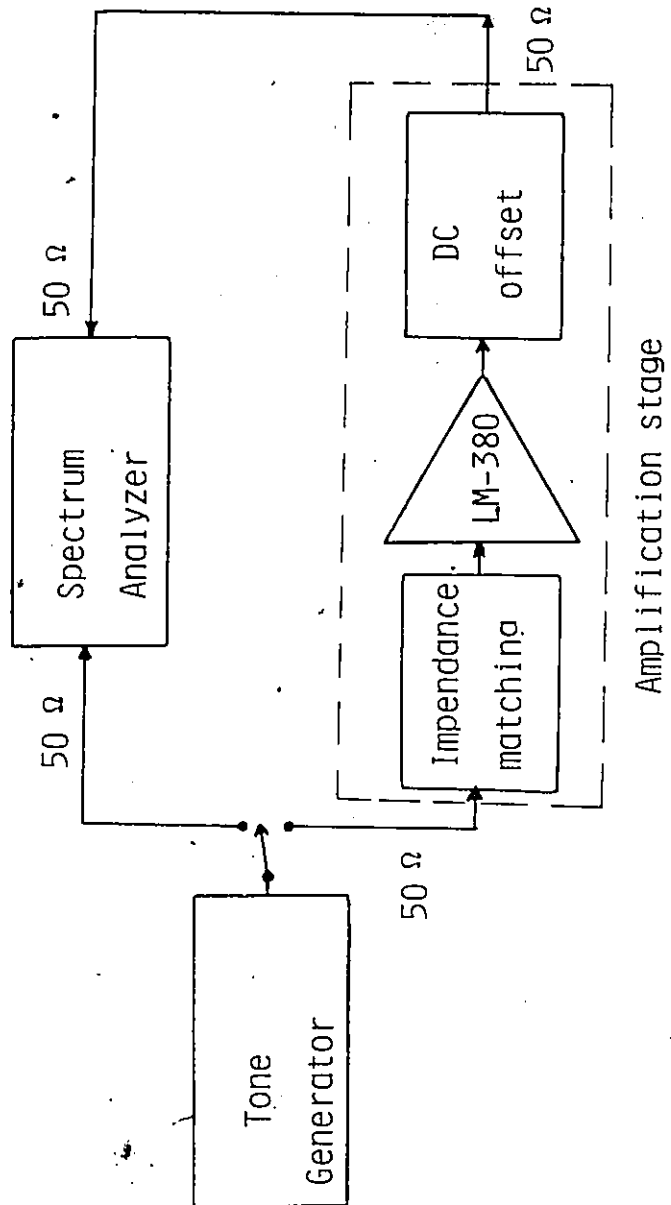


Figure 2.1 . Measurement set-up for the AM-AM characteristic.

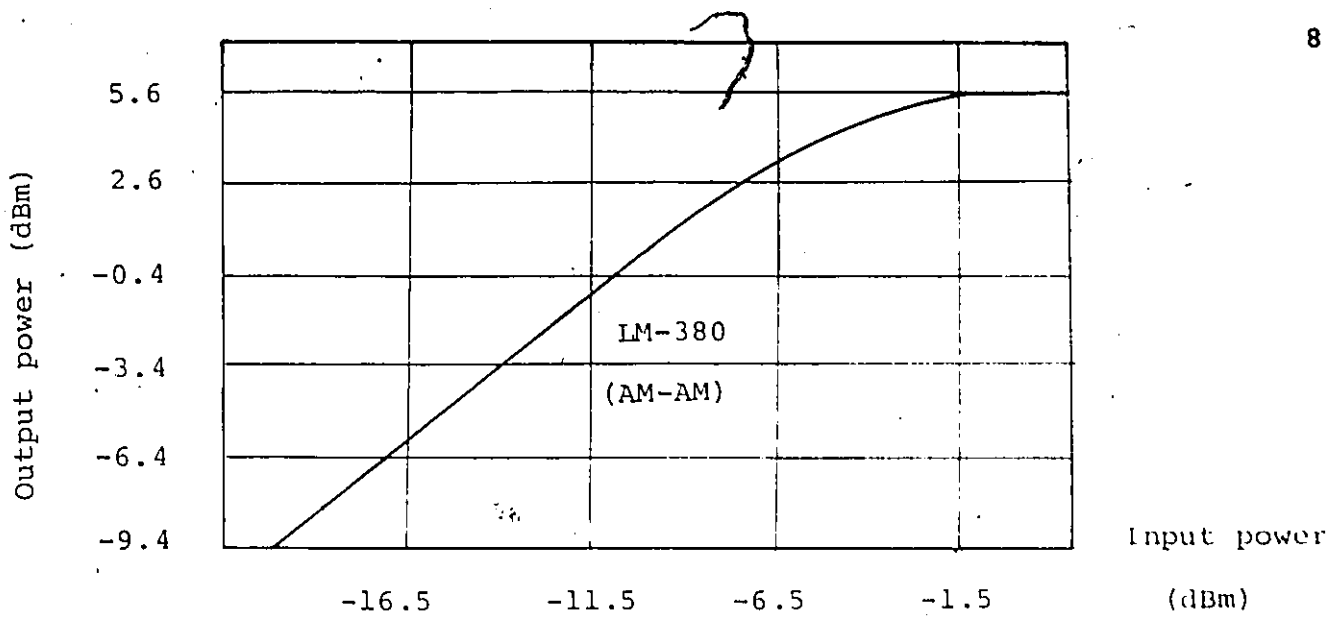


Figure 2.2 (a). The single tone measured AM-AM power characteristic of the LM-380 power amplifier.

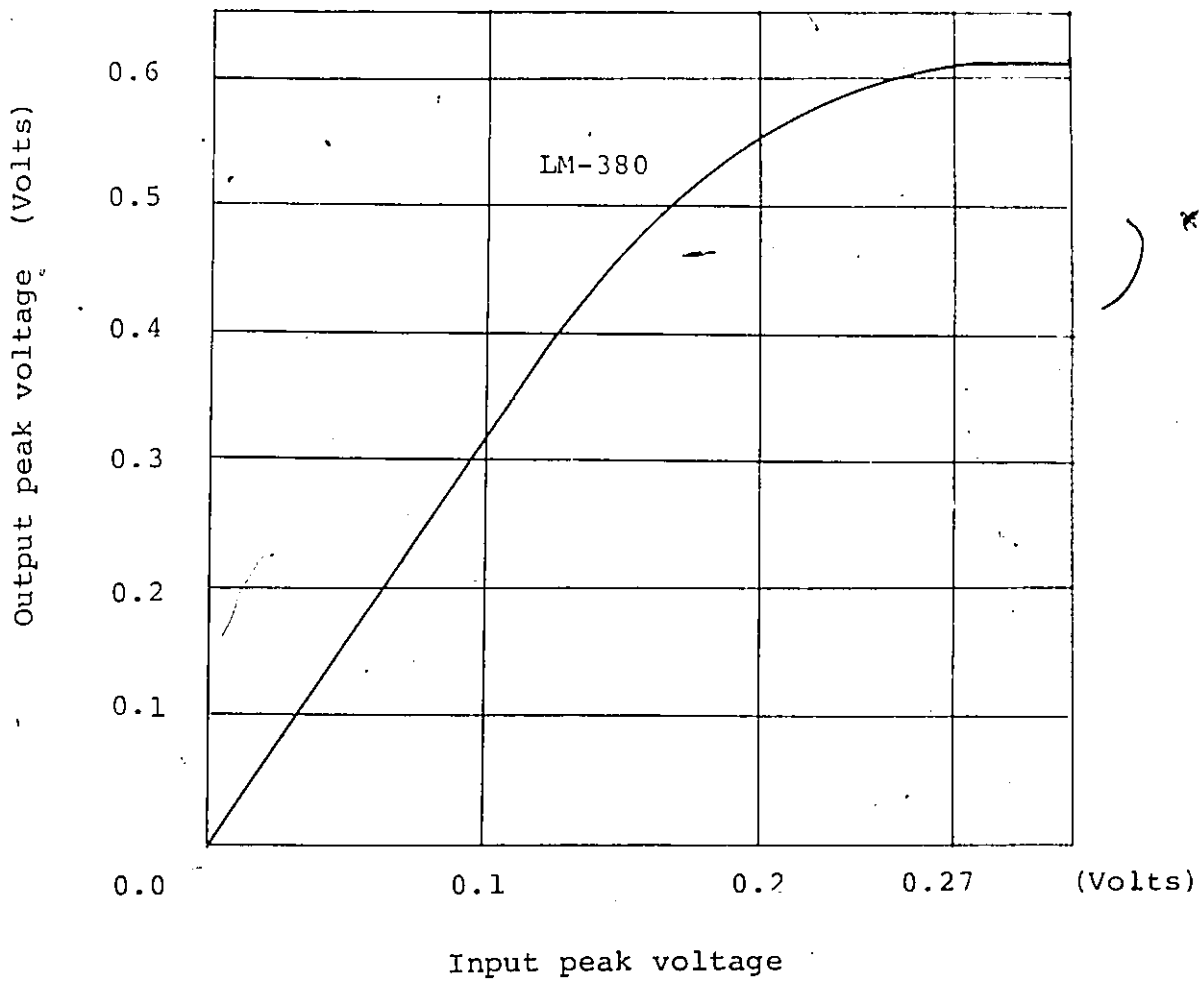


Figure 2.2 (b). Instantaneous amplitude characteristic derived from the measured curve of Fig. 2.2 (a) using the equation 2.1.

The relation between the average envelope power and the instantaneous envelope amplitude, referring to a 50 Ohm resistance is given by the equation :

$$P_{\text{dBm}} = 10 \cdot \log (P_{\text{watts}} / 1\text{mW}) = 10 \cdot \log (V^2 / 2 / 50) / 10^{-3} \quad 2.1$$

Using equation 2.1, the instantaneous amplitude characteristic can easily be obtained from the measured power characteristic. It is drawn for positive input values in Figure 2.2 (b).

2.2 NORMALIZED AM-AM AND AM-PM CHARACTERISTICS

It is usual to express the AM-AM and AM-PM characteristics in terms of Backoff power from saturation [11]. The normalized power characteristic of the LM-380 amplifier, is drawn in Figure 2.3 (a). In the same Figure AM-PM normalized characteristics similar to those of the H-261 and Intelsat-V TWT amplifiers are also drawn.

The corresponding normalized instantaneous envelope-amplitude characteristics are calculated using the equation [9]:

$$V = \pm \sqrt{2} \cdot 10^{-\frac{B}{20}} \quad 2.2$$

where B is the Backoff power in dB, and are drawn (for positive only input values) in Figure 2.3 (b).

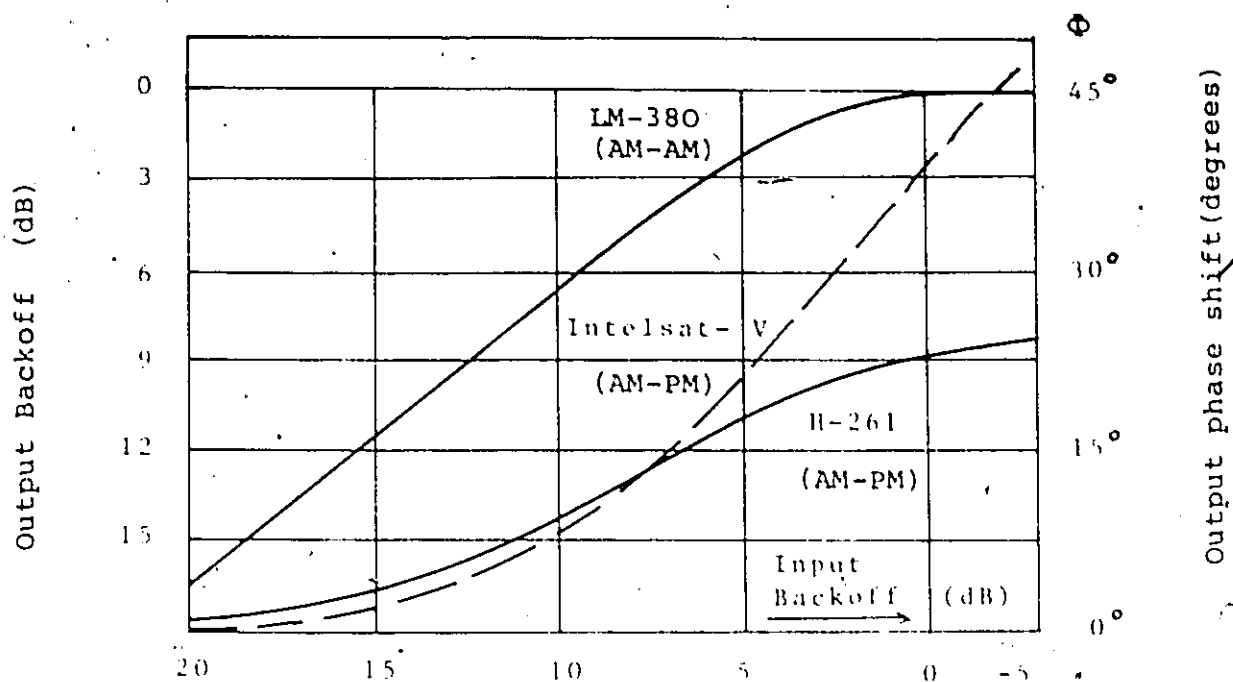


Figure 2.3 (a). The normalized power characteristics with respect to the saturation power of the LM-380 power amplifier.

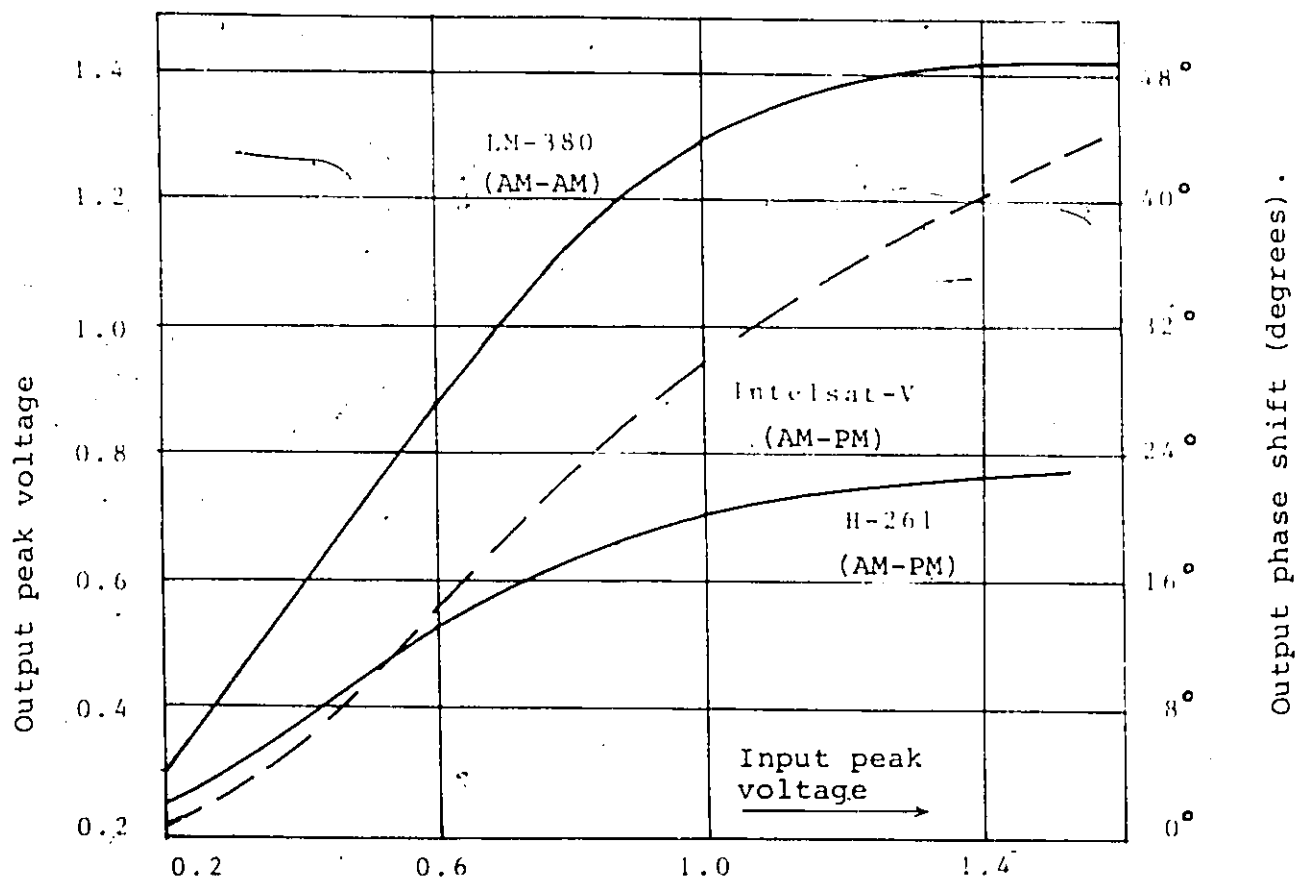


Figure 2.3 (b). Instantaneous amplitude characteristics derived from the curves of Fig. 2.3 (a) using the equation 2.2.

2.3 THE QUADRATURE MODEL

The quadrature model is a model used for representation of band-pass nonlinearities [9]. According to this, if the input to an amplifier is a narrowband radio signal given by the equation:

$$X(t) = R(t) \cos(\omega_c t + \theta(t))$$

the output of the amplifier is given by the equation:

$$Y(t) = g(t) \cos(\omega_c t + \theta(t) + \phi(t))$$

where $R(t)$ is the lowpass envelope of the signal, ω_c is the carrier frequency and $g(t) = g(R(t))$ and $\phi(t) = \phi(R(t))$ are the AM-AM and AM-PM envelope dependent transfer characteristics of the amplifier. The amplifier is assumed to be an effectively memoryless nonlinear element [12]. The equation 2.4 can be written as:

$$Y(t) = P(t) \cos(\omega_c t + \theta(t)) - Q(t) \sin(\omega_c t + \theta(t))$$

where

$$P(t) = g(R(t)) \cos(\phi(R(t)))$$

and

$$Q(t) = g(R(t)) \sin(\phi(R(t)))$$

The inphase and quadrature components $P(t)$ and $Q(t)$, represent only amplitude characteristics. In other words, a phase and an amplitude bandpass nonlinearities can be described (or replaced) by two amplitude nonlinearities. This is the principle of the quadrature model [9], which is shown in Figure 2.4.

A baseband expression of the quadrature model can be derived as follows. Assuming the baseband input to the amplifier is:

$$X(t) = R(t) \quad 2.8$$

the output is given by the equation:

$$Y(t) = G(t) \exp(j\Phi(t)) \quad 2.9$$

where $G(t)=G(R(t))$ and $\Phi(t)=\Phi(R(t))$ are baseband AM-AM and AM-PM nonlinearities similar to the bandpass ones. The equation 2.9 can be written as:

$$Y(t) = G_p(t) + j G_q(t) \quad 2.10$$

where

$$G_p(t) = G(R(t)) \cos(\Phi(R(t))) \quad 2.11$$

and

$$G_q(t) = G(R(t)) \sin(\Phi(R(t))) \quad 2.12$$

As before $G_p(t)$ and $G_q(t)$ represent only amplitude nonlinearities. It is easy to see from equations 2.9, 2.11 and 2.12 that:

$$G(R) = \sqrt{G_p^2(R) + G_q^2(R)} \quad 2.13$$

and

$$\tan \Phi(R) = (G_q(R)/G_p(R))$$

Using equations 2.11 and 2.12 the characteristics of Figure 2.3(b) are converted to the corresponding ones of the Quadrature model, drawn in Figure 2.5. The baseband model will be used in the next Chapters for the representation of the chosen nonlinearities. The reason we chose

this model is the similarity of the equations 2.11, 2.12 and 2.6, 2.7. Due to this similarity $G_p(t)$ and $G_q(t)$ of the baseband model will be also called the inphase and quadrature components respectively. The derived baseband results of Chapters III and V and the approach used in Chapter IV, can be applied to bandpass systems as well.

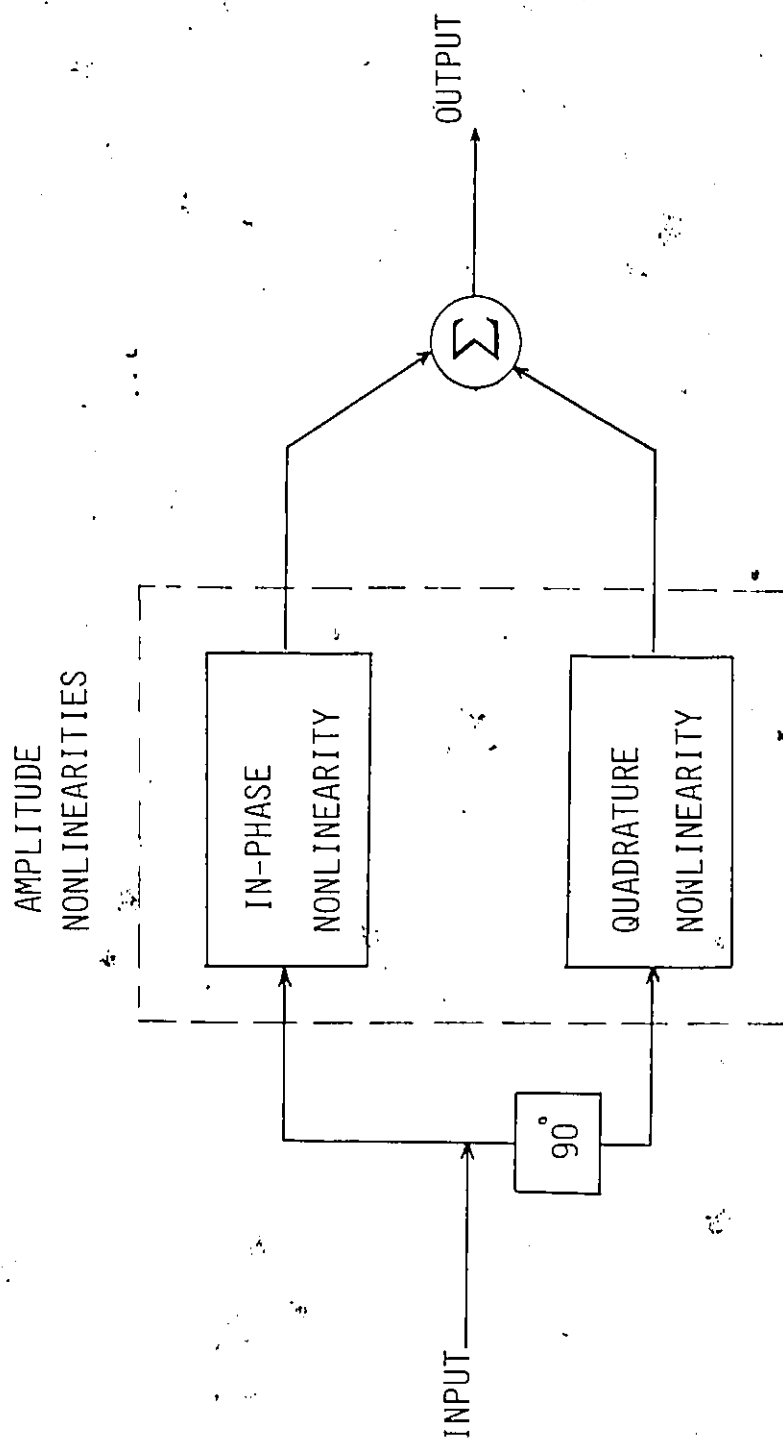


FIGURE 2.4. QUADRATURE MODEL

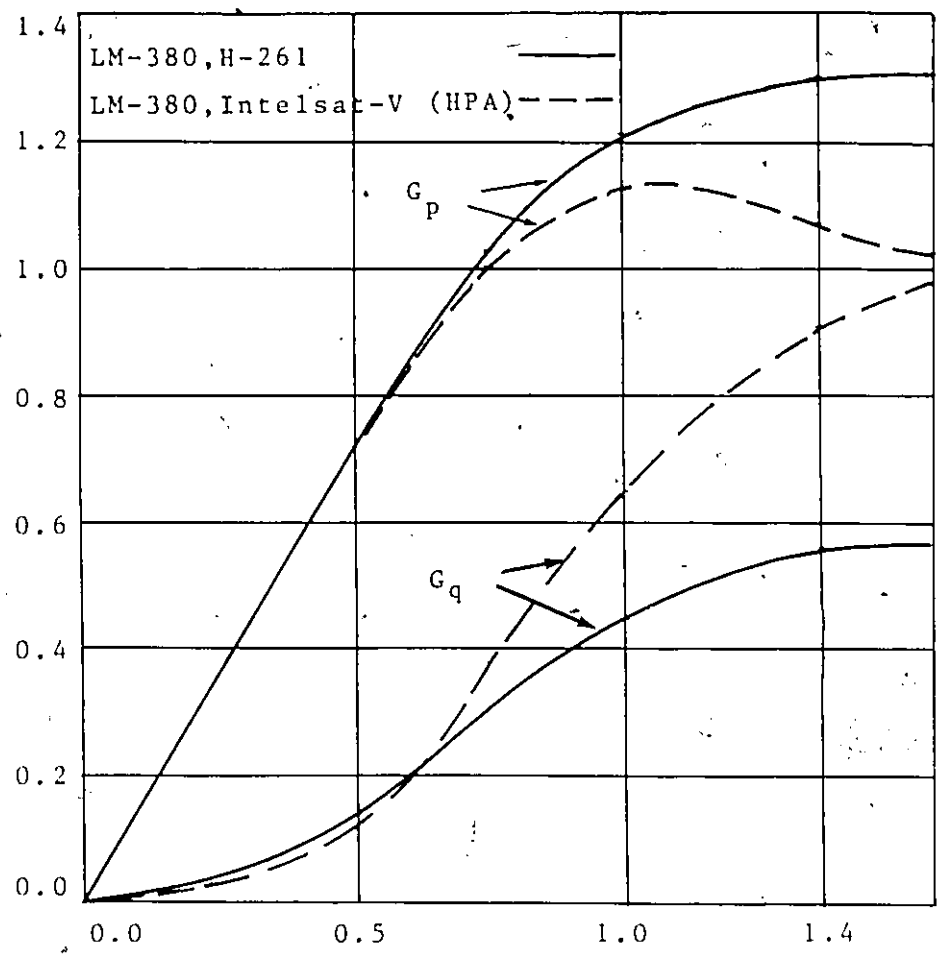


FIGURE 2.5. Amplitude characteristics of the quadrature model, derived from the characteristics of Fig. 2.3 using the equations 2.11 and 2.12.

2.4 MODELS FOR CHARACTERISTIC REPRESENTATION

To calculate the effects of the various nonlinearities we must represent them by proper envelope functions. There are many models proposed [1,3,9,13]. In this section three of these models used in our study are presented.

2.4.1 The polynomial model

This model proposed by Eric [9] uses odd order polynomials for the representation of amplitude nonlinearities and even order polynomials for phase nonlinearities. More analytically, an instantaneous envelope-amplitude characteristic $G(R)=G(R(t))$ can be written as:

$$G(R) = \sum_{n=0}^N C_{2n+1} \cdot R^{2n+1}, \quad -R_1/2 \leq R \leq R_1/2 \quad 2.14$$

while a corresponding phase characteristic $\Phi(R) = \Phi(R(t))$ as:

$$\Phi(R) = \sum_{n=1}^M D_{2n} \cdot R^{2n}, \quad -R_2/2 \leq R \leq R_2/2 \quad 2.15$$

We note that the amplitude characteristic $G(R)$ is an odd function of R while the phase characteristic $\Phi(R)$ is an even function of R . Using the equations 2.11, 2.12, 2.14, 2.15 and the series expansions of $\cos\Phi(R)$, $\sin\Phi(R)$, the amplitude characteristics $G_p(R)$, $G_q(R)$ of the quadrature model can be represented by two odd order polynomials of R , with linear and cubic leading terms respectively:

$$G_p(R) = \sum_{i=0}^N A_{2i+1} \cdot R^{2i+1}, \quad -R_3/2 \leq R \leq R_3/2 \quad 2.16$$

and

$$G_q(R) = \sum_{i=1}^M B_{2i+1} \cdot R^{2i+1}, \quad -R_4/2 \leq R \leq R_4/2 \quad 2.17$$

For small values of R these polynomials are proportional to R and R^3 respectively. The high order terms become significant for large values of R .

The polynomial representation is very accurate, but it requires many terms to fit a characteristic in a long range. It needs many coefficients to be optimized and introduces calculation difficulties due to the high order of the used polynomials. That is the reason simpler models with few coefficients have been proposed.

2.4.2 Hetrakul and Taylor model

This model uses two parameter formulas involving modified Bessel functions of the first kind, in combination with linear and exponential terms [3]. The amplitude characteristics $G_p(R)$, $G_q(R)$ of the quadrature model can be represented by the following equations:

$$G_p(R) = C_1 R \cdot \exp(-C_2 R^2) \cdot I_0(C_2 R^2) \quad 2.18$$

$$G_q(R) = S_1 R \cdot \exp(-S_2 R^2) \cdot I_1(S_2 R^2) \quad 2.19$$

where the parameters C_1, C_2 and S_1, S_2 have to be determined.

We see that this model uses only two parameters for each function but it is still a complicated expression.

2.4.3 Saleh model

Saleh proposed the representation of nonlinearity characteristics by two parameter formulas [1]. An AM-AM characteristic $G(R)$ and an AM-PM characteristic $\Phi(R)$ can be represented as:

$$G(R) = a \cdot R / (1 + b \cdot R^2) \quad 2.20$$

and

$$\Phi(R) = c \cdot R^2 / (1 + d \cdot R^2) \quad 2.21$$

while the amplitude characteristics $G_p(R), G_q(R)$ of the quadrature model can be represented as:

$$G_p(R) = a_1 \cdot R / (1 + b_1 \cdot R^2) \quad 2.22$$

and

$$G_q(R) = c_1 \cdot R^3 / (1 + d_1 \cdot R^2)^2 \quad 2.23$$

We notice that for small values of R equations 2.20 and 2.22 are proportional to R . For large values of R the equations 2.20, 2.22 and 2.23 become proportional to $1/R$ while the equation 2.21 is almost constant. The parameters a, b, c, d can be calculated using optimization procedures [1], (Appendix D).

Compared with the previous models, Saleh model is simpler but not necessarily more accurate, as we found during our study.

2.4.4 Representation of the used characteristics

In this section the models used for the representation of the characteristics of Figures 2.2 to 2.5 and their coefficients are given. A particular characteristic is represented by more than one models. In our study, depending on the nature of application the more suitable model is chosen (chapters III, IV). The coefficients were calculated using optimization subroutines and are given in tables 2.1 to 2.7. The absolute RMS error was also calculated according to the equation:

$$E_{rms} = \sqrt{\frac{1}{N} \sum_{i=1}^N (a_i - d_i)^2}$$

where a_i and d_i are the derived and estimated values, respectively.

MODEL	LM-380.	ERROR	RANGE
Polynomial	C1 = 1.4621649 C3 = -0.0998297 C5 = 0.5981663 C7 = -0.8914303 C9 = -0.8178380 C11 = 2.0430622 C13 = -1.2413568 C15 = 0.2490590	0.00731	$ R \leq 1.35$
Hetrakul Taylor	C1 = 1.6446420 C2 = 0.2892350	0.05750	$ R \leq 1.5$

TABLE 2.1 . The coefficients of the normalized LM-380
AM-AM characteristic of Figure 2.3 (b)

MODEL	LM-380	ERROR	RANGE
Hetrakul	C1 = 3.590262	0.01437	$ R \leq 0.4$
Taylor	C2 = 7.462000		

TABLE 2.2 . The coefficients of the LM-380 AM-AM characteristic of Figure 2.2 (b) .

MODEL	H-261	ERROR	RANGE
Polynomial	D2 = 1.032361	0.00219	$ R \leq 1.4$
	D4 = -1.202852		
	D6 = 0.164144		
	D8 = 1.191000		
	D10 = -1.267618		
	D12 = 0.503055		
	D14 = -0.059495		
	D16 = -0.004849		
Saleh	c = 1.390587 d = 2.988430	0.02670	$ R \leq 1.5$

TABLE 2.3 . The coefficients of the normalized H-261 AM-PM characteristic of Figure 2.3 (b) .

MODEL	LM-380, H-261	ERROR	RANGE
Polynomial	A1 = 1.4630000 A3 = -0.1424000 A5 = 0.0573800 A7 = -2.5463552 A9 = 3.4320452 A11 = -1.9768057 A13 = 0.5927067 A15 = -0.0695557	0.00209	$ R \leq 1.35$
Hetrakul Taylor	C1 = 1.6013820 C2 = 0.3257130	0.02259	$ R \leq 1.35$

TABLE 2.4 . The coefficients of the inphase nonlinearity $G_p(R)$ derived from the LM-380 and H-261 characteristics (Figure 2.5).

MODEL	LM-380, H-261	ERROR	RANGE
Polynomial	B3 = 1.1649265 B5 = 0.0535739 B7 = -4.4133043 B9 = 7.7314234 B11 = -6.0660324 B13 = 2.2945530 B15 = -0.3384920	0.02426	$ R \leq 1.4$
Saleh	c1 = 1.6446420 d1 = 0.2892350	0.01113	$ R \leq 1.4$

TABLE 2.5. The coefficients of the quadrature nonlinearity $G_q(R)$ derived from the LM-380 and H-261 characteristics (Figure 2.5).

MODEL	LM-380, INTEL. -V	ERROR	RANGE
Polynomial	A1 = 1.4619360 A3 = -0.0975490 A5 = 0.4134734 A7 = -2.3335270 A9 = 2.9813547 A11 = -1.7313000 A13 = 0.4804000 A15 = -0.0510523	0.00385	$ R \leq 1.4$

TABLE 2.6. The coefficients of the inphase nonlinearity $G_p(R)$ derived from the LM-380 and Intelsat-V characteristics (Figure 2.5).

MODEL	LM-380, INTEL. -V	ERROR	RANGE
Polynomial	B3 = 0.1769764 B5 = 6.0393476 B7 = -15.5881000 B9 = 20.5560000 B11 = -13.4176200 B13 = 4.4521000 B15 = -0.5910000	0.01792	$ R \leq 1.5$

TABLE 2.7. The coefficients of the quadrature nonlinearity $G_q(R)$ derived from the LM-380 and Intelsat-V characteristics (Figure 2.5).

Chapter III

EFFECTS OF AMPLITUDE AND PHASE NONLINEARITIES ON PAM SIGNALS

In this Chapter, the computer simulation and experimental set-ups used in our study are described. The effects caused by amplifier nonlinearities on PAM schemes are presented. The degradation in the error performance and the spectral regrowth of various PAM schemes, with the nonlinearities given in chapter. II are computed. The optimum operating points for all the schemes are found.

3.1 COMPUTER SIMULATION SET-UP.

The computer simulation model we used, is shown in Figure 3.1. A brief explanation of the model follows, while all the simulation programs we used are given in details in Appendix D.

Binary data are generated by a Random Generator. A PAM encoder translates them to a multilevel stream, long enough to contain all the possible combinations of the generated levels. For an M-ary PAM scheme these levels are given by the formula [22]:

$$A_m = 2^{m-1} - M, \quad m=1, 2, \dots, M$$

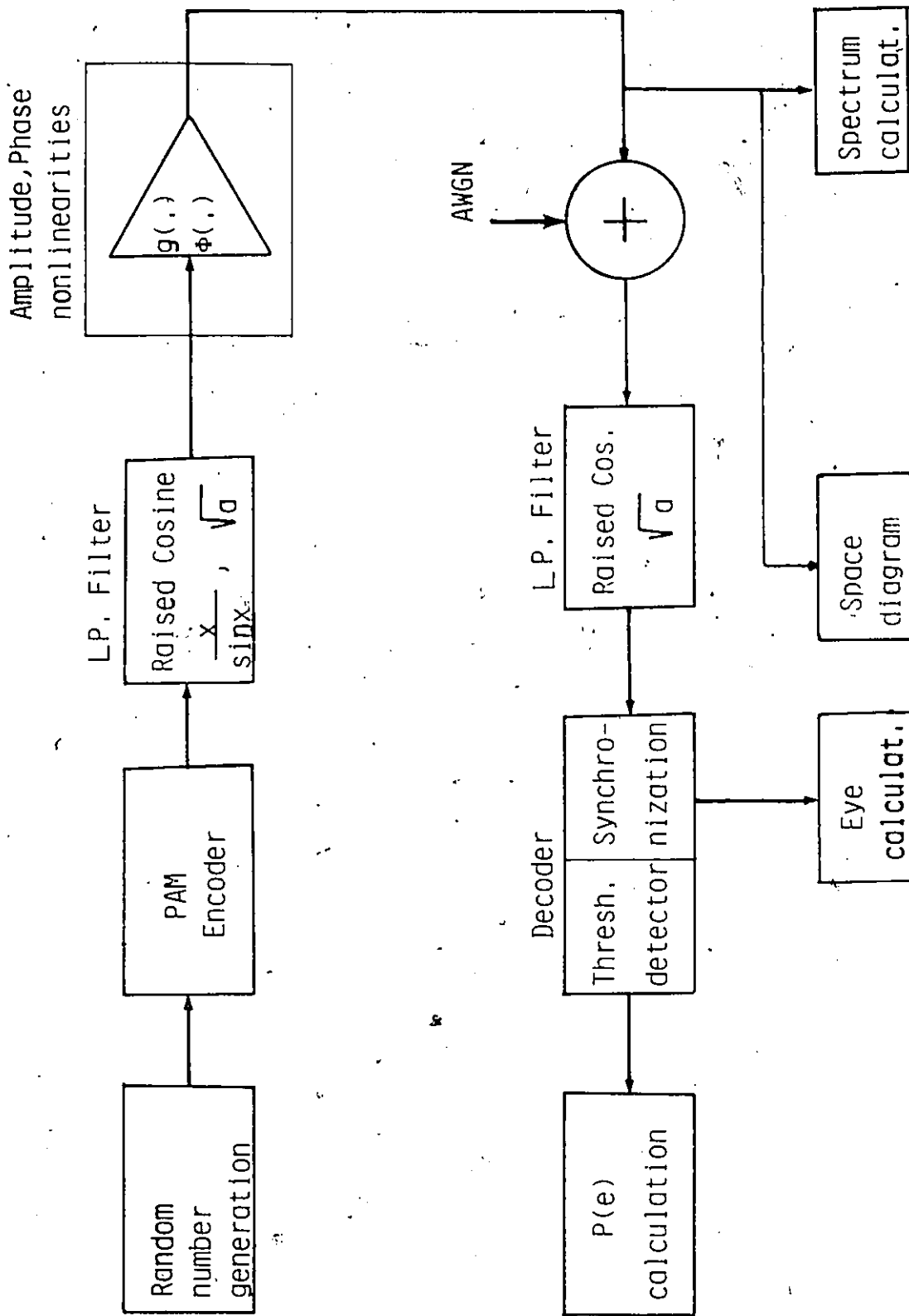


Figure 3.1. Computer simulation set up.

The transmit and receive filters are ideal square root of raised cosine filters, having a roll-off factor α . The transmit filter is $x/\sin x$ amplitude equalized so that the overall system satisfies the Nyquist first criterion.

The channel impairments assumed are, distortions due to the amplitude and phase nonlinearities given in Chapter II and Additive White Gaussian Noise (AWGN).

The different levels of the distorted signal, are detected by comparing them to suitable thresholds ($T_k = 2k - M$, $k=1, \dots, M-1$). The error probability of the i -th received symbol is computed using the equations [21]:

$$P_S^i(e) = \begin{cases} 1/2 \cdot \operatorname{erfc} \left(\frac{\operatorname{abs}(A_m^i - T_k^i)}{\sqrt{2N_0}} \right) & , \quad m=1, M \quad , \quad k=1, M-1 \\ 1/2 \cdot \left[\operatorname{erfc} \frac{\operatorname{abs}(A_m^i - T_k^i)}{\sqrt{2N_0}} + \operatorname{erfc} \frac{\operatorname{abs}(T_{k-1}^i - A_m^i)}{\sqrt{2N_0}} \right] & k=2, \dots, M-2 \quad , \quad m=2, \dots, M-1 \end{cases} \quad 3.1$$

where A_m^i is the magnitude of the optimum sample of the i -th received symbol, T_k^i and T_{k-1}^i are the lower and upper corresponding thresholds and N_0 is the equivalent to the receiving Nyquist filter noise power. Assuming Gray coding for the PAM scheme, the total bit error probability for a sequence of N symbols is calculated as:

$$P(e) = 1/\log_2 M \cdot (1/N \sum_{i=1}^N P_S^i) \quad 3.2$$

The eye and space diagrams as well as the spectrum of the signal are calculated at the points shown in Figure 3.1. The filtering of the signal is performed using FFT algorithms.

Assuming ideal carrier and timing recovery, the baseband simulation model of Figure 3.1 is equivalent to a bandpass one with similar nonlinearities (the AM-AM, AM-PM characteristics we used are assumed to be frequency independent) [11]. In all the simulation results given in this and the following chapters the S/N and C/N ratios are equivalent.

3.2 MEASUREMENT SET-UP.

Measured results on the performance of a 4-PAM signal with the LM-380 amplifier were also obtained in order to justify the computer simulation results. The used baseband measurement set-up is drawn in Figure 3.2. A description of the set-up follows.

An HP-1647 Data error analyzer was used for the generation of a 413.3 kb/s binary stream. This is actually a pseudorandom periodic data stream that it is considered random if it is long.

A 4-PAM encoder-decoder was implemented for the translation of binary stream to a 4 level stream. The diagram and the performance of this circuit are explained in detail in Appendix A. The generated 4-PAM signal has a rate of 206.66 kBaud.

413.3 Kb/s 206.66 Kbaud 124 KHz

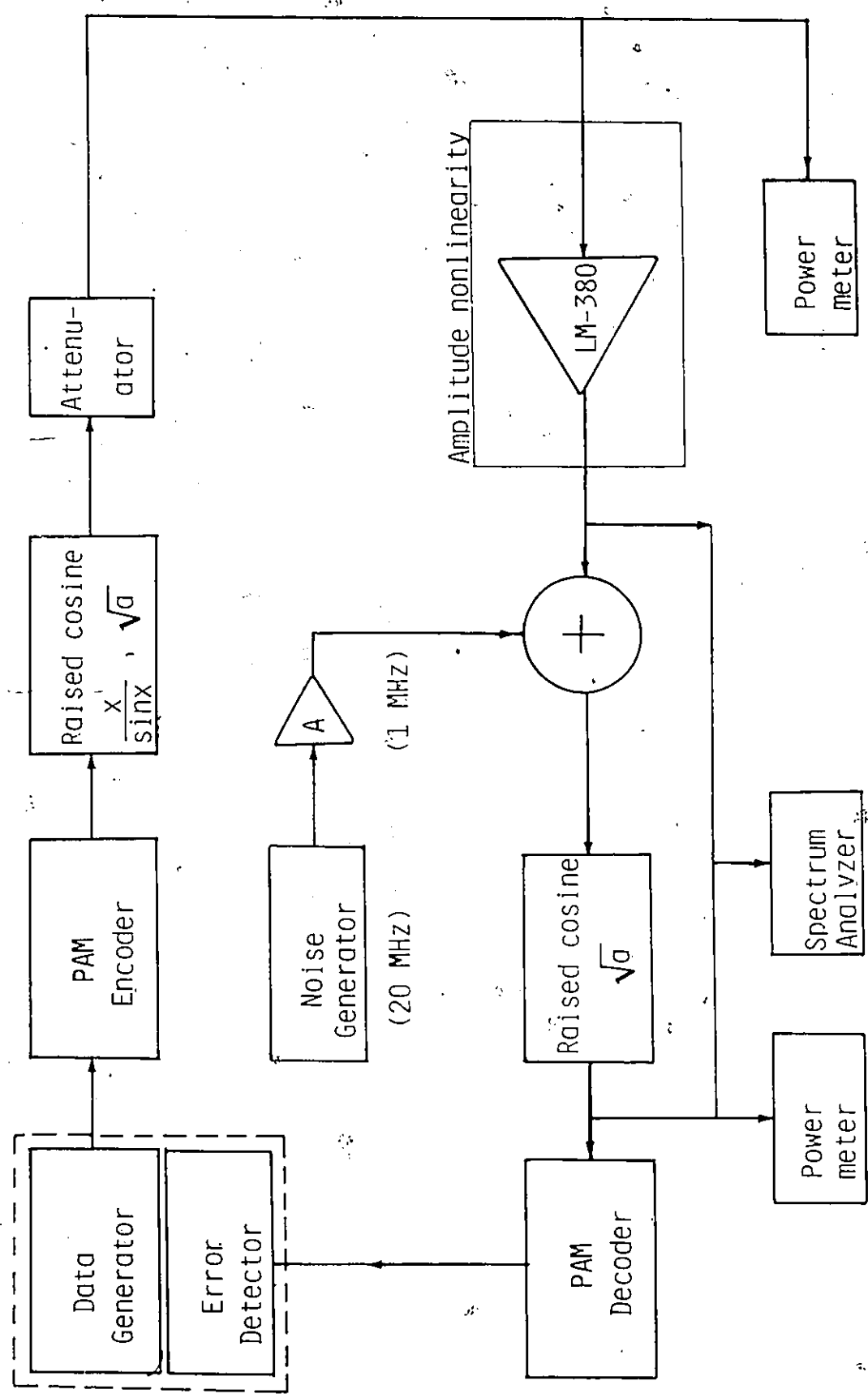


Figure 3.2. Measurement set-up.

The transmit and receive filters are square root of raised cosine filters with a roll-off factor $\alpha = 0.2$. The transmit filter is $x/\sin x$ amplitude equalized and the overall system satisfies the Nyquist first criterion. The filter is manufactured by Karkar Electronics Inc. and has a Nyquist Frequency of 103.3 kHz and an out of band rejection of 50 dB at 124 kHz. The receiver filter is also used for the noise limitation.

The signal is distorted by the LM-380 amplifier. The distortion depends on the input power level which is controlled by a variable attenuator. The operation point is changed from the linear region of the amplifier to the saturation. The signal power at the output of the amplifier is measured by a true RMS power meter.

Additive Gaussian noise is added to the signal. The noise is amplified and bandlimited before the addition. The final noise bandwidth is wide enough (1 MHz), compared to the signal bandwidth and thus the noise is considered white.

The error probability is measured with the HP-1647 Data error analyzer. The decoded signal plus noise is compared with the stored in memory transmitted signal and the errors are counted. The S/N ratio is measured by a true RMS power meter (HP-3400 A) at the output of the receiver filter. We must mention here that different values of the S/N ratio are measured by changing the noise power, while the signal power is kept constant:

3.3 EFFECTS ON THE SIGNAL PERFORMANCE.

The impact of the nonlinear channel impairments on the error performance of PAM schemes is explained in this section.

3.3.1 Analysis of the effects.

A baseband PAM scheme is characterized by the equation [22]:

$$R(t) = \sum_{k=0}^{\infty} A_k \cdot u(t - kT_s) \quad 3.3$$

where A_k takes the M discrete values (levels)

$$A_m = 2m-1-M \quad , \quad m=1,2,\dots,M$$

for a given M . T_s is the signal rate and $u(t)$ the signal pulse. In our study $u(t)$ is a Nyquist shape pulse, given ideally by the equation [11]:

$$u(t) = \frac{\sin(\eta t/T_s)}{\eta t/T_s} \cdot \left[\frac{\cos(\alpha t/T_s)}{1 - 4\alpha^2 t^2/T_s^2} \right] \quad 3.4$$

where α is the channel roll-off factor.

A signal like that of equation 3.1 is distorted due to the AM-AM envelope dependent response of the power amplifiers. If we operate close to or into the nonlinear region of the amplifier AM-AM characteristic, we notice that the envelope dependent amplification causes suppression of the higher signal levels compared to the lower levels. On the other hand, the interaction of the envelope depended response with the enve-

lope fluctuations due to the filtering of the transmitted signal, give rise to intersymbol interference. Both effects are shown in Figures 3.3 to 3.5 for a 4-PAM signal with the LM-380 AM-AM characteristic. We notice that the distortion becomes more severe as the operation point is changed from the linear region of the characteristic to saturation.

The above effects cause significant degradation in the error performance of the transmitted signal as it is shown in the next section. The major contribution to the degradation comes from the higher level. We call amplitude margin the percentage of the higher level suppression that causes system failure (fig. 3.6). As it is shown in Table 3.1 the amplitude margin decreases when we move to higher schemes.

No of levels	Amplitude margin
2	100 %
4	33 %
8	14.3 %
16	6.7 %
32	3.2 %

TABLE 3.1 Amplitude margin of PAM schemes.

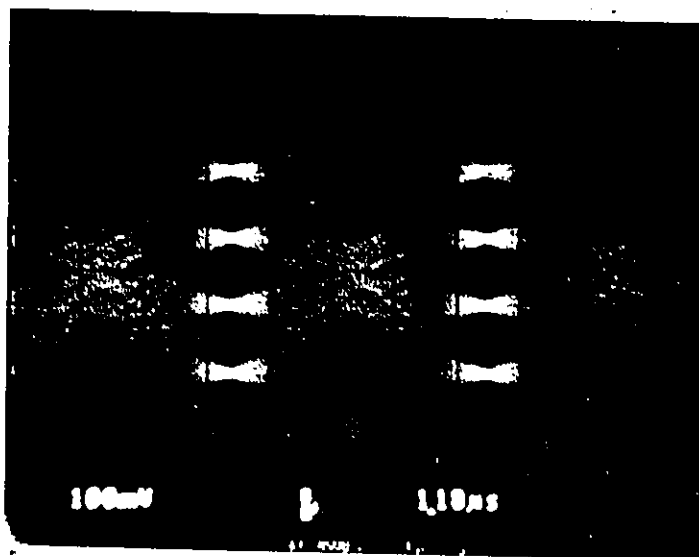


Figure 3.3. Measured eye diagram of a 4-PAM signal with the LM-380 amplifier. Linear region. Nyquist filters with $\alpha=0.2$ are used. The signal rate is 413.3 kb/s.

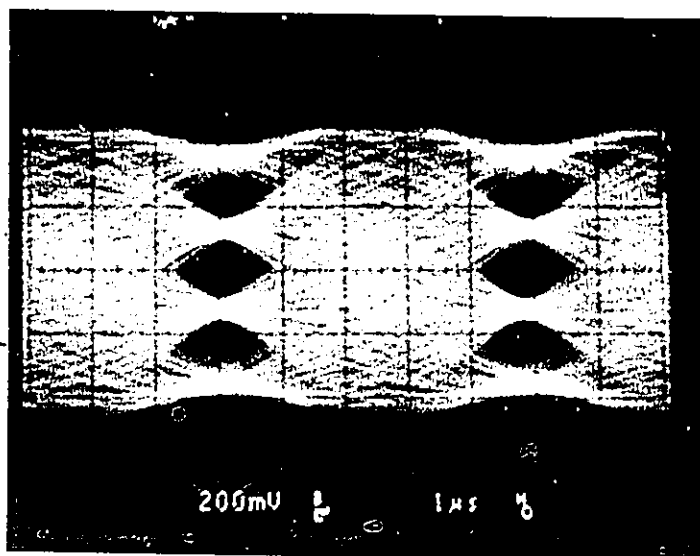


Figure 3.4. Measured eye diagram of a 4-PAM signal with the LM-380 amplifier (3 dB Output Backoff). Nyquist filters with $\alpha=0.2$ are used. The signal rate is 413.3 kb/s.

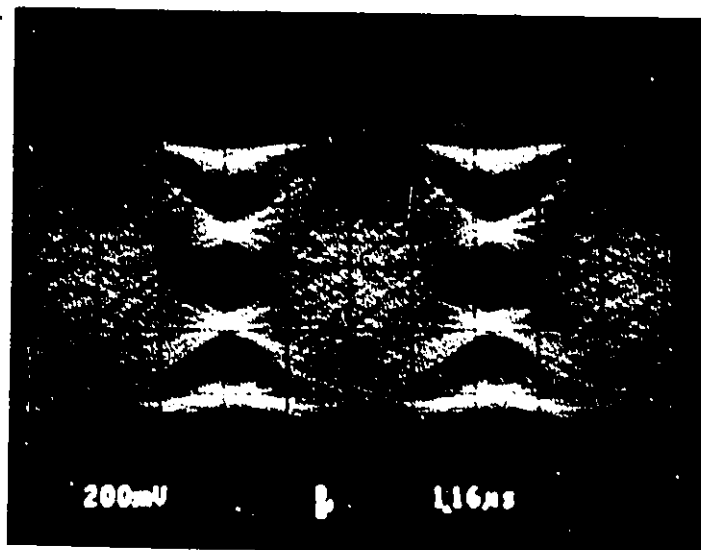


Figure 3.5. Measured eye diagram of a 4-PAM signal with the LM-380 amplifier (2 dB Output Backoff). Nyquist filters with $\alpha=0.2$ are used. The signal rate is 413.3 kb/s.

4 dB Out.Backoff

Amplitude margin=

$$= \frac{L-1}{L} \%$$

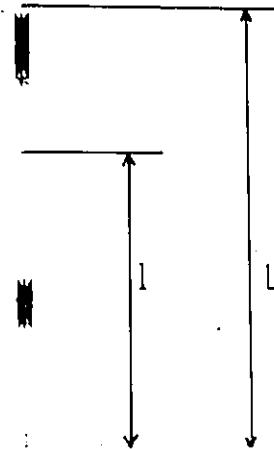


Figure 3.6. Space diagram of a 4-PAM scheme with the LM-380 characteristic. Computer simulation results with $\alpha=0.2$ Nyquist filters. The initial transmitted levels were $\pm 1, \pm 3$. The gain of the LM-380 amplifier has been removed.

A phase nonlinearity (AM-PM conversion) causes envelope dependent phase rotation of the incoming signal levels with the following results.

Assuming only AM-PM conversion, the output of the amplifier can be written as (equation 2.9):

$$Y(t) = R(t) \exp(j\Phi(t)) = R_p(t) + j R_q(t) \quad 3.5$$

where

$$R_p(t) = R(t) \cos(\Phi(t)) = R(t) \cos(\Phi(R(t))) \quad 3.6$$

and

$$R_q(t) = R(t) \sin(\Phi(t)) = R(t) \sin(\Phi(R(t))) \quad 3.7$$

We note that the original one dimensional signal, is expressed as a two dimensional signal according to the equation 3.5 (see also Figure 3.7). Since our decoding system is one dimensional, only the in-phase component R_p will remain after demodulation. The result is a level dependent suppression according to the $\cos(\Phi(R(t)))$. Additional inter-symbol interference is also expected.

The above effects degrade the error performance of the system. Once more, the major contribution to the degradation comes from the higher level. We call phase margin the amount of rotation of the higher level that causes system failure (Fig 3.7). In Table 3.2 we note that the phase margin decreases as we move to higher schemes.

10 dB Out.Backoff.

PHASE MARGIN

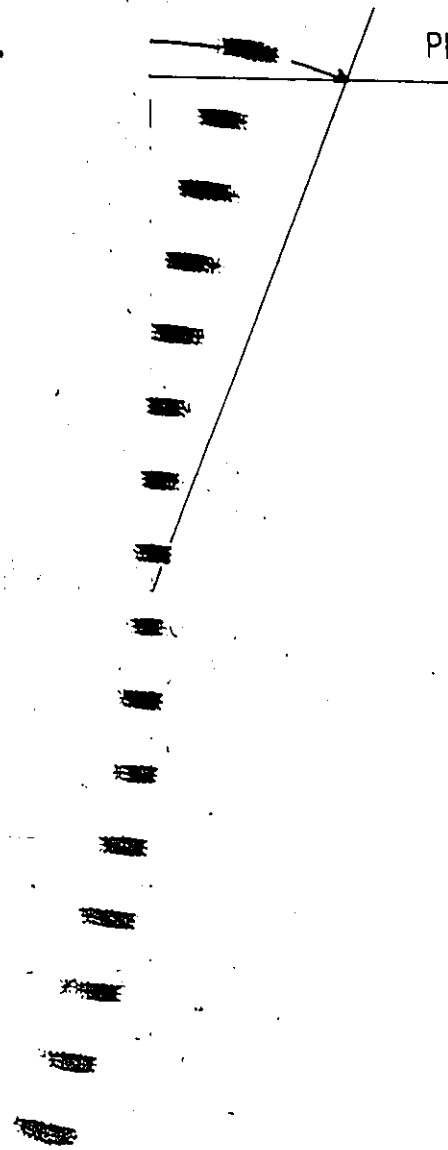


Figure 3.7. Space diagram of a 16-PAM scheme with the H-261 AM-PM characteristic. Computer simulation results with $\alpha=0.2$ Nyquist filters. The Out.Backoff refers to the LM-380 characteristic. The initial transmitted levels were $\pm 1, \pm 3, \pm 5, \pm 7, \pm 9, \pm 11, \pm 13, \pm 15$.

No of levels	Phase margin (degrees)
2	90
4	48
8	31
16	21
32	14.6

TABLE 3.2 . Phase margin of PAM schemes.

The signal distortion due to the combined AM-AM and AM-PM effects is much more severe than the distortion of each effect. The signal levels are suppressed and rotated simultaneously. The distortion is more severe for the higher levels. This is shown clearly in Figures 3.8 and 3.9 for an 8-PAM signal with the LM-380 and H-261 nonlinearities. We notice that the higher transmitted levels (± 7), have almost reach their corresponding decoding thresholds, which means that the system has almost failed.

At this point, we must make a remark about the simulated space diagrams and eye diagram of Figures 3.6 to 3.9. We should expect the received signal power to be higher than the power of the transmitted signal. We should also expect the received signal power to increase as Backoff is decreased. However this does not seem so. This happens because in our simulations we remove the gain of the amplifier. Thus in the above Figures we see only the effects of the amplifier nonlinearities.

We mentioned in the preceding analysis, that the higher schemes are more sensitive to the effects of the channel nonlinearities and that their error performance is expected to be worst than that of the lower schemes. The advantage of using schemes with high number of levels is to accomplish spectral efficiency. The bandwidth requirements for transmitting PAM signals can be found by the formula [22]:

$$W = R / (2 \log_2 M)$$

where W is the baseband signal bandwidth, R the signal rate in b/s and M the number of signal levels. The bandwidth efficiency for PAM as measured by the ratio R/W in bits per second per Hertz is given in Table 3.3.

No of levels	Bandwidth efficiency b/s/Hz
2	2
4	4
8	6
16	8
32	10

TABLE 3.3 . Bandwidth Efficiency of PAM signals.

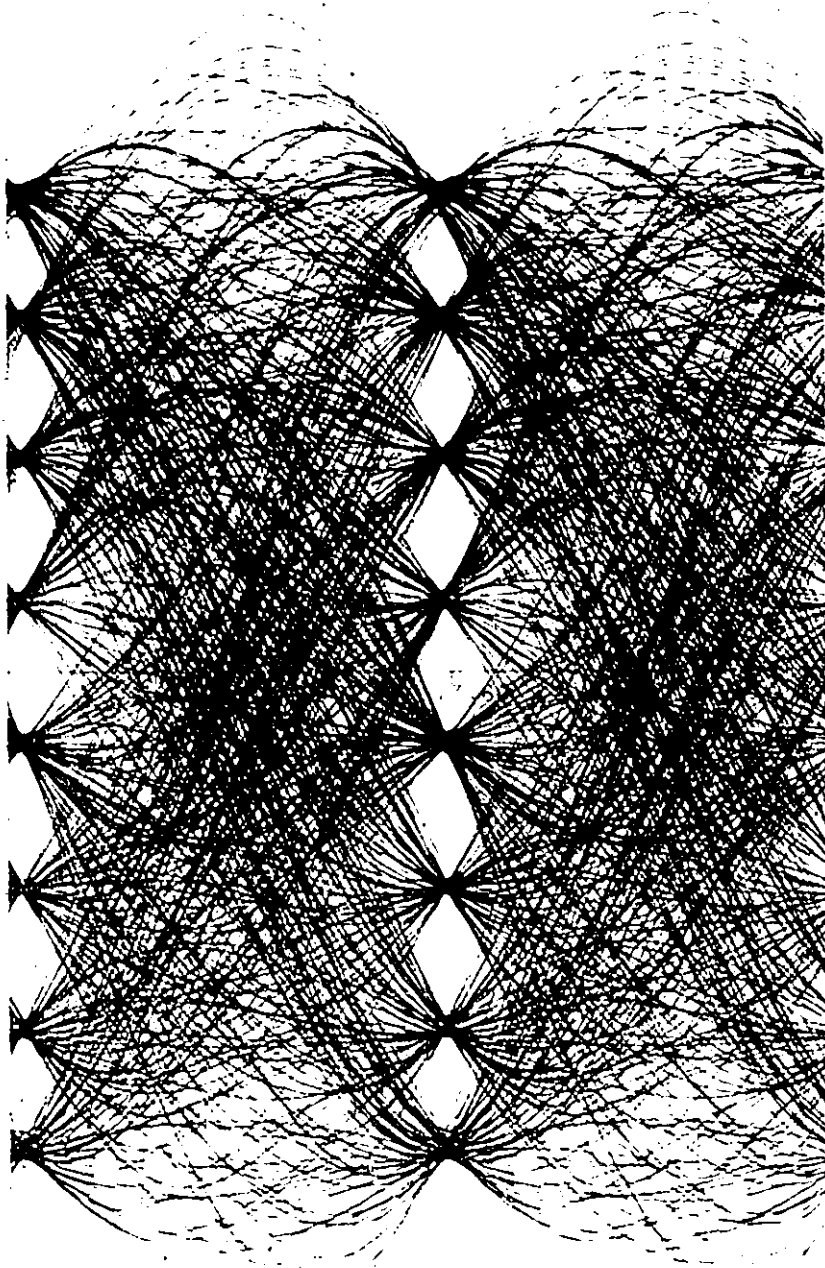


Figure 3.8. Eye diagram of an 8-PAM scheme with the LM-380, H-261 characteristics (6 dB Out.Backoff). Computer simulation results with $\alpha=0.2$ Nyquist filters. The initial transmitted levels were $\pm 1, \pm 3, \pm 5, \pm 7$. The gain of the LM-380 amplifier has been removed.

6 dB Output Backoff

Figure 3.9. Space diagram of an 8-PAM scheme with the LM-380,H-261 characteristics. Computer simulation results with $\alpha=0.2$ Nyquist filters. The initial transmitted levels were $\pm 1, \pm 3, \pm 5, \pm 7$. The gain of the LM-380 amplifier has been removed.

3.3.2 Calculation of the error performance.

Using the described simulation set-up, the probability of error $P(e)$ was calculated for 2, 4, 8, 16 and 32 PAM schemes and for different operating points of the nonlinear characteristics. For better accuracy the polynomial representation was preferred (see Tables 2.1 to 2.7). The quadrature model with the characteristics of Figure 2.5 was used for the AM-AM and AM-PM nonlinearities.

In Figure 3.10, the error performance of a 4-PAM signal with the LM-380 AM-AM characteristic is shown. The different operating points are expressed as Output Backoff. We notice that the performance degrades when the Backoff is decreasing. In order to obtain a good performance the power amplifiers must be operated at average power levels which are significantly below saturation. This makes the system less power efficient. The same observations are made when the AM-PM and the AM-AM, AM-PM combined effects are considered (Figures 3.11, 3.12).

The observed degradation in the error performance is due to the nonlinear distortions of the signal, explained in Section 3.3.1. The vertical eye openings (see Figures 3.3 to 3.9), decrease due to the envelope dependent suppression and rotation of the signal levels. In other words, the distances $A_m - T_k$ ($m = 1, \dots, M$, $k = 1, \dots, M-1$) of the equations 3.1 become smaller, resulting in higher probability of error ($\text{erfc}(x)$ increases when x decreases). The degradation of the performance increases when the operation point is changed towards saturation, because the nonlinear distortions become more severe.

The measured Probability of bit error for a 4-PAM signal and for various operating points of the LM-380 characteristic is shown in Figure 3.13. To measure the S/N ratio for a particular operating point (Output Backoff), we changed the noise power while the signal power was kept constant. Comparing the measured results with those of computer simulation (Fig. 3.10) we observe that:

i) For $P(e)=10^{-4}$ and without the amplifier (linear channel), there is a 0.6 dB degradation in the S/N ratio from the simulated performance. This is due to Hardware imperfections of the 4-PAM circuit, impedance mismatching and filter Group delay (see Appendix A). These impairments generate Intersymbol Interference.

ii) For $P(e)=10^{-4}$ and with the LM-380 amplifier operating in the "linear" region there is an additional 0.4 dB degradation in the S/N ratio. This is due to a basic difference between the simulation and the measurement models. In the simulation model the LM-380 amplifier is assumed to be phase equalized. In Appendix B we show that the above degradation is mainly due to the phase of the LM-380 amplifier which is drawn in Figure B.2 .

iii) The effects of the above imperfections become more severe when we operate closer to saturation, due to the very small vertical opening of the signal outer eyes.

As we see in Figure 3.14, the difference between computer simulation and measured results for $P(e)=10^{-4}$ is between 1 to 1.5 dB. Considering the above remarks we can say that the measured results justify the simulated ones.

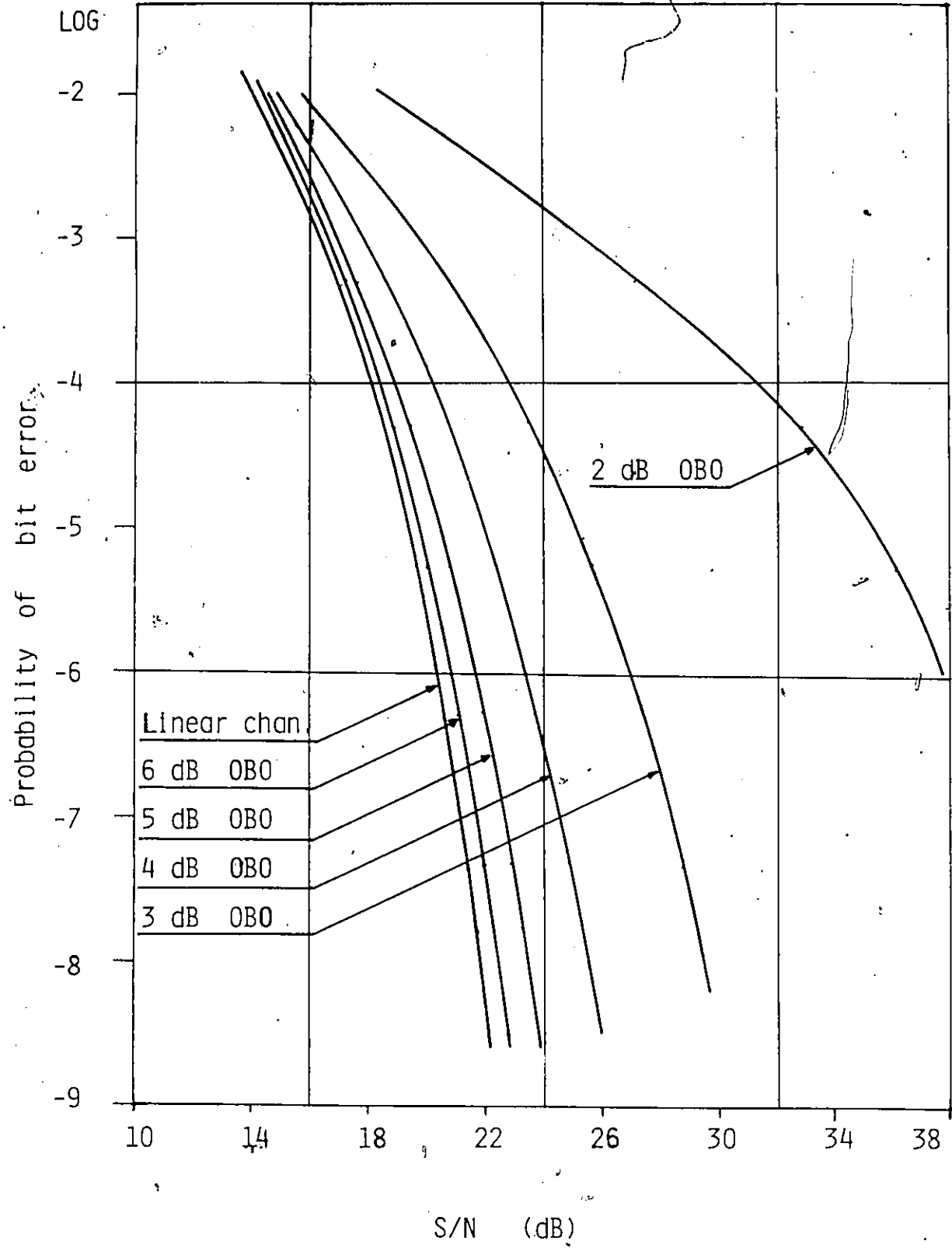


Figure 3.10. Performance of a 4-PAM signal with the LM-380 AM-AM characteristic. Computer simulation results with $\alpha=0.2$ Filters. The S/N ratio is measured in the Nyquist bandwidth at the output of the receiver LPF.

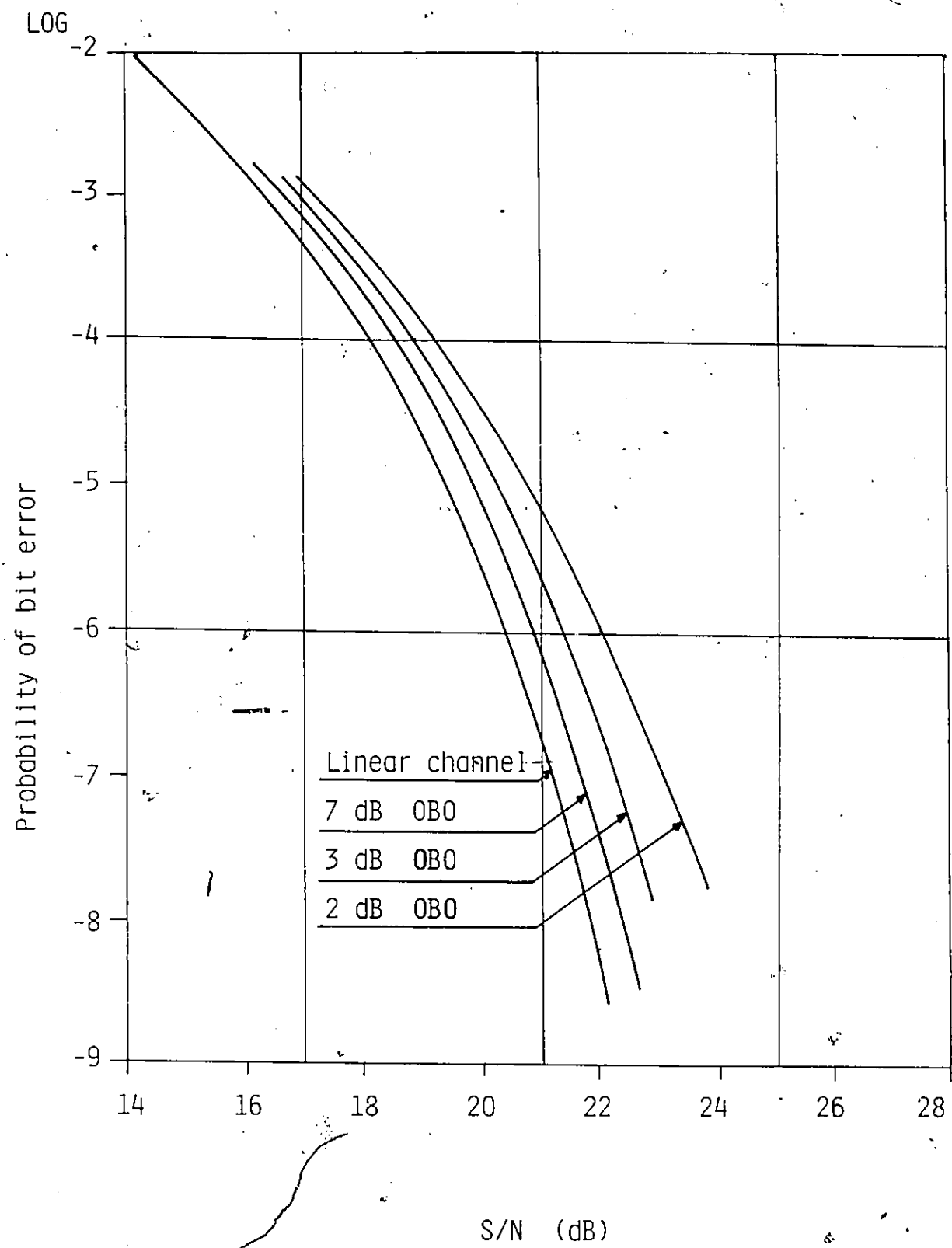


Figure 3.11. Performance of a 4-PAM signal with the H-261 AM-PM characteristic. Computer simulation results with $\alpha=0.2$ Filters. The S/N ratio is measured in the Nyquist bandwidth at the output of the receiver LPF. The Output Backoff refers to the LM-380 characteristic.

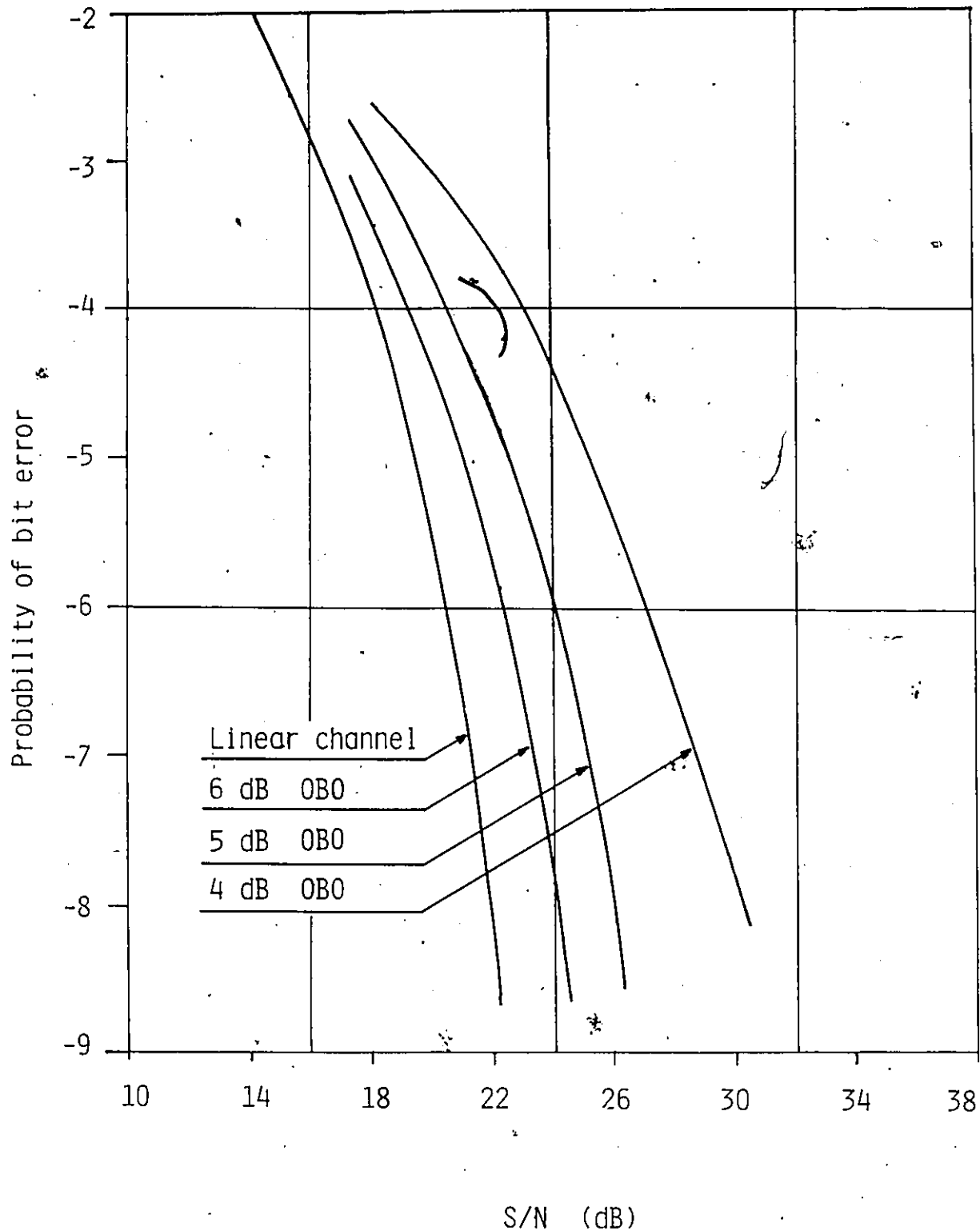


Figure 3.12: Performance of a 4-PAM signal with the LM-380 and H-261 characteristics. Computer simulation results with $\alpha=0.2$ Filters. The S/N ratio is measured in the Nyquist bandwidth at the output of the receiver LPF.

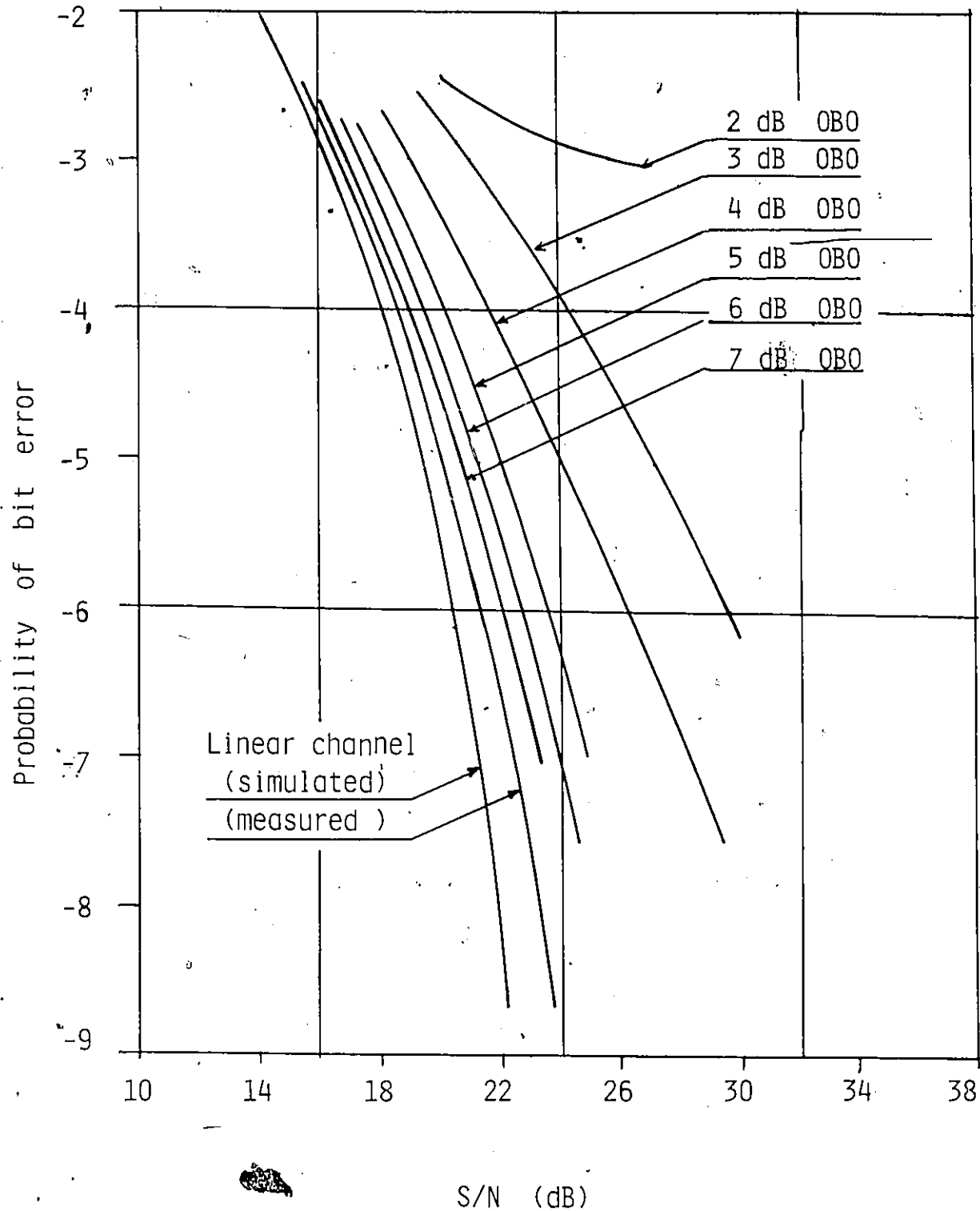


Figure 3.13. Performance of a 4-PAM signal with the LM-380 AM-AM characteristic. Measured results with $\alpha=0.2$ Filters. The S/N ratio is measured in the Nyquist bandwidth at the output of the receiver LPF.

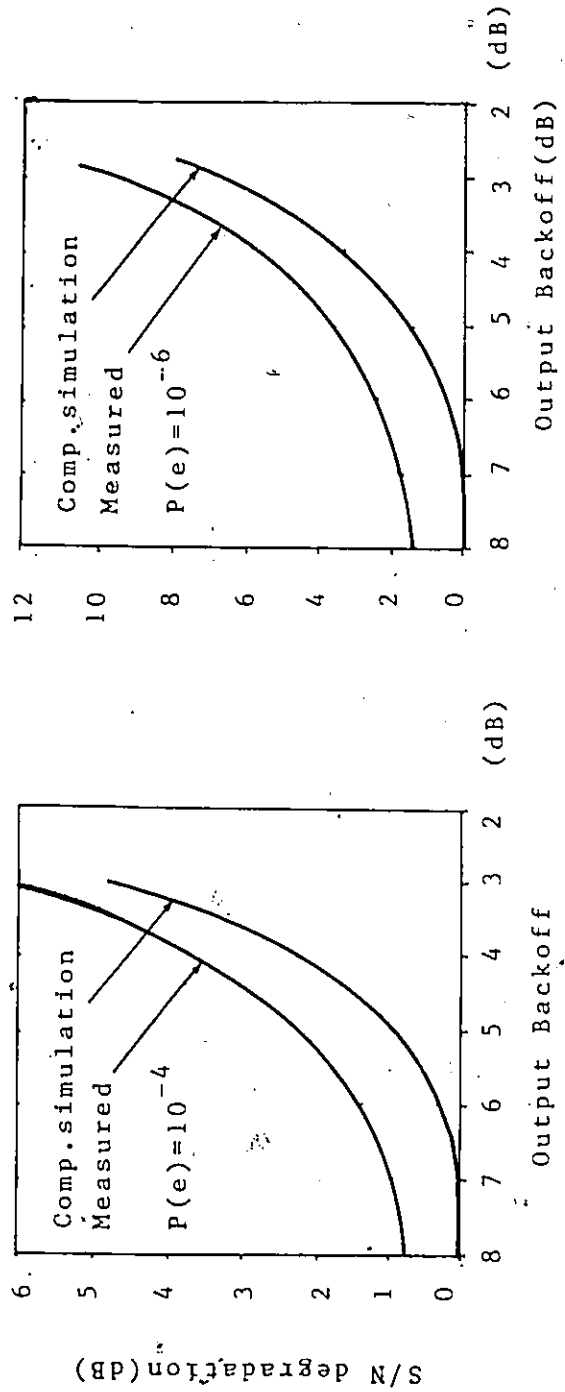


FIGURE 3.14. C/N DEGRADATION OF A 4-PAM SIGNAL WITH THE LM-380 AM-AM CHARACTERISTIC. COMPUTER SIMULATION AND MEASURED RESULTS WITH $\alpha = 0.2$. NYQUIST FILTER.

The degradation in the error performance for various PAM schemes has also been computed. The sum of the S/N degradation (dB) and Output Backoff (dB) versus Output Backoff, for $P(e)=10^{-6}$ is drawn in Figures 3.15 to 3.17. This is done because in a communication link, in order to find the best operating point both the S/N degradation and the Output Backoff must be considered. According to these Figures the following conclusions are made:

i) The closer to saturation we operate the greater the degradation is. As we explained before, this happens because the nonlinear distortions become more severe.

ii) The higher the scheme the more sensitive is to the nonlinear effects. This is due to the significantly lower amplitude and phase margins of the higher schemes (see Tables 3.1, 3.2). In Figure 3.15 we see that for an acceptable performance, and with an 8-PAM signal we must operate more than 5 dB Output Backoff while with a 32 PAM signal we must operate more than 12 dB Output Backoff.

iii) There is a small dependence of the nonlinear distortion on the shape of the transmit filter. The performance for roll-off factors $\alpha=0.2$ and $\alpha=0.5$ is drawn in Figures 3.15 and 3.17. We note that the degradation increases as the roll-off factor decreases. This is expected since the smaller the roll-off factor, the greater the envelope fluctuation of the signal and therefore the greater the distortions caused by the envelope dependent nonlinearities. We also observe that the higher schemes are less sensitive to the filter shape. This is because they exhibit high envelope fluctuations even before filtering.

iv) The severity of the degradation depends also on the nature of the amplifier characteristics. The H-261 characteristic allows less Back-off than the Intelsat V characteristic, since it exhibits lower phase shifts (Figure 3.17).

v) Comparing Figures 3.15 and 3.16, we observe that the degradation due to the AM-PM conversion is for the higher schemes more critical than the degradation due to AM-AM conversion. For these schemes the phase margin is comparable to the phase rotation caused by the chosen AM-PM characteristics. However, generally there is no consistent explanation to identify whether the major cause of performance degradation is due to the AM-AM or the AM-PM characteristic of the amplifier [2,13].

vi) The degradation caused by the combined AM-AM, AM-PM effects is greater than the sum of the degradation of each effect. This is due to the interaction of the envelope dependent suppression and rotation of the signal levels.

From the obtained results we can find the optimum operating points when both the S/N degradation and the Output Backoff are considered. They are given in table 3.4 and they justify the conclusions we made.

OPTIMUM OPERATING POINTS (Out.Backoff,dB). $P(e)=10^{-6}$

<div style="display: flex; align-items: center;"> <div style="writing-mode: vertical-rl; transform: rotate(180deg);">scheme</div> <div style="margin-left: 10px;"> 2 PAM </div> </div>	<div style="display: flex; align-items: center;"> <div style="writing-mode: vertical-rl; transform: rotate(180deg);">4 PAM</div> </div>	<div style="display: flex; align-items: center;"> <div style="writing-mode: vertical-rl; transform: rotate(180deg);">8 PAM</div> </div>	<div style="display: flex; align-items: center;"> <div style="writing-mode: vertical-rl; transform: rotate(180deg);">16 PAM</div> </div>	<div style="display: flex; align-items: center;"> <div style="writing-mode: vertical-rl; transform: rotate(180deg);">32 PAM</div> </div>	
<div style="display: flex; align-items: center;"> <div style="writing-mode: vertical-rl; transform: rotate(180deg);">nonlin.</div> </div>					
LM-380	0	5	7	9	11
H-261	0	0	3	11	13
Intel.-V	0	5	/	/	/
LM-380					
H-261	0	6	9	12	14
LM-380					
Intel.-V	0	7.5	/	/	/

TABLE 3.4

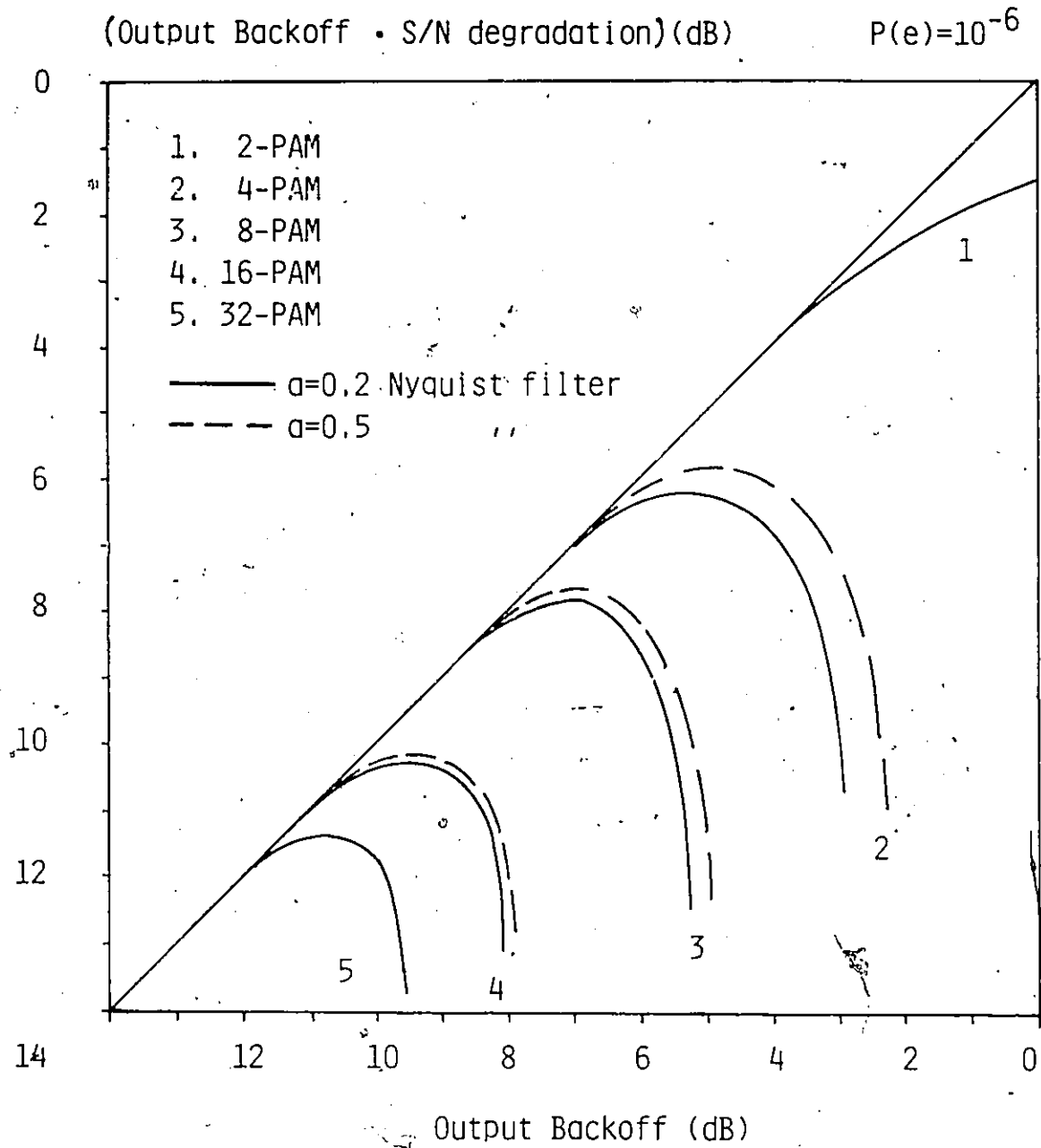


Figure 3.15 Degradation due to Amplitude conversion (LM-380 characteristic). Computer simulation results.

(Output Backoff • S/N degradation) (dB)

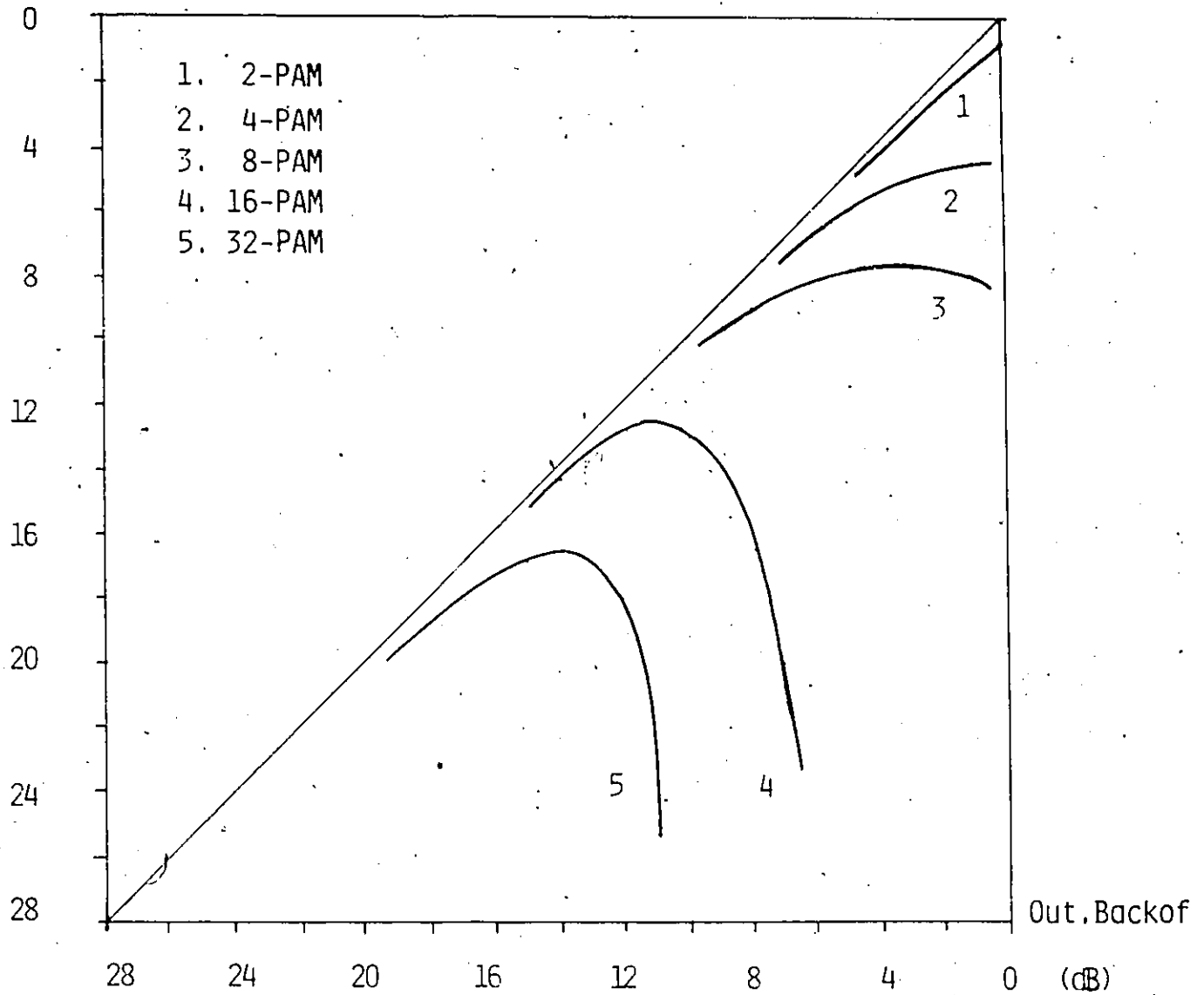
 $P(e)=10^{-6}$ 

Figure 3.16. Degradation due to AM-PM conversion (H-261 characteristic). The Output Backoff refers to the LM-380 characteristic. Computer simulation results with $\alpha=0.2$ Nyquist filters. The S/N ratio is measured in the Nyquist bandwidth at the output of the receiver LPF.

(Output Backoff • S/N degradation) (dB)

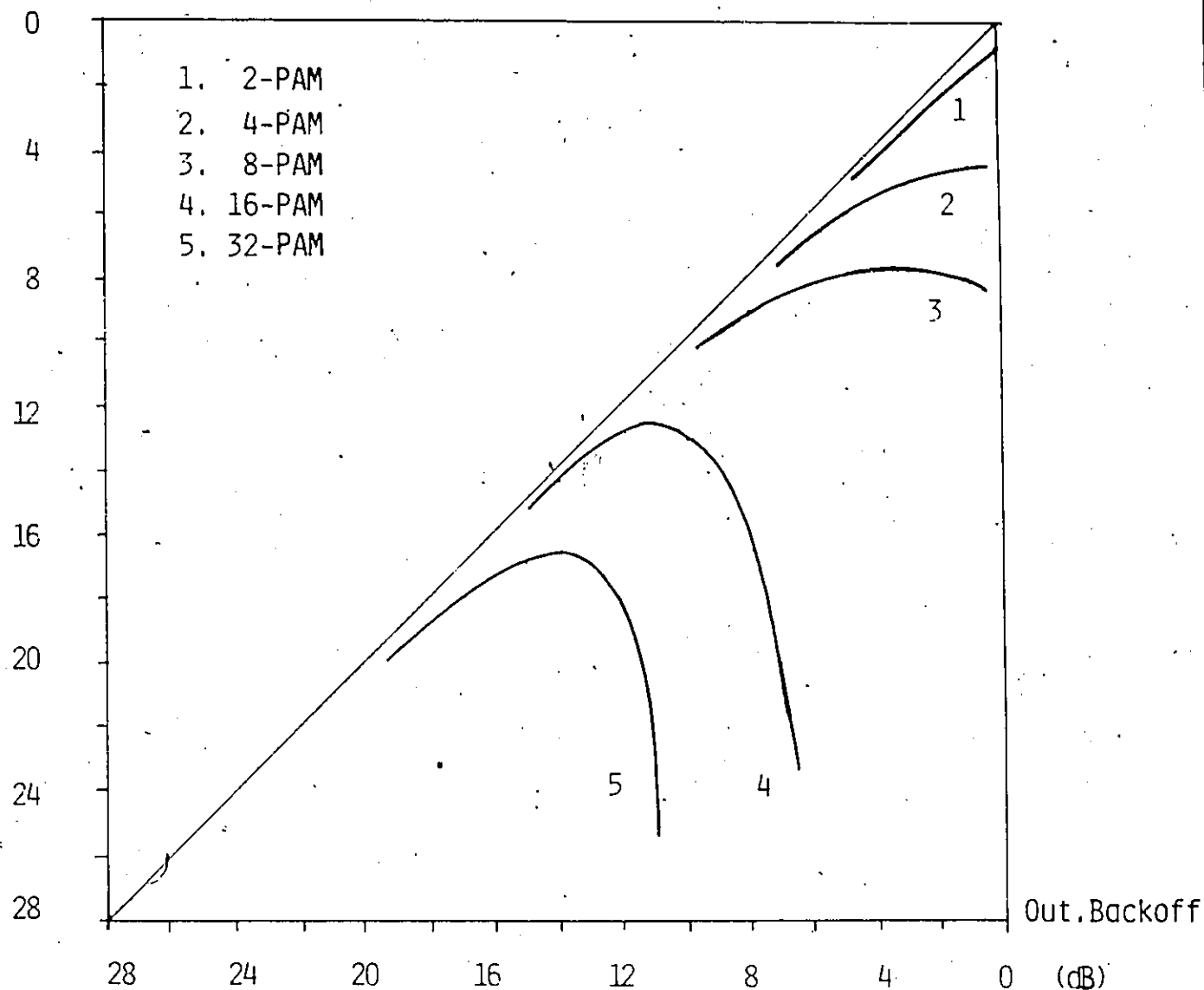
 $P(e)=10^{-6}$ 

Figure 3.16. Degradation due to AM-PM conversion (H-261 characteristic). The Output Backoff refers to the LM-380 characteristic. Computer simulation results with $\alpha=0.2$ Nyquist filters. The S/N ratio is measured in the Nyquist bandwidth at the output of the receiver LPF.

3.3.3 Spectral regrowth

Spectral regrowth is another severe problem caused by power amplifier nonlinearities. In spite of the bandwidth limitation of the transmitted signal by the transmit filter, spectral sidelobe regrowth is observed at the output of the amplifier (usually the filter is prior to the amplifier). This is due to the increase of the signal envelope fluctuations, caused by the amplitude and phase nonlinearities. The amount of the OBE is dependent upon the operating Backoff of the amplifier and the amount of envelope fluctuation of the incoming signal.

The measured spectral regrowth for a 4-PAM scheme due to the LM-380 amplifier is shown in Figures 3.18 (a), (b). We note that for operation in the "linear" region of the amplifier (8 dB Out. Backoff), there is some spectral regrowth. This is consistent with the obtained degradation in the error performance which is shown in Figure 3.13 and is due to the phase of the LM-380 amplifier (Appendix B).

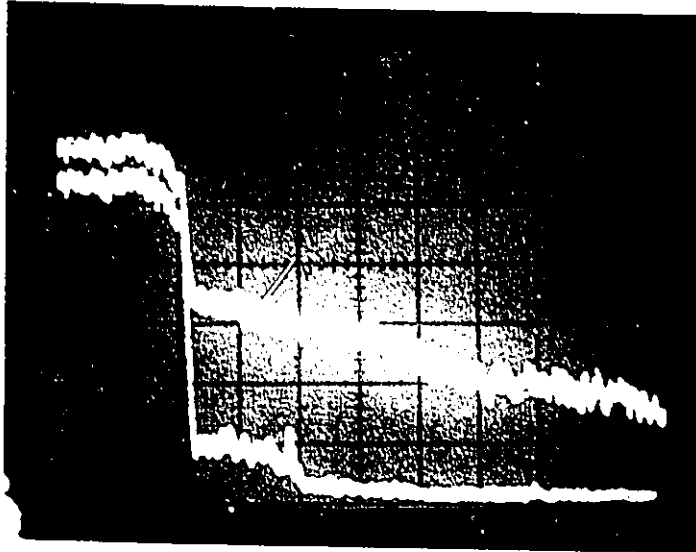
For the combined AM-AM, AM-PM effect we computed the spectral regrowth of the inphase and quadrature components (Equation 3.4). They are shown in Figure 3.19 (a), (b).

The following conclusions can be made:

i) For operation far below saturation the AM-PM conversion has the major contribution to the spectral regrowth (compare the In-phase and Quadrature spectrum). However, this is generally dependent on the nature of the nonlinear characteristics.

ii) As the operation point is changed towards saturation, the spectral regrowth increases. This is expected since, due to the severity of the nonlinear distortions close to saturation, the signal envelope fluctuations become more significant. We also note that the AM-AM conversion becomes the major contributor.

The spectral regrowth can become a cause for adjacent and cochannel interference. That is why we usually want to suppress it. In chapter VI we will show that the spectral regrowth can be reduced by using linearization techniques.

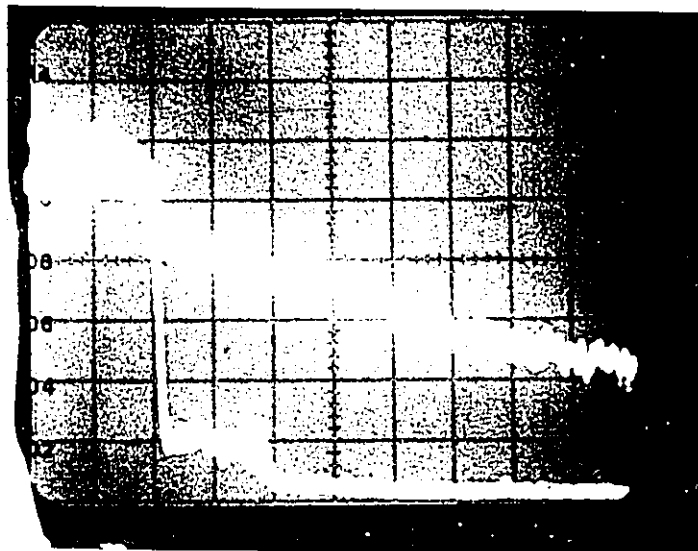


Vert. 10 dB/div.
 Horiz. 50KHz/div.
 Up.ref.lev. 0 dBm

4 dB Out.Backoff.

8 dB Out.Backoff.

(a)



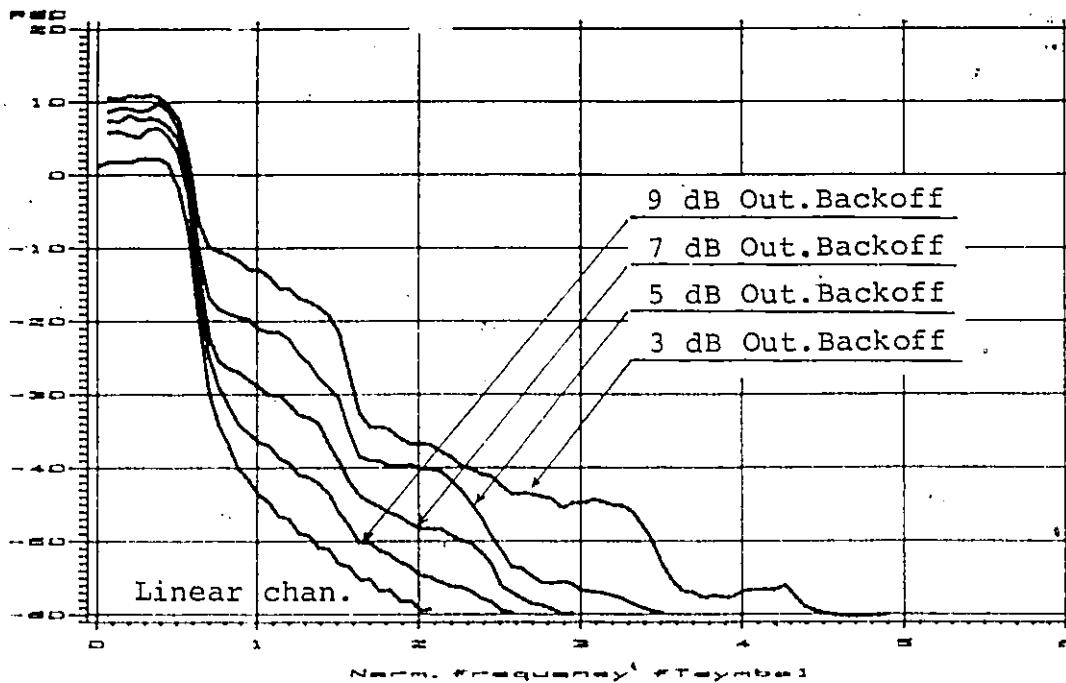
Vert. 10 dB/div.
 Horiz. 50KHz/div.
 Up.ref.lev. 0 dBm

2 dB Out.Backoff.

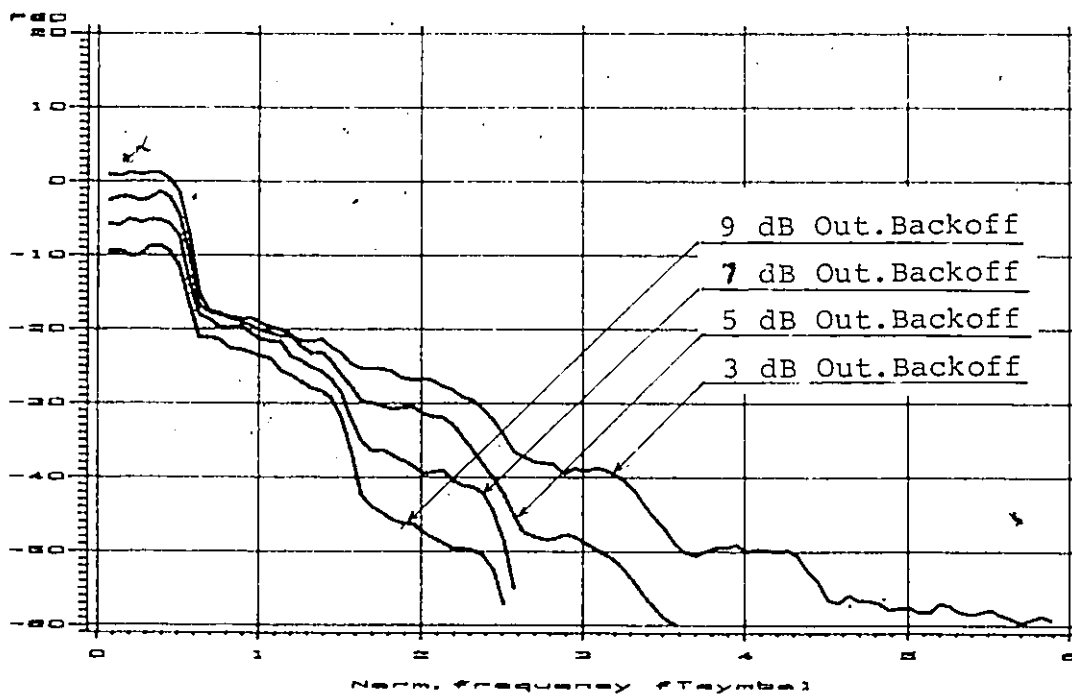
8 dB Out.Backoff.

(b)

Figure 3.18. Measured spectrum diagrams of a 4-PAM signal with the LM-380 amplifier. The signal rate is 413.3 kb/s. Nyquist filters with $\alpha=0.2$ were used.



(a) Inphase component spectrum.



(b) Quadrature component spectrum.

Figure 3.19. Spectral regrowth of a 4-PAM signal due to the LM-380 and H-261 nonlinearities. Computer simulation results with $Q = 0.2$ Nyquist filters.

Chapter IV

LINEARIZATION OF THE AMPLIFIER CHARACTERISTICS

The characteristics of predistortion linearizers for the amplifier nonlinearities used in chapter IV are calculated. The overall linearizer-amplifier characteristic is more linear and exhibits low phase shifts. Baseband linearization models are proposed and a baseband linearizer for the LM-380 amplifier is implemented.

4.1 GENERAL

The reduction of the distortion due to amplifier nonlinearities, is approached here by the introduction of a source of complementary nonlinear distortion in the signal path (linearizer), so that the overall transfer characteristic becomes more linear. For microwave transmitters in Microwave or Satellite links, predistortion linearization is preferred (Fig. 4.1), for the following reasons [4,6].

i) Because of the high microwave power at the output of the power amplifiers predistortion applications are less costly. The predistorter is not required to handle as much power and thus it is easier to be implemented.

ii) It is possible to apply predistortion in the RF, IF or baseband sections of the transmitter.

A drawback of predistortion linearization is that for perfect compensation, all the significant frequencies produced by the predistorter should be applied without shaping to the input of the power amplifier. This is difficult to be satisfied in practice.

The above considerations affect the decision on where to introduce the predistorter. In RF, IF or baseband. RF predistorters have the advantage of operating at smaller fractional bandwidths and thus achieving minimum frequency shaping. Baseband and IF predistorters on the other hand, are more flexible in signal processing and less costly [4].

The predistorter considered in our study is such that the overall predistorter-amplifier amplitude characteristic approaches that of a soft limiter and the overall phase characteristic is almost zero. These characteristics although suboptimal [3], yield significant performance improvements.

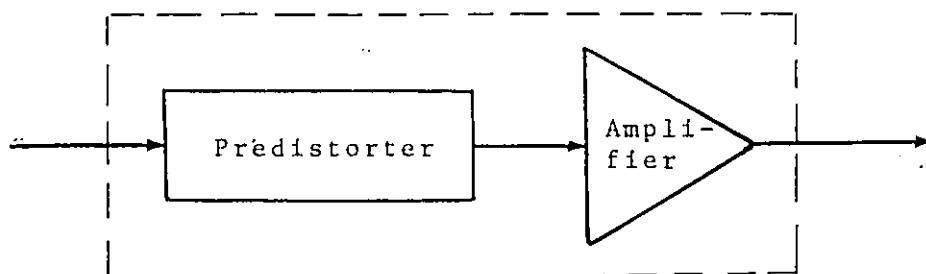


Figure 4.1. Predistortion linearization.

4.2 LINERIZATION OF THE LM-380 AM-AM CHARACTERISTIC

Here the phase rotation is considered zero. The LM-380 characteristic (Fig.2.2 (b)) is represented by the Hetrakul-Taylor model (Table 2.2) given by the equation:

$$Z(R) = 3.590262 \cdot R \cdot \exp(-7.462 R^2) \cdot I_0(7.462 \cdot R^2) \quad 4.1$$

where R is the input to the power amplifier. The reason for using this model instead of the more accurate polynomial model is explained later.

The predistorter linearizer is modeled as a $2m-1$ order polynomial:

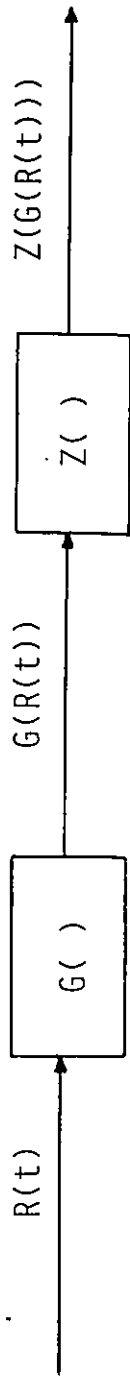
$$G(R) = \sum_{i=1}^m a_{2i-1} R^{2i-1} \quad 4.2$$

where the coefficients a_k are to be determined. In Figure 4.2 the cascade combination of the linearizer and the LM-380 amplifier is shown. We want the overall characteristic to be:

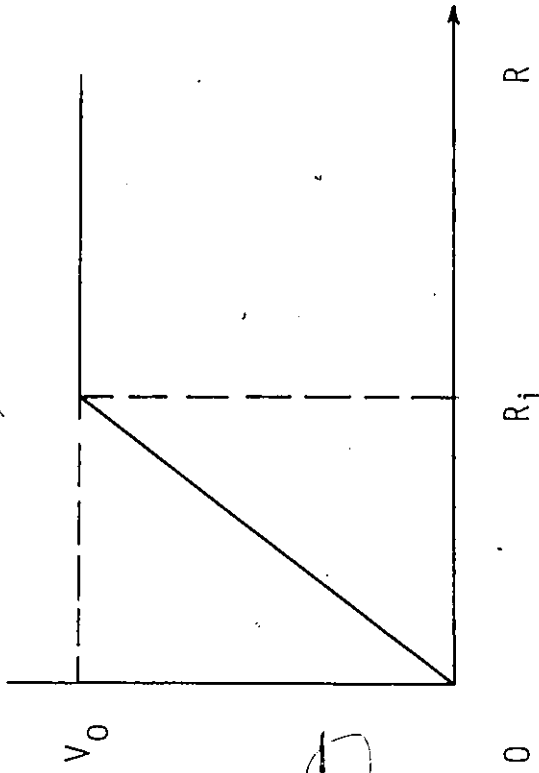
$$Z(G(R)) = \begin{cases} V_0 R/R_i & , 0 \leq |R| \leq R_i \\ V_0 & , |R| \geq R_i \end{cases} \quad 4.3$$

where V_0 is the saturation voltage and R_i the minimum voltage corresponding to the saturation of the soft limiter (Fig. 4.2). From equations 4.1, 4.2 and 4.3 we get:

$$Z(G(R)) = 3.590262 \cdot \left(\sum_{i=1}^m a_{2i-1} R^{2i-1} \right) \cdot \exp(-7.462 \cdot \left(\sum_{i=1}^m a_{2i-1} R^{2i-1} \right)^2) \cdot I_0(7.462 \cdot \left(\sum_{i=1}^m a_{2i-1} R^{2i-1} \right)^2) = \begin{cases} V_0 \cdot R/R_i & , 0 \leq |R| \leq R_i \\ V_0 & , |R| \geq R_i \end{cases} \quad 4.4$$



(a)



(b)

Figure 4.2. (a) Predistortion linearization of AM-AM nonlinearity.
 (b) Required overall characteristic.

From the equations 4.3 and 4.4, we see that in order to calculate the predistorter coefficients, the polynomial $G(R)$ must be inserted into the equation 4.1. If the polynomial representation were chosen for the $Z(R)$, the resulting polynomial $Z(G(R))$ would have terms of very high order. These terms may cause overflow or underflow in the simulation. That is the reason we chose the Hetrakul-Taylor model which has lower power terms. This model was found more accurate than the Saleh model.

Using a conventional curve fitting optimization subroutine (Appendix D) the coefficients a_k were determined for different values of m . Their values for $m=2,3$ and 4 and $R_i=0.183$, $V_0=0.6063$ are given in table 4.1.

$a_k \backslash m$	2	3	4
a_1	0.991	0.98102	0.98520
a_3	4.663	3.80665	3.78135
a_5		104.19950	101.53210
a_7			-205.13100

TABLE 4.1 . Coefficients of the LM-380 predistorter.

In Figure 4.3 the linearizer and linearized characteristics are drawn for $m=2,3$. For $m=3,4$ the characteristics are almost the same and much more linear than $m=2$. In the next chapter the case for $m=3$ is considered.



A baseband linearizer was implemented for the LM-380 amplifier. A diode wave shaping circuit was considered [19,20]. The single-tone measured characteristic of the linearizer is a piece-wise linear approximation of the simulated one and is drawn in Figure 4.4. The analytical circuit of the linearizer is given and explained in Appendix C.

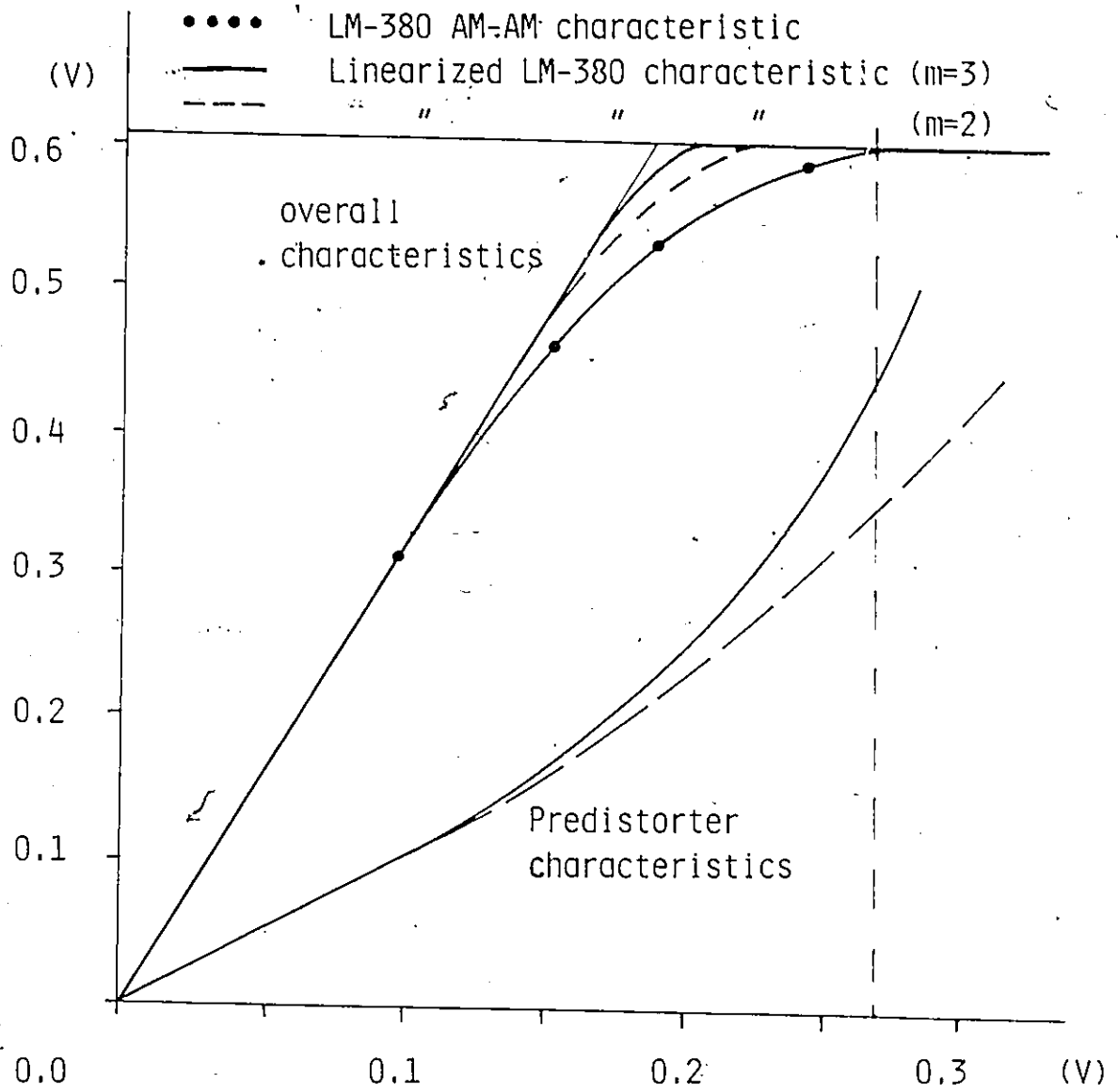


Figure 4.3. Linearization of the LM-380 AM-AM characteristic.

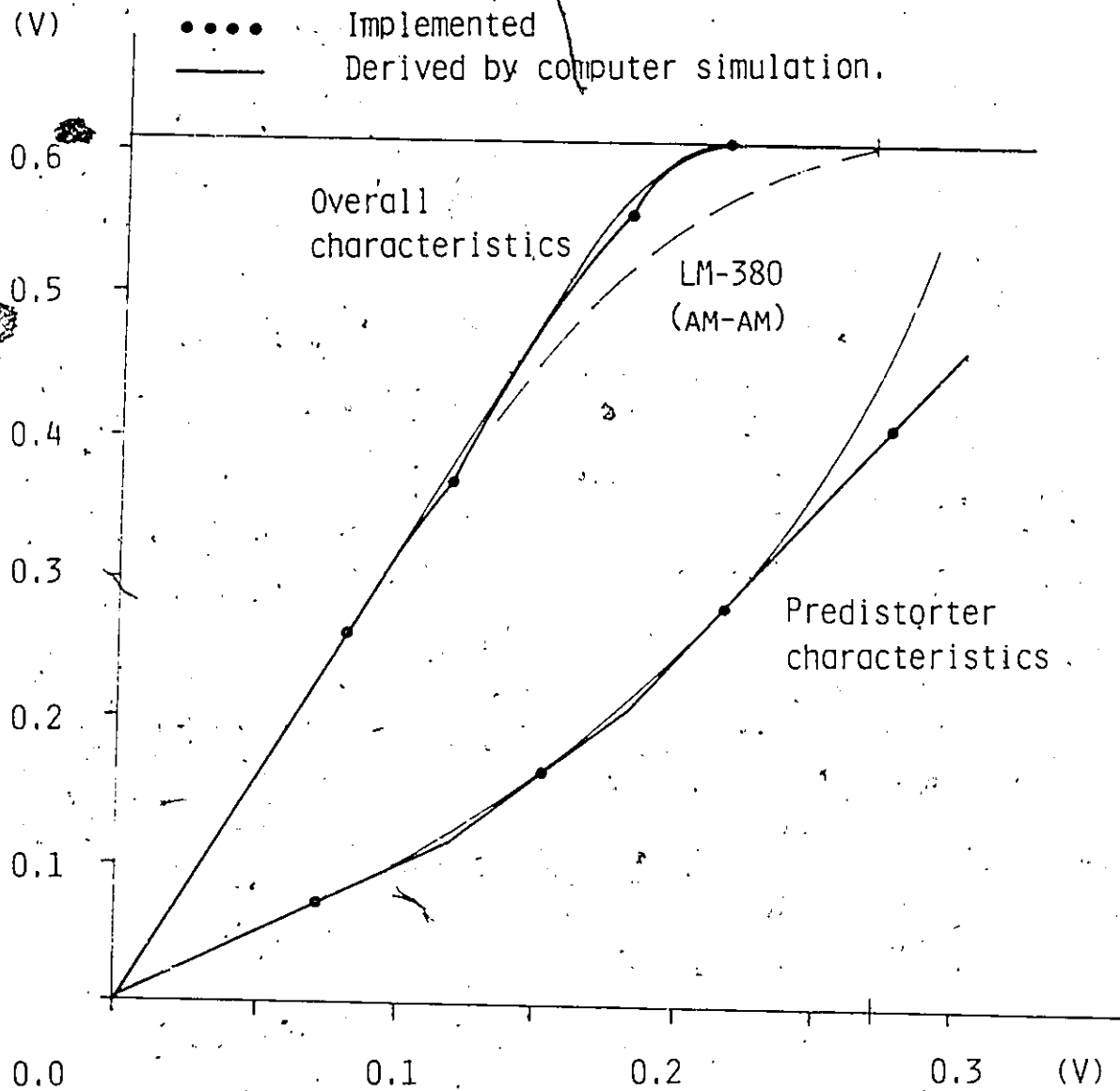


Figure 4.4 . Implemented piece-wise linear approximation of the LM-380 predistorter characteristic.

4.3 COMPENSATION OF THE LM-380 AND H-261 CHARACTERISTICS.

We want the overall predistorter-amplifier AM-AM characteristic to approach that of a soft limiter and the overall AM-PM characteristic to be zero. We use the quadrature model of the normalized LM-380 and H-261 characteristics. The corresponding inphase and quadrature envelope nonlinearities are represented as (see Tables 2.4,2.5):

$$\begin{aligned} Z_p(R) &= 1.60138 \exp(-0.325713 R^2) \cdot I_0(0.325713 \cdot R^2) \\ Z_q(R) &= 1.887482 R^3 / (1 + 1.063857 \cdot R^2)^2 \end{aligned} \quad 4.5$$

These models were chosen for the same reason explained in Section 4.2. The Hetrakul-Taylor model was found more accurate for the representation of the $Z_p(R)$, while the Saleh model was found more accurate for the representation of the $Z_q(R)$. The predistorter is modeled as a second quadrature nonlinearity having the inphase and quadrature envelope nonlinearities $G_p(R), G_q(R)$ represented by two odd order polynomials:

$$\begin{aligned} G_p(R) &= \sum_{i=1}^m a_{2i-1} R^{2i-1} \\ G_q(R) &= \sum_{i=1}^n a_{2i+1} R^{2i+1} \end{aligned} \quad 4.6$$

A block diagram of the overall predistortion model is shown in Figure 4.5. According to this we get for the overall amplitude and phase characteristics:

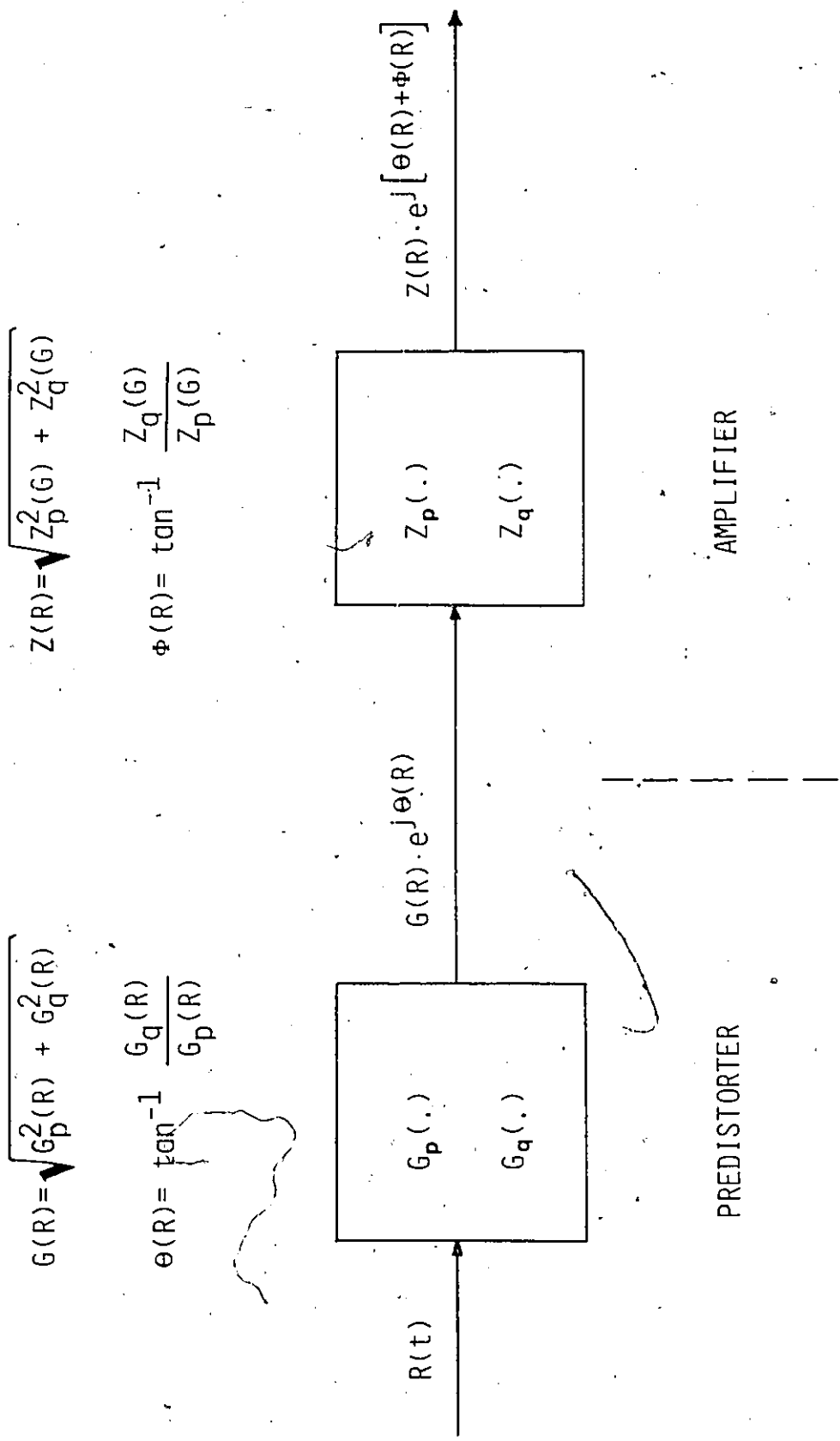


Figure 4.5. Predistortion compensation for AM-AM and AM-PM nonlinearities.

$$Z(R) = \sqrt{Z_p^2(R) + Z_q^2(R)} =$$

$$\sqrt{Z_p^2(\sqrt{G_p^2(R) + G_q^2(R)}) + Z_q^2(\sqrt{G_p^2(R) + G_q^2(R)})} =$$

$$= \begin{cases} V_0 R/R_i & 0 \leq |R| \leq R_i \\ V_0 & |R| \geq R_i \end{cases}$$

4.7

and

$$\theta(R) + \phi(G(R)) = \tan^{-1}(G_q(R)/G_p(R)) +$$

$$+ \tan^{-1}(Z_q(\sqrt{G_p^2(R) + G_q^2(R)})/Z_p(\sqrt{G_p^2(R) + G_q^2(R)})) = 0 \quad 4.8$$

where $R_i = 0.966$ and $V_0 = 1.414$. Using equations 4.5 to 4.8 and an optimization subroutine (Appendix D) the coefficients of the predistorter characteristics were computed. They are given in table 4.2.

The compensated overall AM-AM and AM-PM characteristics for the above coefficients are drawn in Figure 4.6.

A baseband implementation of a predistorter with characteristics similar to the $G_p(R), G_q(R)$ could be the one shown in Figure 4.7 [7].

The circuit is a hardware realization of the equation:

$$G(R) \exp(j\theta(R)) = G(R) \cdot \cos(\theta(R)) +$$

4.9

$$j G(R) \cdot \sin(\theta(R)) = G_p(R) + j G_q(R)$$

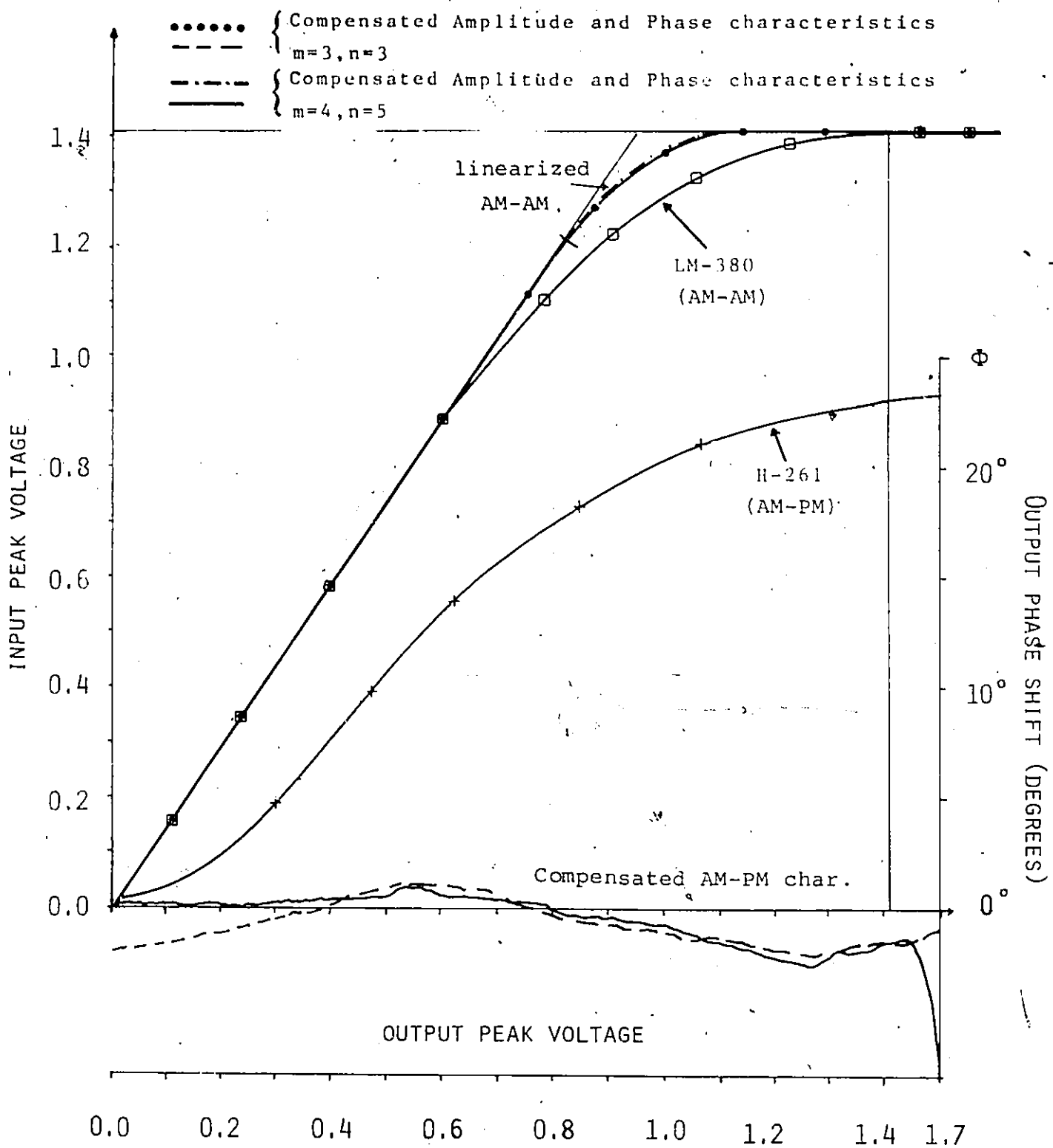


Figure 4.6. Compensation of the normalized LM-380,H-261 characteristics...

k	a_k	b_k
1	1.024364	
3	-0.215228	-0.525770
4	0.287643	0.151374
7		-0.038831
1	1.020762	
3	-0.201450	-0.879726
5	0.274770	1.138574
7	0.003371	-1.135015
9		0.522154
11		-0.089051

TABLE 4.2 . Coefficients of equations 4.6.

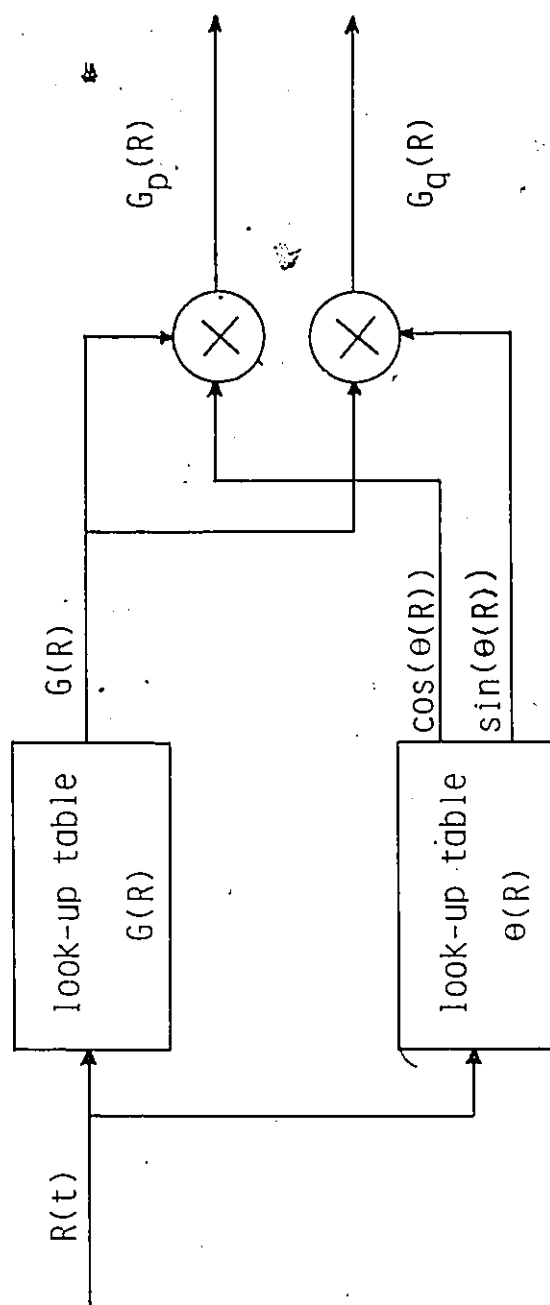


Figure 4.7. Baseband predistorter for AM-AM, AM-PM nonlinearities.

4.4 AMPLITUDE COMPENSATION FOR THE LM-380 AND H-261 CHARACTERISTICS

This time we use only amplitude predistortion for both the LM-380 and H-261 nonlinearities. Our objective is the overall amplitude characteristic to approach that of a soft limiter and the overall phase characteristic to be better than that of the H-261. Since the H-261 characteristic is envelope dependent, the smaller the gain of the predistorter the lower the overall phase response will be. We chose gain equal to one ($V_0 = R_i = 1.414$). The predistorter is modeled again as an odd order polynomial:

$$G(R) = \sum_{i=1}^m a_{2i-1} R^{2i-1} \quad 4.10$$

The block diagram of the predistorter-amplifier is drawn in Figure 4.8. According to this we get for the overall AM-AM and AM-PM characteristics.

$$Z(R) = \sqrt{Z_p^2(G(R)) + Z_q^2(G(R))} = \begin{cases} R & , \quad 0 \leq |R| \leq 1.414 \\ 1.414 & , \quad |R| \geq 1.414 \end{cases} \quad 4.11$$

$$\Phi(G(R)) = \tan^{-1} \left[Z_q(G(R)) / Z_p(G(R)) \right] \quad 4.12$$

Using equations 4.5, 4.10, 4.11 with an optimization subroutine the coefficients of the predistorter characteristic were computed (Table 4.3). The procedure is that of section 4.3 with $G_q(R) = 0$.

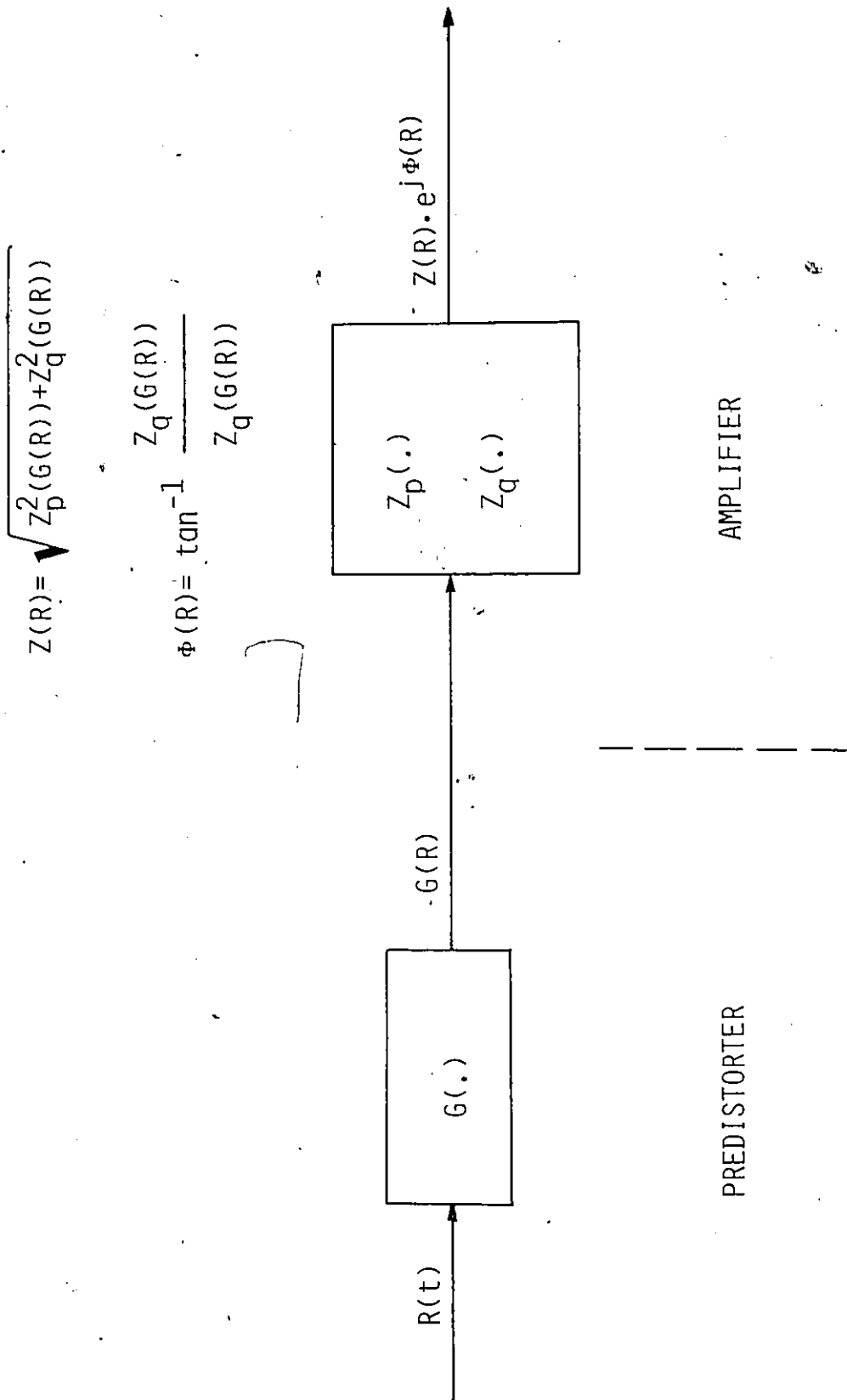


Figure 4.8. AM-AM predistortion compensation for AM-AM, AM-PM nonlinearities.

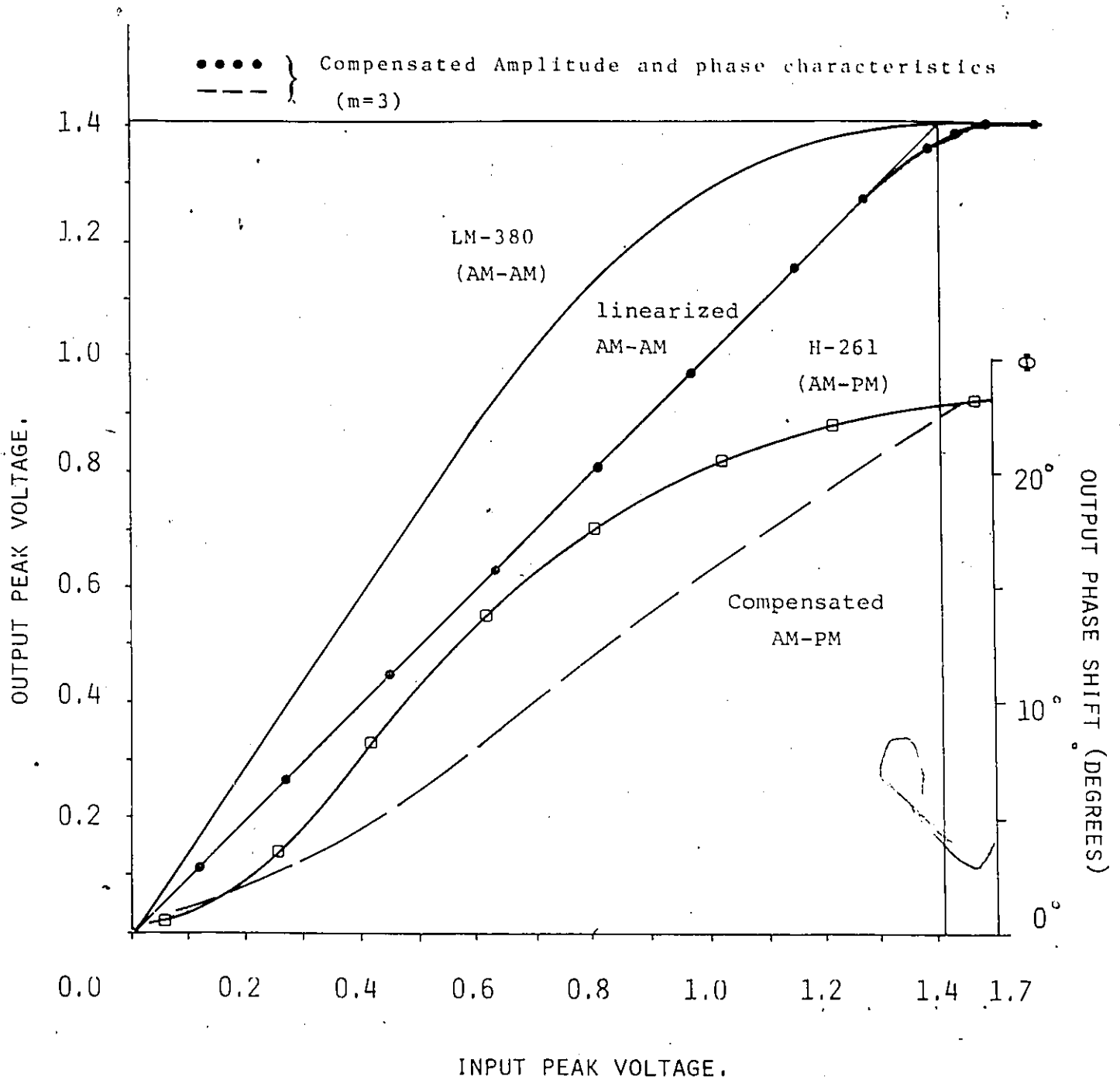


Figure 4.9. AM-AM compensation of the LM-380, H-261 characteristics.

k	a_k
1	0.693974
3	-0.065900
5	0.067550

TABLE 4.3. Coefficients of equation 4.8 .

The corresponding overall AM-AM and AM-PM characteristics are drawn in Figure 4.9. We note that a small improvement in the AM-PM response is also accomplished.

Chapter V

LINEARIZATION RESULTS.-IMPROVEMENTS IN THE ERROR PERFORMANCE BY ADJUSTING THE DECODING THRESHOLDS.

The performance of the linearized systems in combination with threshold adjustment is investigated. The obtained results are compared with those of the conventional system.

5.1 PERFORMANCE WITH THE LINEARIZED LM-380 CHARACTERISTIC AND THRESHOLD ADJUSTMENT.

The error performance of a 4-PAM scheme with the linearized LM-380 characteristic and with or without threshold adjustment is shown in Figures 5.1 to 5.4. For the linearization results the equation 4.4 with the coefficients of Table 4.1 ($m=3$) were used. For the threshold adjustment an optimization procedure was used in order to set the decoding thresholds at the middle of each eye. This is done because after the suppression of the higher levels due to the nonlinearity effects (see section 3.3), the conventional decoding thresholds are not optimum any more (Figure 5.4).

For the results, the computer simulation and measurement set-ups described in Sections 3.1 and 3.2 were used. In the simulation model the LM-380 characteristic was replaced by the linearized LM-380 characteristic. In the measurements the LM-380 amplifier was replaced by the cascade combination of the implemented linearizer (see section 4.2) and the LM-380 amplifier.

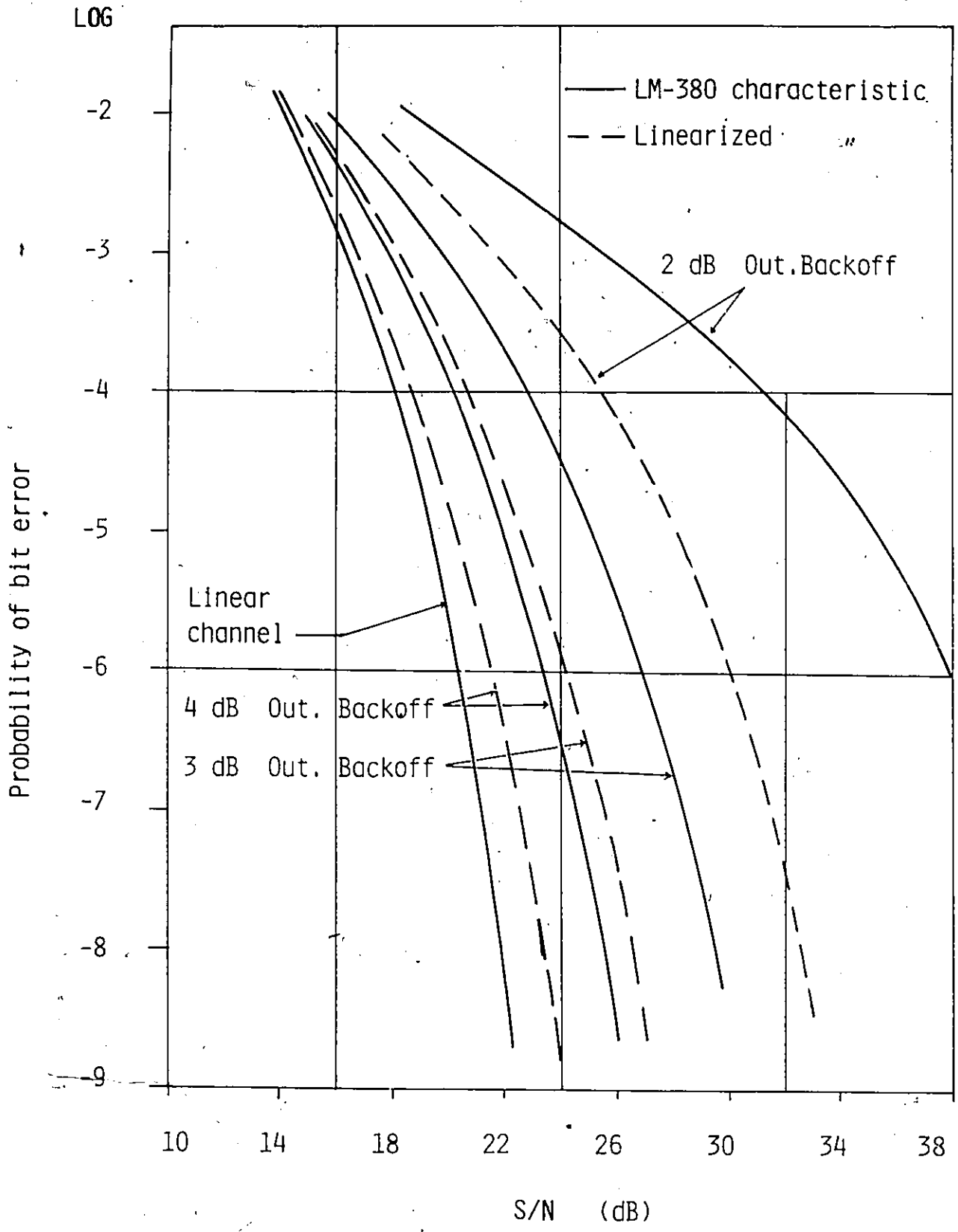


Figure 5.1 . Improvement in the error performance of a 4-PAM signal obtained by linearizing the LM-380 characteristic. Computer simulation results with $\alpha=0.2$ Nyquist filter.

Once more we mention that the S/N ratio was measured at the output of the receiver filter, by changing the noise power while the signal power was kept constant. The procedure was repeated for various operating points (Output Backoff).

The following remarks can be made for the obtained results.

i) The total improvement obtained in the error performance using the above techniques is significant. The best operating point (where the sum of the S/N degradation and Out.Backoff is minimum) is moved about 2 dB closer to saturation.

ii) Considering the remarks of section 3.3.2 we conclude that the measured results of Figure 5.2 when only threshold adjustment is considered, are satisfactory. For the measured results when both linearization and threshold adjustment are considered, we note an additional degradation of 0.3 dB (for $P(e)=10^{-6}$) which is due to the piece-wise linear nature and Hardware imperfections of the implemented predistorter.

The improvement obtained by linearizing the LM-380 characteristic, is due to the reduction of the nonlinear distortion. This means that the envelope dependent suppression of the signal levels and the generated ISI (see Section 3.3), become less significant. The vertical opening of the signal eyes increases, resulting in better system performance. In Figure 5.5 measured eye diagrams of a 4-PAM signal before and after linearization are given. We note that the outer eyes of the signal have opened slightly and the ISI has been reduced. On the other hand, by

adjusting the decoding thresholds we increase the distances of the received signal levels from their corresponding lower thresholds (see Section 3.1 and Figure 5.4). This results in an additional improvement in the error performance.

The spectral regrowth reduction accomplished by linearizing the LM-380 characteristic, is shown clearly in Figure 5.6. It is due to the reduction of the signal envelope fluctuation. The reduction of the spectral regrowth is important since it also reduces the adjacent channel interference.

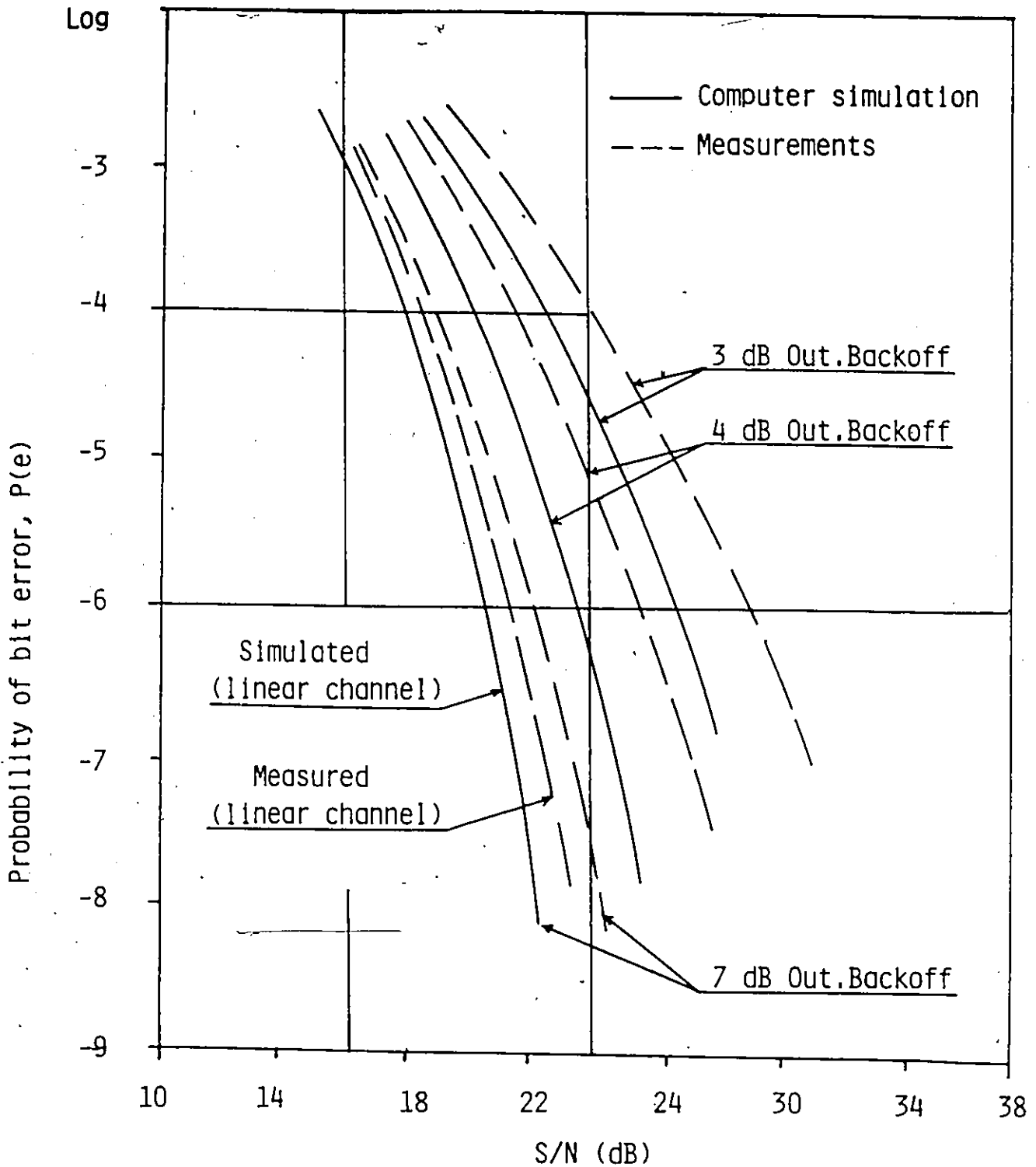


FIGURE 5.2 Performance of a 4-PAM signal distorted by the LM-380 amplitude characteristic. The signal rate is 413.3 kb/s. Filters with $\alpha=0.2$ are used. The S/N ratio is defined in the Nyquist bandwidth at the output of the receiver LPF.

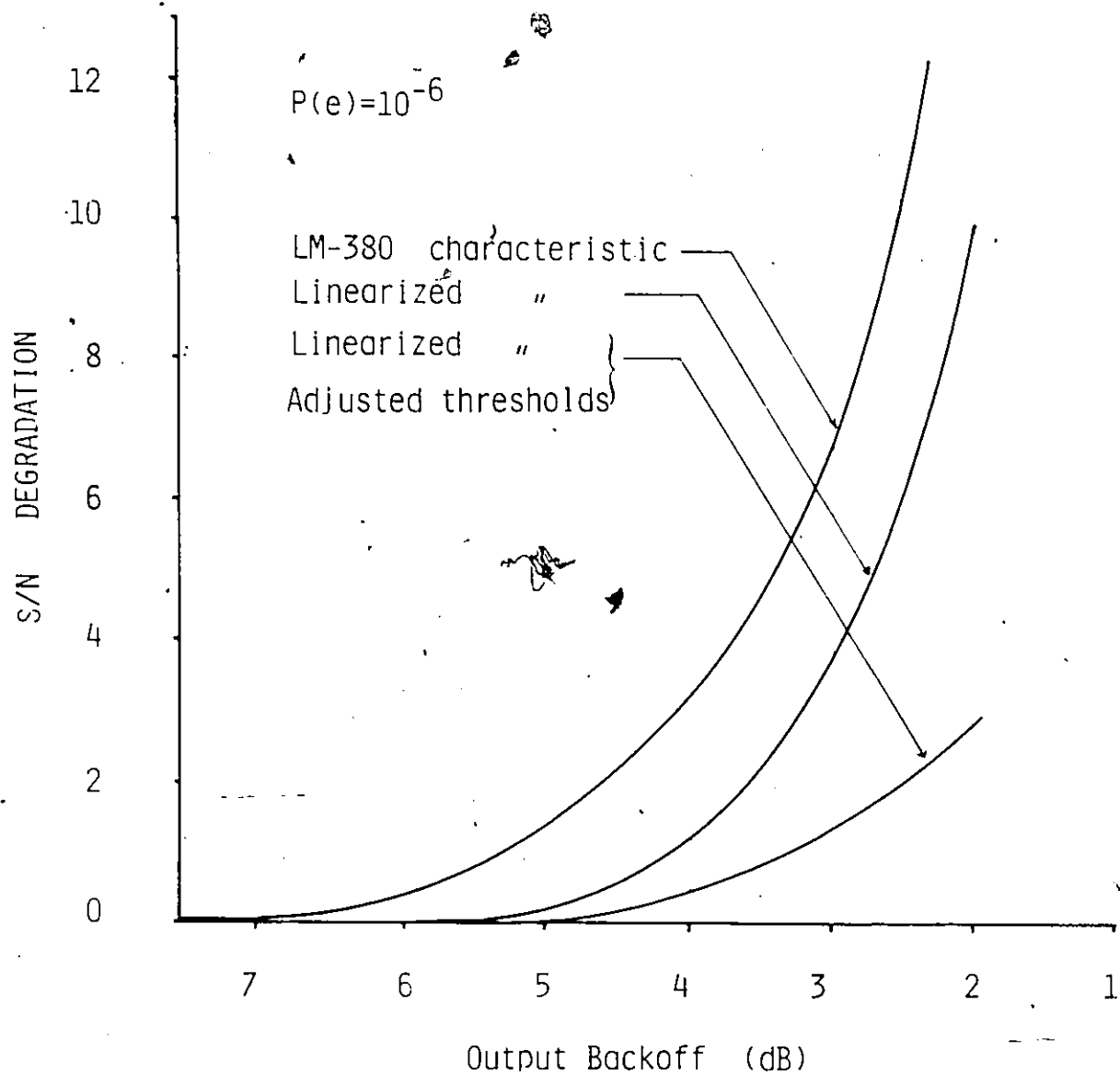


Figure 5.3 . Improvements in the $\overline{S/N}$ ratio degradation of a 4-PAM signal, obtained by linearizing the LM-380 characteristic and by adjusting the decoding thresholds.

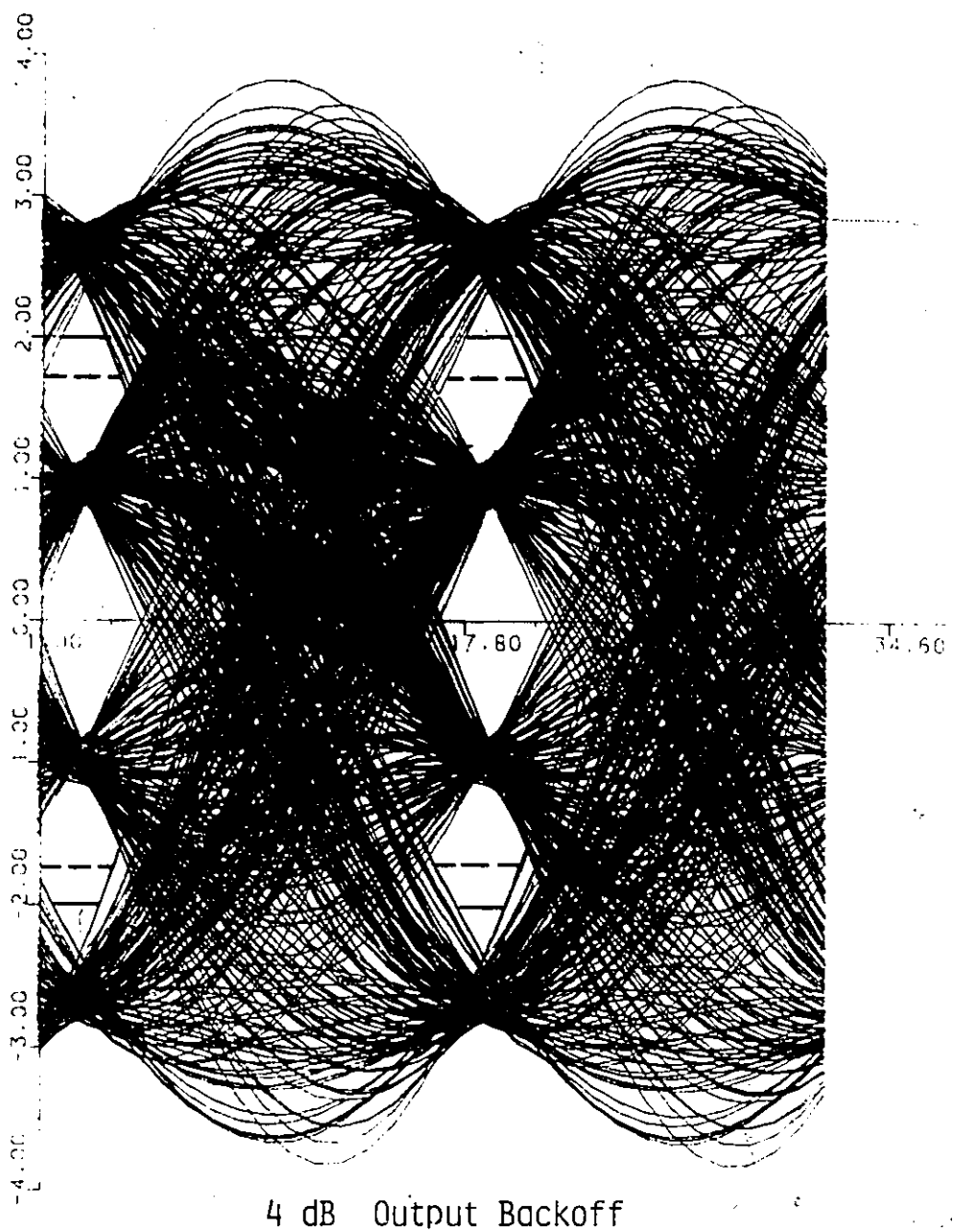
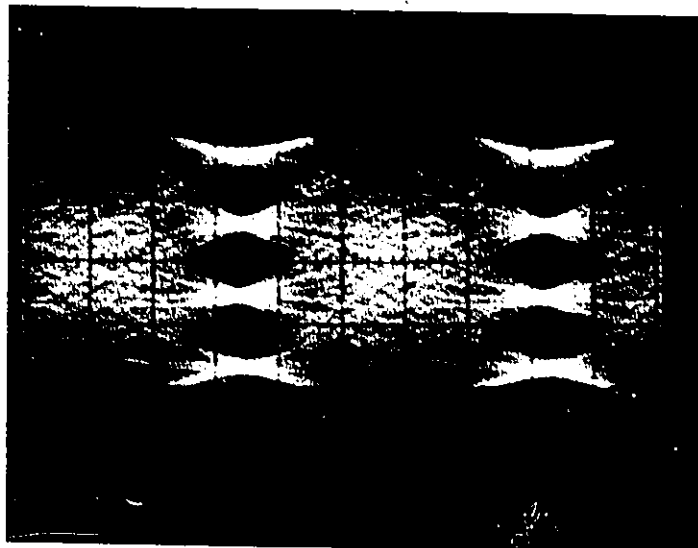


Figure 5.4. Eye diagram of a 4-PAM signal with the LM-380 amplifier. Computer simulation results with $\alpha=0.2$ Nyquist filters. The initial transmitted levels were $\pm 1, \pm 3$. The gain of the amplifier has been removed.



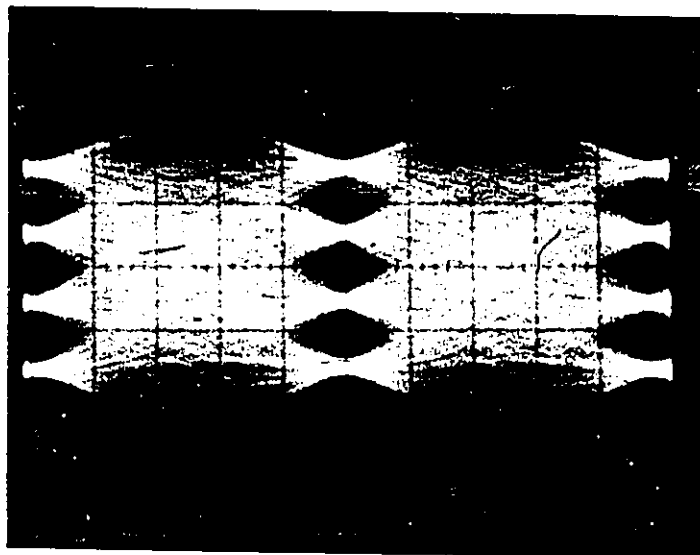
Horiz. 1 μ s/div.

Vert. 200 mV/div.

$f_b = 413.3$ kb/sec.

4 dB Out.Backoff.

Fig. 5.5(a). Measured eye diagram of a 4-PAM signal with the LM-380 amplifier. Filters with $\alpha=0.2$ were used.



Horiz. 1 μ s/div.

Vert. 200 mV/div.

$f_b = 413.3$ kb/sec.

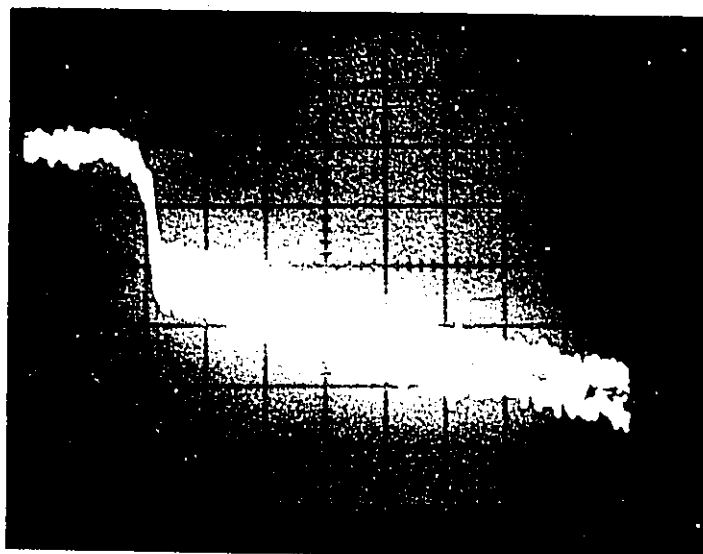
4 dB Out.Backoff.

Fig. 5.5(b). Measured eye diagram of a 4-PAM signal with the linearized LM-380 amplifier. Filters with $\alpha=0.2$ were used.



Vert. 10 dB/div.
Horiz. 50 KHz/div.
Up.ref.lev. 0 dBm.

4 dB Out.Backoff



Vert. 10 dB/div.
Horiz. 50 KHz/div.
Up.ref.lev. 0 dBm.

2 dB Out.Backoff

Figure 5.6. Reduction of the spectral regrowth of a 4-PAM signal by linearizing the LM-380 AM-AM characteristic. The signal rate is 413.3 Kb/s. Nyquist filter with $\alpha=0.2$ is used.

5.2 PERFORMANCE WITH THE COMPENSATED LM-380 , H-261 CHARACTERISTICS AND THRESHOLD ADJUSTMENT.

5.2.1 Error performance

The error performance of various PAM schemes with the LM-380, H-261 and the compensated LM-380, H-261 characteristics, was computed using equations 4.7. The coefficients of Table 4.2. with $m=3$ and $n=3$ were used. The error performance of the various PAM schemes when both threshold adjustment and linearization are considered was also computed. The obtained results which are drawn in Figures 5.7 and 5.8 show that:

i) The total improvement obtained in the error performance is very significant. The best operating point (where the sum of S/N ratio and Output Backoff is minimum) is moved closer to saturation, 3 dB for a 4-PAM scheme and more than 5 dB for a 32 PAM scheme. This increases the power utilization efficiency of the system. The reasons which led to the performance improvement were explained in the previous Section.

ii) The improvement obtained by linearization (compensation) is more significant for the higher schemes, while the improvement obtained by adjusting the decoding thresholds is more significant for the lower schemes. The reasons are the following. As we mentioned before, the nonlinear distortions affect the opening of the signal eyes. The size of the eyes of the higher schemes are sufficiently smaller than that of the lower schemes (assuming the same transmitted power for all schemes), which makes them more sensitive to the nonlinear distortions. Thus it should be expected that the reduction of the distortion obtained

by linearization will affect more the higher schemes. On the other hand, the threshold adjustment can be more significant in large size eyes and thus it will affect more the lower schemes.

iii) For each scheme the improvement obtained by adjusting the thresholds becomes negligible over a particular operating point. This happens because the outer eyes of the signal are almost closed due to the nonlinear effects and the system has almost failed.

5.2:2

Spectral regrowth reduction

The spectral regrowth reduction due to the compensation of the LM-380 and H-261 characteristics is shown in Figures 5.9 (a) and (b), where the inphase and quadrature spectrum for a 4-PAM scheme are drawn. It is due to the reduction of the signal envelope fluctuations. We notice that the improvement obtained in the spectrum of the inphase component for operation at 7 dB Out. Backoff is about 8 dB. The improvement obtained in the spectrum of the quadrature component is even more significant. This is expected, since due to the low phase rotations of the compensated system the quadrature component is not significant. In the compensated system the AM-AM conversion has the major contribution to the spectral regrowth.

Due to the spectral regrowth reduction the adjacent and cochannel channel interference are also reduced.

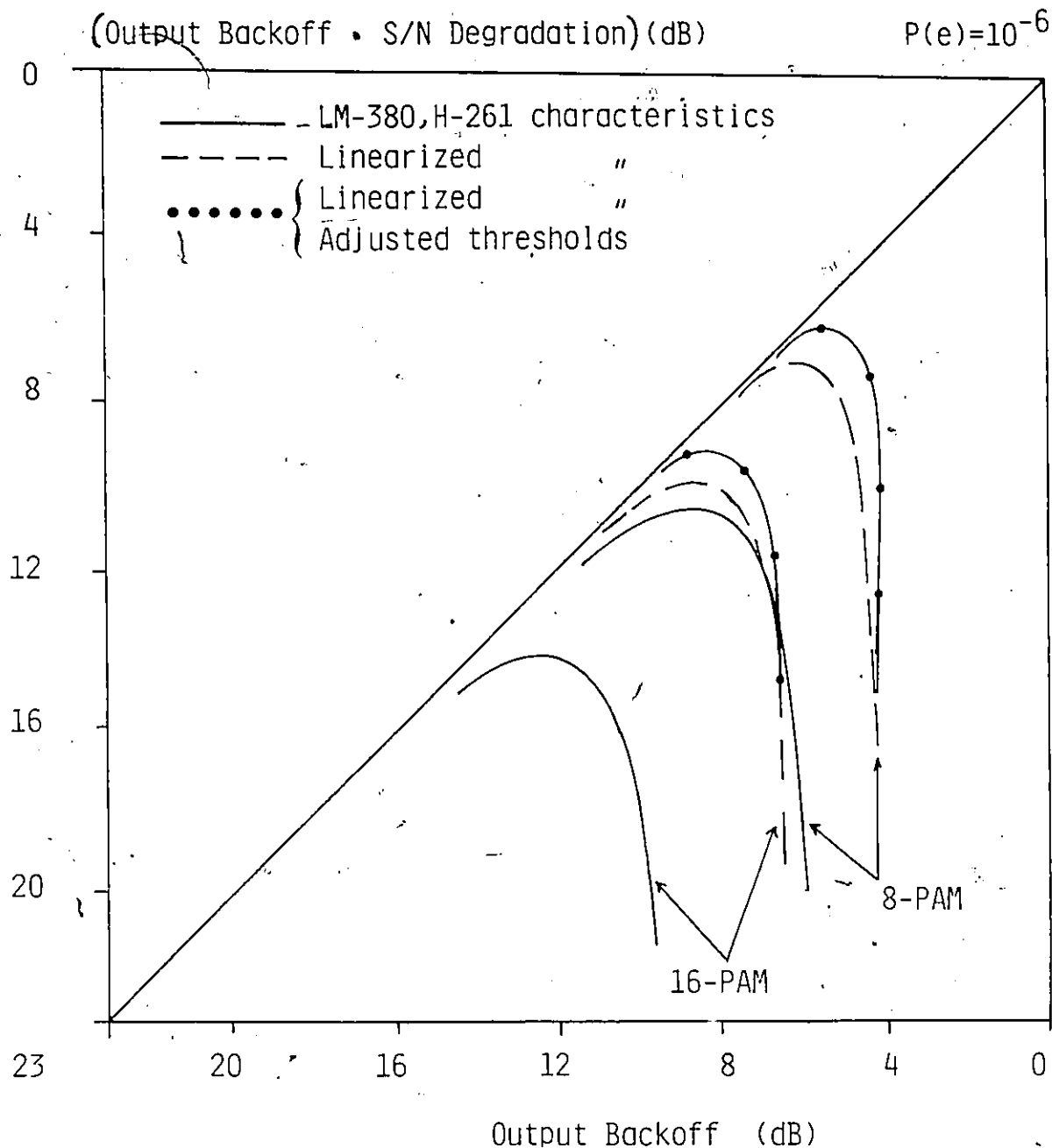


Figure 5.7. Improvements in the performance of 8 and 16 PAM signals obtained by linearizing the LM-380, H-261 characteristics and by adjusting the decoding thresholds. Computer simulation results with $\alpha=0.2$ Nyquist filter. Both signals have the same symbol rate.

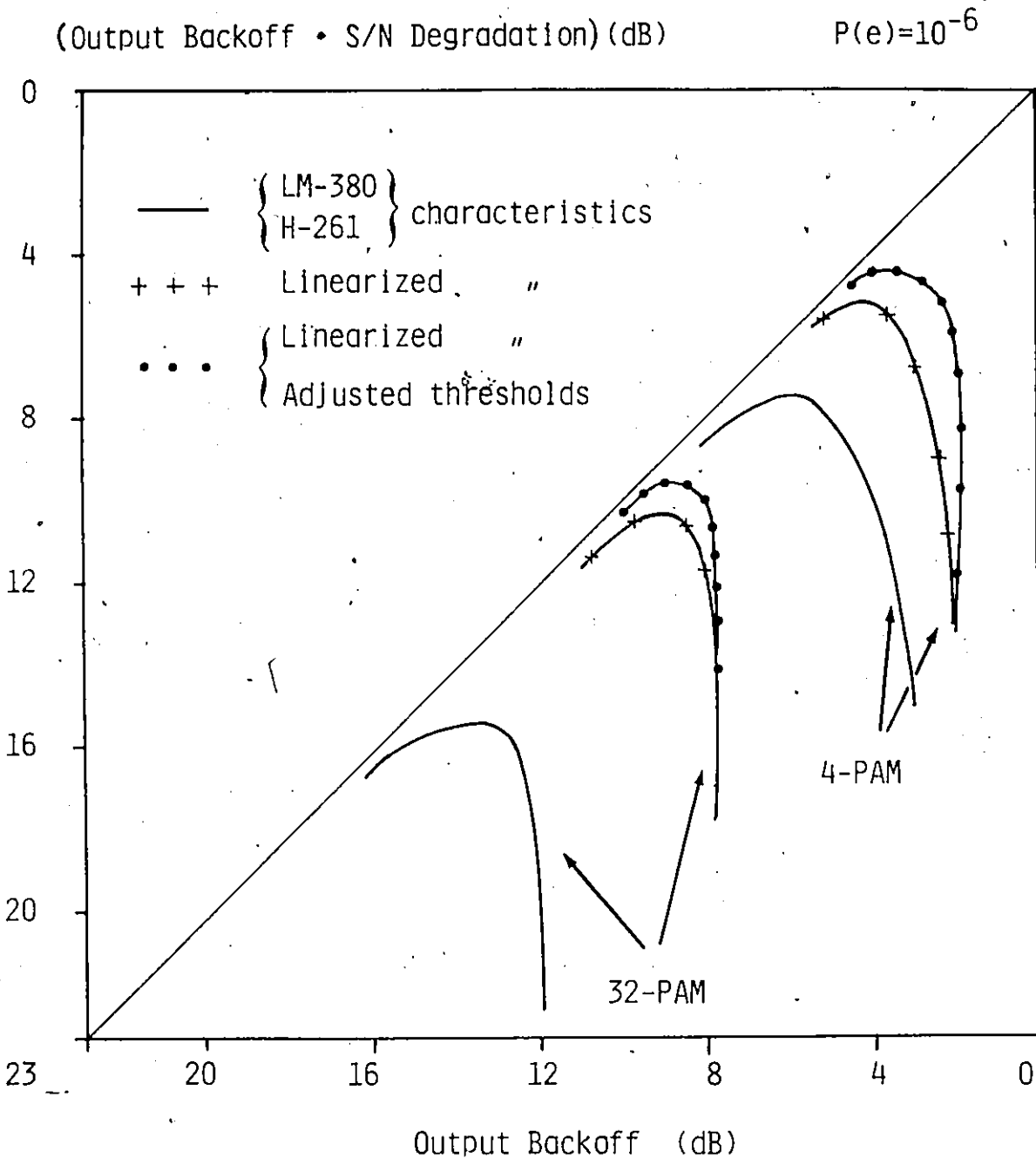
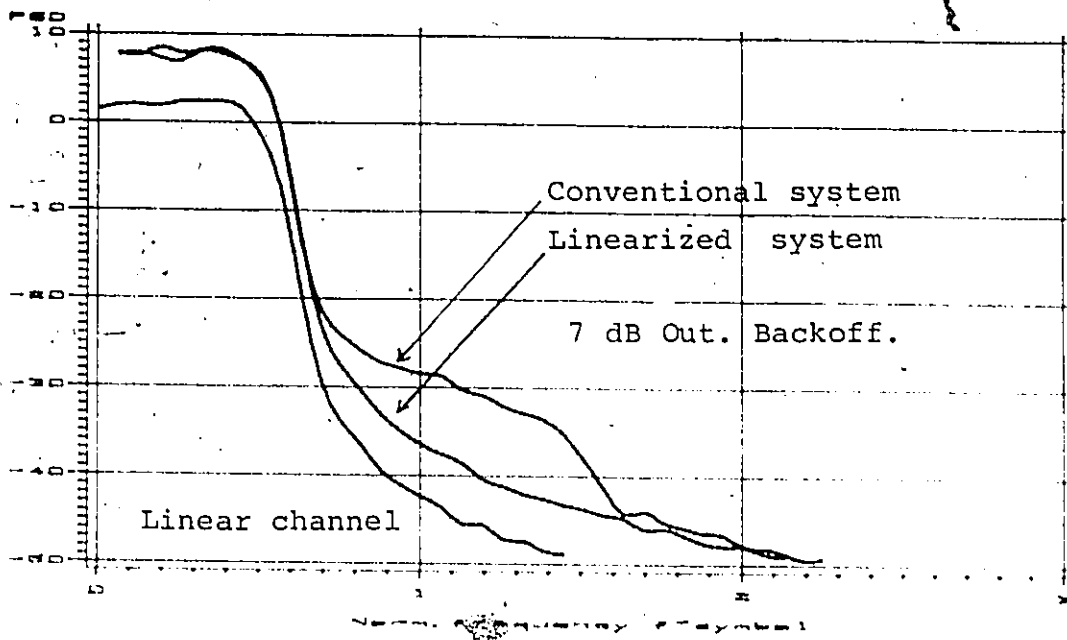
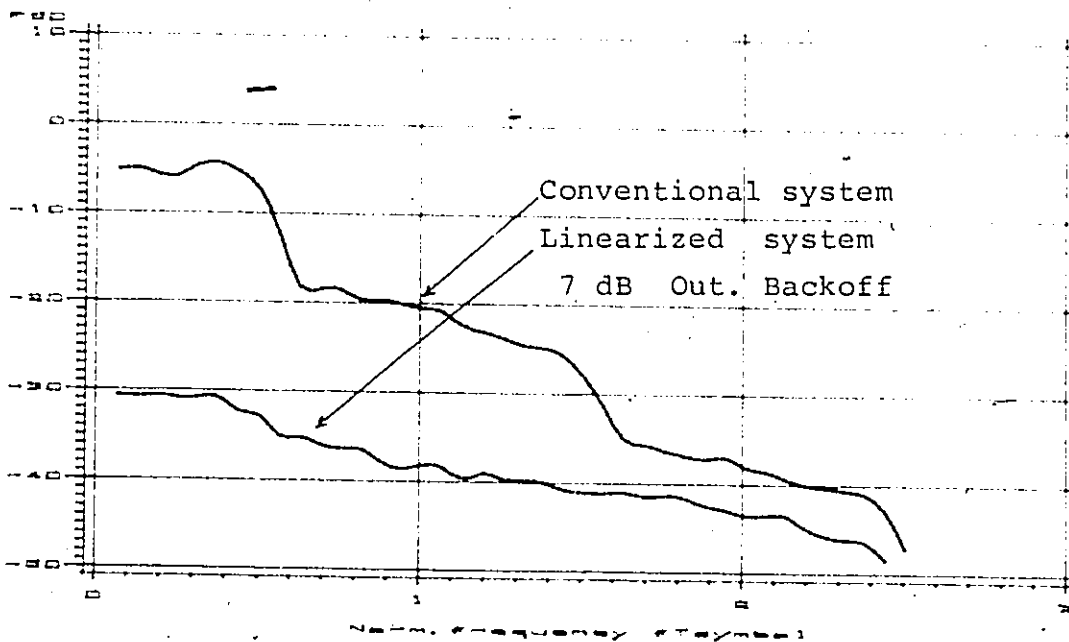


Figure 5.8. Improvements in the performance of 4 and 32 PAM signals obtained by linearizing the LM-380, H-261 characteristics and by adjusting the decoding thresholds. Computer simulation results with $\alpha=0.2$ Nyquist filter. Both signals have the same symbol rate.



(a) Inphase component spectrum.



(b) Quadrature component spectrum.

Figure 5.9. Reduction in the spectral regrowth of a 4-PAM signal obtained by linearizing the LM-380 and H-261 characteristics. Computer simulation results with $Q=0.2$ Nyquist filters.

5.3 PERFORMANCE WHEN ONLY AMPLITUDE OR PHASE COMPENSATION FOR AM-AM AND AM-PM NONLINEARITIES IS CONSIDERED.

Following the analysis of section 4.1.4 we computed the improvement in the S/N degradation, when only Amplitude linearization or Phase compensation is considered for the combined AM-AM and AM-PM effect. From the results drawn in Figure 5.10 we conclude that:

i) The improvement obtained when only amplitude linearization is considered is not significant compared to the improvement obtained when both amplitude and phase linearization are employed.

ii) The improvement obtained when only phase compensation is considered is more significant than the amplitude linearization. However, generally this depends on the nature of the AM-AM and AM-PM characteristics.

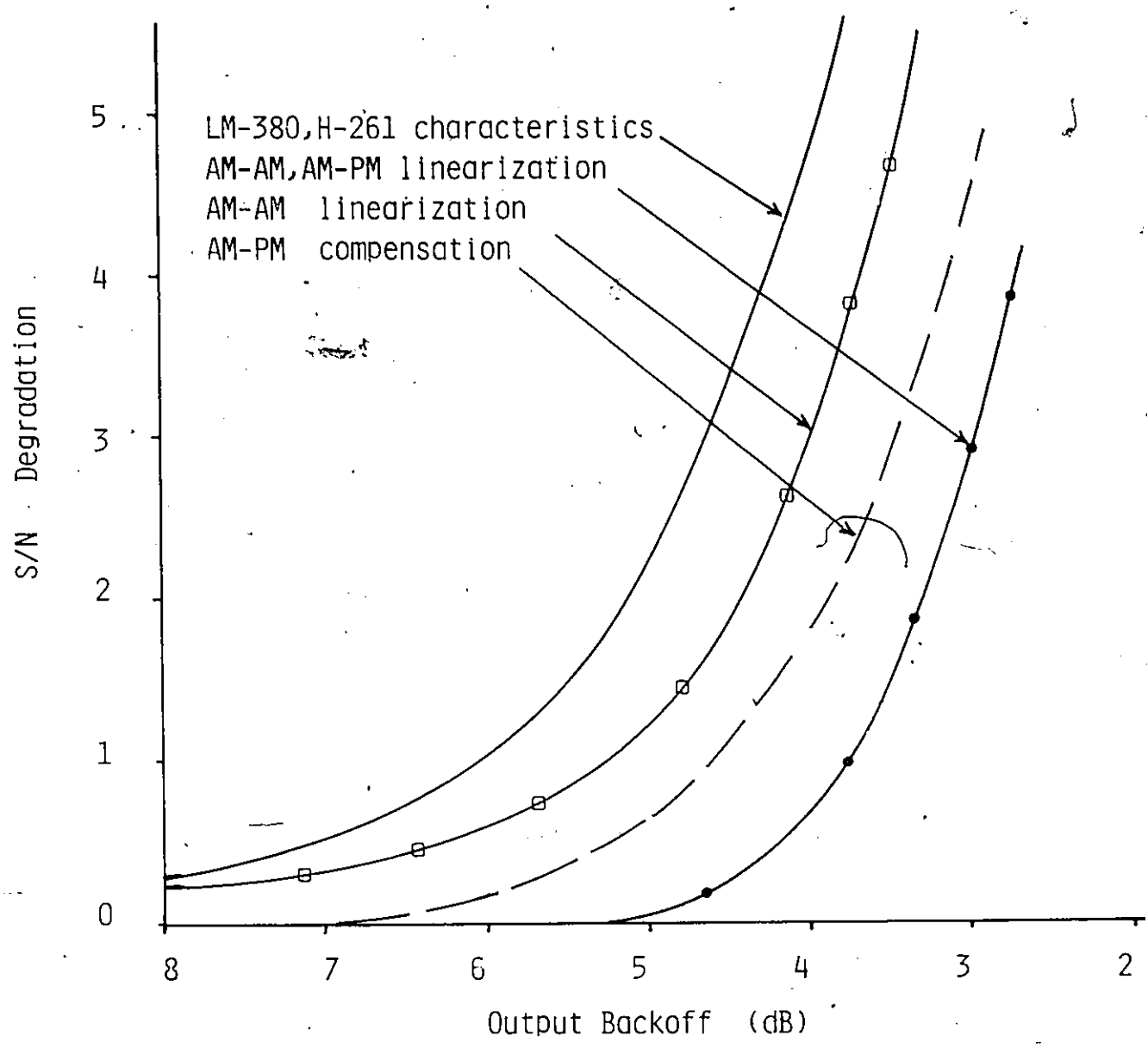


Figure 5.10. Improvements in the S/N degradation of a 4-PAM signal obtained by linearizing (compensated) the LM-380 and H-261 characteristics. Computer simulation results with $\alpha=0.2$ Nyquist filter.

Chapter VI

CONCLUSION

In this chapter the most important results of our study are summarized.

The effects of amplitude and phase nonlinearities on multilevel PAM signals were investigated. Specific AM-AM and AM-PM amplifier characteristics were used. The conclusions that can be made by analyzing the obtained simulation and experimental results are the following.

i) The degradation in the system performance, is dependent on the nature of the channel nonlinearities, the number of the signal levels and the transmit filter shape. The sensitivity of the signal to the nonlinearities increases rapidly with the number of levels. The degradation increases significantly, when the operation point is changed from the linear region of the amplifier characteristic towards saturation.

ii) The interaction of envelope fluctuations due to filtering, with the nonlinear distortions caused by the power amplifiers, give rise to spectral regrowth effects which cause adjacent and cochannel channel interference.

iii) It is found that for the higher schemes, the major cause of performance degradation is due to the AM-PM conversion. However, generally this depends on the nature of the AM-AM and AM-PM characteristics.

iv) The means to limit signal distortions, are either to operate the power amplifiers at average power levels which are significantly below the output saturation power, or to predistort the signal before amplification so as to make the overall system more linear. Predistortion linearization increases the power utilization efficiency and reduces the spectral regrowth. The improvements obtained are very significant especially for the higher schemes.

v) Significant improvement in the error performance was obtained by adjusting the conventional decoding thresholds. The improvement is more significant for the lower schemes.

REFERENCES

1. A.M.SALEH, "Frequency independent and Frequency dependent Nonlinear Models of TWT Amplifiers." IEEE Trans. on Commun., November 1981.
2. M.BORGNE. "Comparison of high level modulation schemes for high capacity Digital radio systems." IEEE Trans. on commun., Vol.COM-33, no.5, May 1985.
3. P.HETRACUL, D.P.TAYLOR, "Compensators for Bandpass Nonlinearities in Satellite communications". IEEE Trans. on Aerospace and Electronic systems, Vol AES-12, no.4, July 1976.
4. D.R.GREEN. "Characterization and compensation of nonlinearities in microwave transmitters. Globecom 1982.
5. A.R.KAYE, D.A.GEORGE, M.J.ERIC. "Analysis and compensation of Bandpass Nonlinearities for communications." IEEE Trans. on comm. p. 965-972, Oct. 1971.
6. H.GIRARD, K.FEHER. "A new Baseband Linearizer for more Efficient Utilization of Earth Station Amplifiers used for QPSK transmission. IEEE Journal on select.areas in commun., VOL.SAC-1, No.1, August 1983.
7. G.SATOH, T.MIZUNO. "Impact of a new TWTA Linearizer Upon QPSK/TDMA Transmission performance" IEEE Journal on sel.ar.on commun.Vol. SAC-1, no.1, Jan. 1983.
8. X.T.VUONG, H.J.MOODY. "Realization of Predistortion compensators of memoryless Nonlinear Devices." Globecom 1980.
9. M.J. ERIC. "Intermodulation analysis of Nonlinear Devices for multiple carrier inputs." Commun. Research Center. Report no.1234, Nov. 1972.
10. K.FEHER. "Digital Microwave Applications" Prentice Hall, Englewood Cliffs, N.J, 1981.
11. K.FEHER. "Digital Communication-Satellite/Earth Station Engineering." Prentice Hall, N.J., 1983.
12. X.T.VUONG, A.F.GUIBORD. "Modeling of Nonlinear Elements with Memory." Proc. of the IEEE-SCC '83. Ottawa, pp.5.6.1-5.6.4 .

13. K.SREENATH."A study on the influence of channel nonlinearities on digital radio systems."Candidacy paper submitted to the Dpt.of Electr. Eng.,Univ. of Ottawa,December 1985.
14. A.L.BERMAN,C.H.MAHLE."Nonlinear phase shift in Travelling Wave Tubes as applied to multiple access communication Satellites."IEEE Trans. on Commun.,Vol.COM-18,pp.37-43,February 1970.
15. H.YAYAMOTO."Advanced 16-QAM techniques for digital microwave radio" IEEE Trans. on Commun.,COM-19,pp.36-45,1981.
16. S.BENEDELTO,E.BIGLIER,R.BAFFARA."Performance of Multilevel Baseband Digital systems in a nonlinear environment" IEEE Trans. on commun. pp.1166-1174,Oct.1976.
17. D.BAINS,H.BALSHEM."GaAs FET Power amplifier for 64-QAM Digital Radio System",Microwave Journal,pp.101-109,October 1985.
18. I.SASASE,K.T.WU,H.FEHER."Comparison of improved efficiency 225-QPRS and 256-QAM in distorted channels."Proc.of the IEEE-ICC-85,pp.15.3.1-15.3.5, June 1985.
19. L.STRAUSS."Wave Generation and Shaping."Mc Graw Hill,1960.Chapter 2.
20. R.G.IRVINE."Operational Amplifier-characteristics and applications." Prentice Hall,Englewood Cliffs,NJ 1981.
21. WOZENCRAFT J.M and I.M.Jacobs."Principles of Communications Engineering." Wiley,New York,1965.
22. J.PROAKIS."Digital Communications",McGraw-Hill 1983

Appendix A

IMPLEMENTATION AND PERFORMANCE EVALUATION OF A 4-PAM SYSTEM

A.1 DESCRIPTION OF THE HARDWARE IMPLEMENTATION.

A photograph of the implemented 4-PAM encoder-decoder circuit is shown in Figure A.1. We explain the system operation in the following paragraphs.

A.1.1 Description of the Encoder circuit.

The following description refers to circuit diagram of the 4-PAM encoder drawn in Figure A.2. The symbol rate clock (clock-2), is derived through 3B by dividing the bit rate clock (clock-1) by two. The incoming binary data stream consisting of 1 and 0 which are represented by 5V and 0V respectively, is serial to parallel converted by 2A and 4B. The D/A converter (3A) converts the input parallel binary signals (Q1 and Q2) to a 4 level (i.e. 0,1,2,3) waveform according to Table A.1.

Q1	Q2	A
1	1	3
1	0	2
0	1	1
0	0	0

Table A.1. Encoding table with reference to Figure A.2.

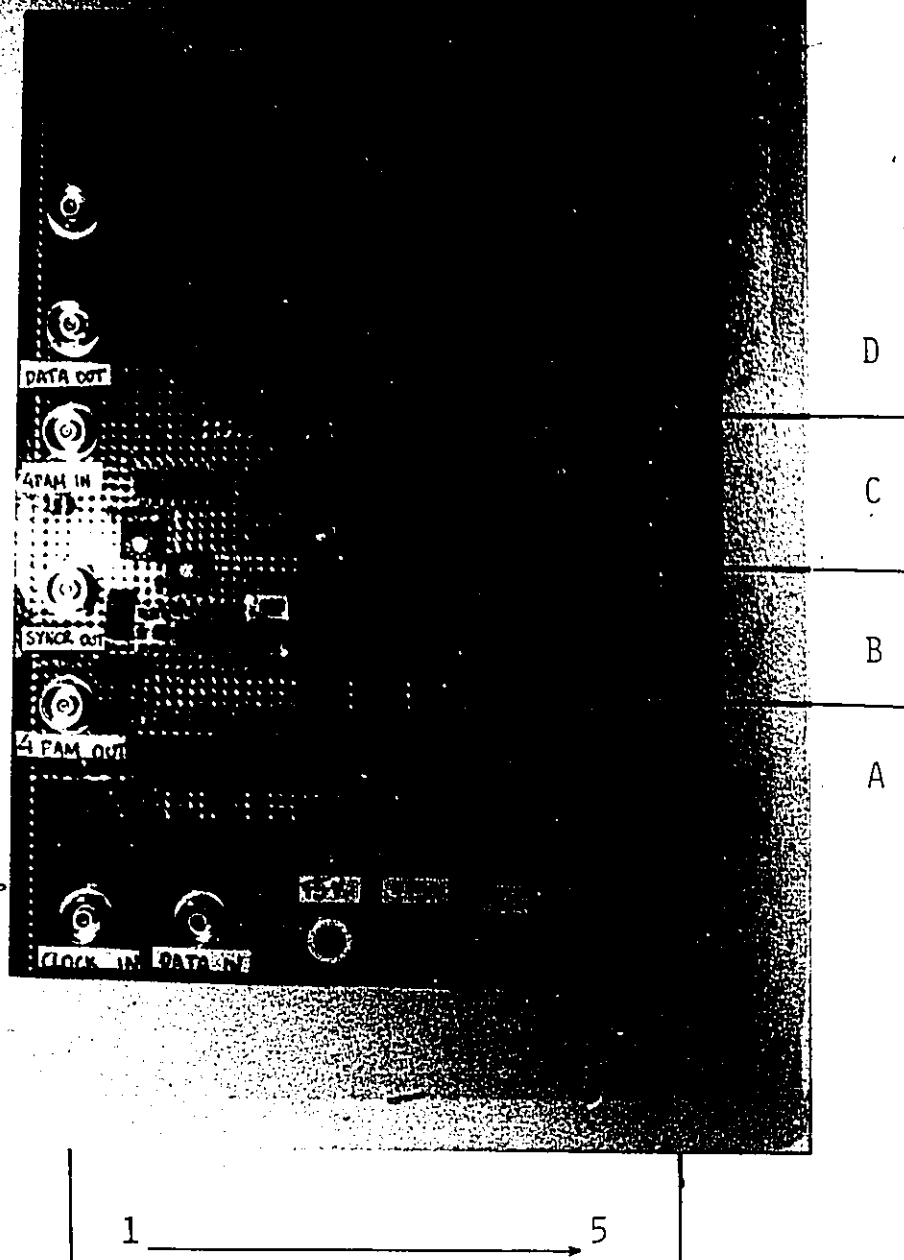


Figure A.1. Photograph of the implemented 4-PAM encoder-decoder.

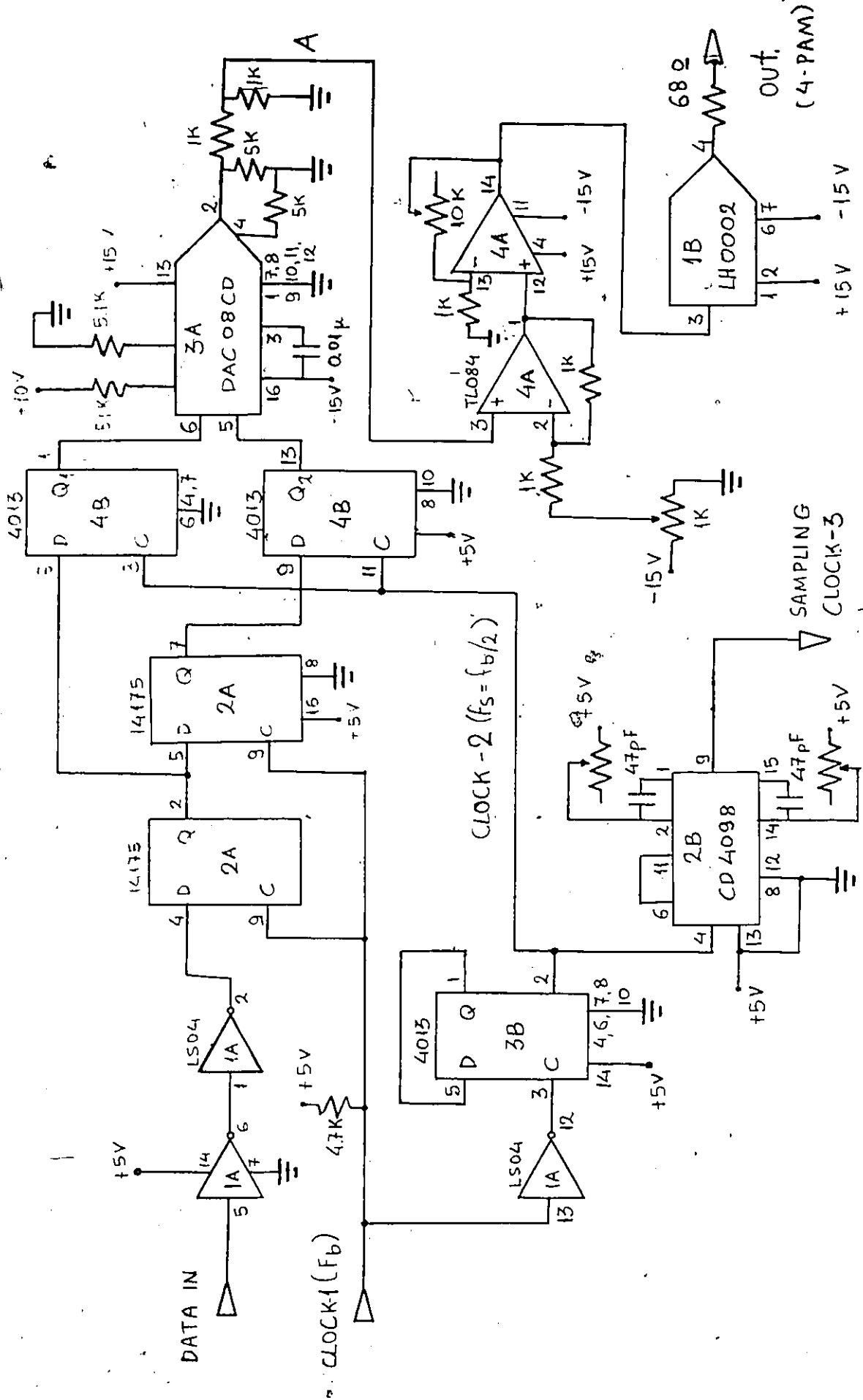


FIGURE A.2. Implemented 4-PAM Encoder.

A dc balancing adjustment and level magnitude control is provided by 4A. A current amplifier (1B) is used to drive a 75 Ohm load which is the input impedance of the used raised cosine filter. The wideband generated signal will be bandlimited by the filter to achieve spectral efficiency.

The symbol rate clock triggers a set of two one-shot multivibrators (2B) to generate the required sampling clock (clock-3) which will be wired to the decoder. The delay and pulse width of the sampling clock is adjusted by two potentiometers.

A.1.2 Description of the Decoder circuit.

Referring to Figure A.3 the received signal $r(t)$ is first amplified by 1C. After the amplification the signal is passed through a 4-level quantizer consisting of three voltage comparators (2C-4C) and three D flip-flops (5C). The threshold voltages V_1, V_2, V_3 are set properly in the middle of each eye of the eye diagram. We define as r_k the sampled value of $r(t)$ at $t=kT + \tau$, i.e.,

$$r_k = r(t) \Big|_{t=kt + \tau}$$

where k is an integer and τ is the sampler's phase which is to be adjusted to the optimum sampling instants. The output of 5C depends on the location of r_k , as illustrated by Table A.1.

Finally the two parallel bits (A,B outputs) are converted to a serial bit stream (1D to 4D). This completes the description of the circuit operation.

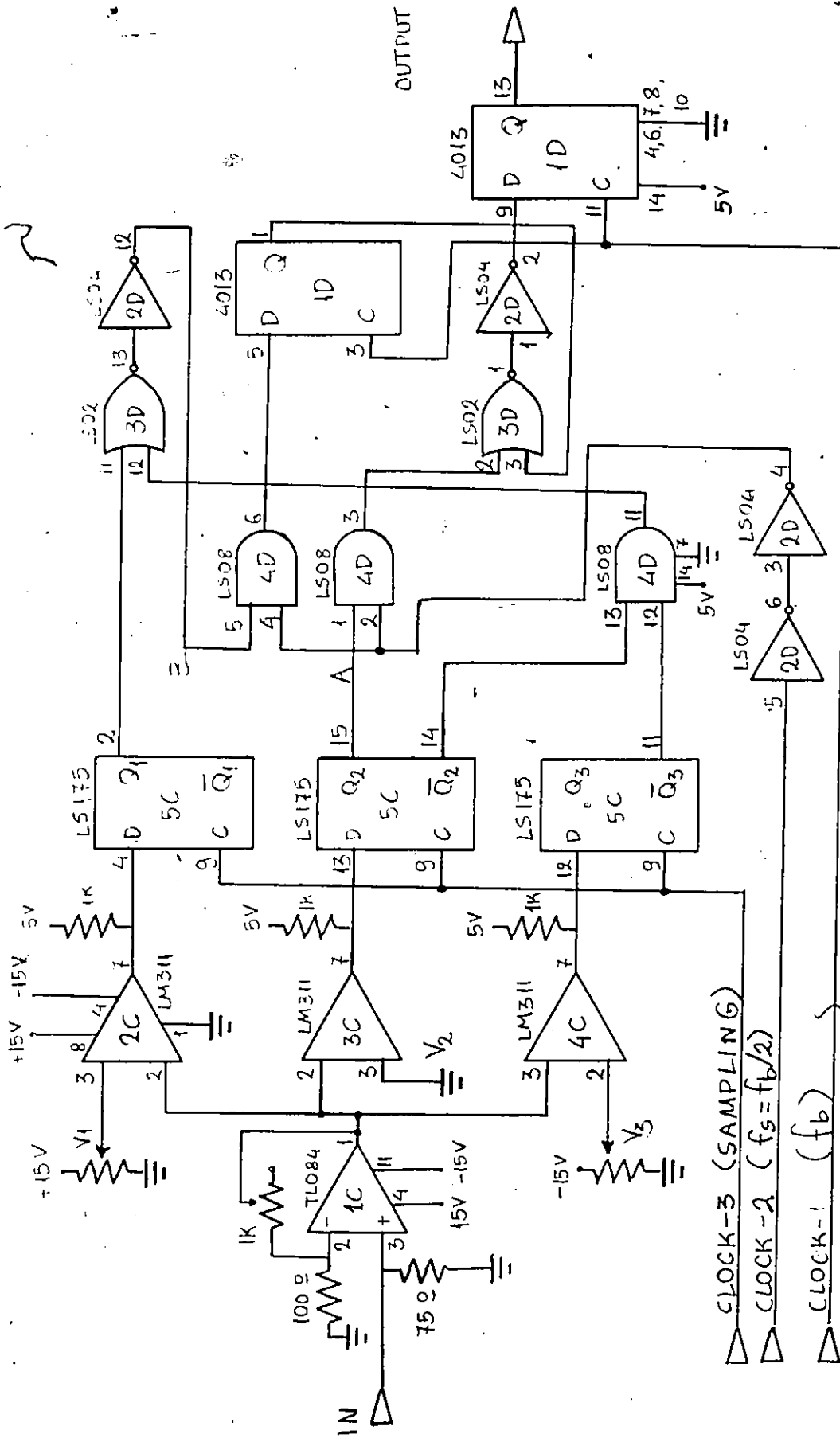


FIGURE A.3 . Implemented 4-PAM Decoder.

Range	74174			7408	
	Q1	Q2	Q3	A	B
$V1 \leq r_k$	1	1	0	1	1
$V2 \leq r_k \leq V1$	0	1	0	1	0
$V3 \leq r_k \leq V2$	0	0	0	0	1
$r_k \leq V4$	0	0	1	0	0

Table A.2. Decoding table with reference to Figure A.3.

A.2 EXPERIMENTAL RESULTS AND DISCUSSIONS.

The data pattern and the corresponding spectrum of the generated wideband 4-PAM signal are shown in Figure A.4 while the eye diagram and spectrum of the bandlimited received signal are shown in Figure A.5. Raised cosine filters with $\alpha = 0.2$ were used. The transmit filter is $x/\sin x$ amplitude equalized. The filter bandwidth is 124 KHz (given by the designer). The 3 dB cutoff frequency is:

$$f_{3dB} = 124 / (1 + \alpha) = 124 / 1.2 = 103.33 \text{ kHz.}$$

Thus the filter is designed for transmitting data at a symbol rate of:

$$f_s = 2 \cdot f_{3dB} = 206.66 \text{ kBaud}$$

For the 4-level PAM the nominal bit rate is

$$f_b = 2 \cdot 206.66 = 413.3 \text{ kb/sec}$$

The BER performance versus S/N was measured for the described system. The signal and noise powers were measured at the output of the lowpass filter just before the threshold detectors. The results are

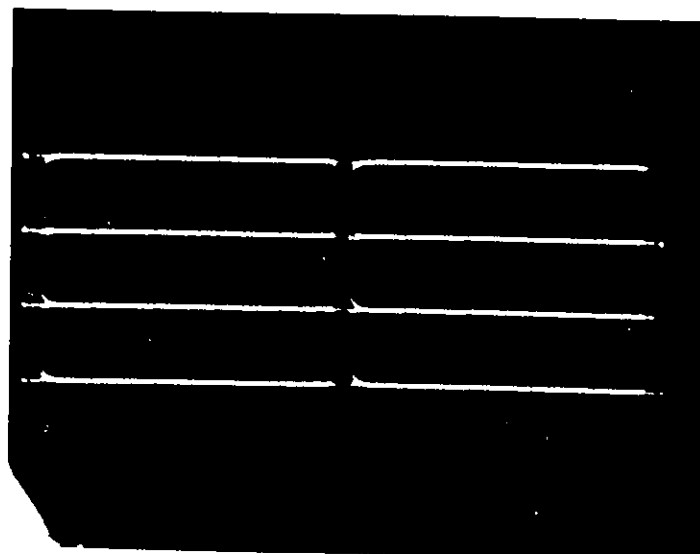
shown in Figure A.6. As we note for $P(e)=10^{-6}$ the difference between measured and simulated results is about 1 dB. This is due to the following.

i) Hardware imperfections of the implemented circuit and impedance mismatching.

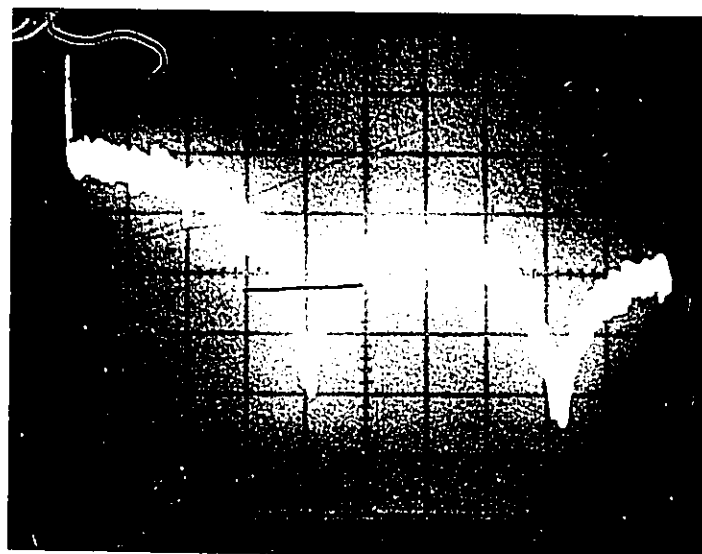
ii) Filter group delay which is not considered in the computer simulation.

iii) In the simulation Gray encoding of the 4-PAM signal is assumed while the generated 4-PAM signal is not Gray encoded.

The measurement set up is shown in Figure A.7.

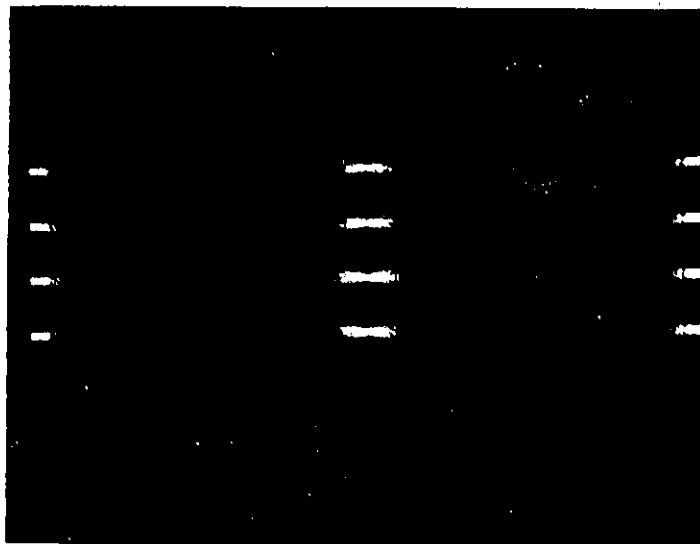


Horiz. 890ns/div.
Vert. 500mV/div.

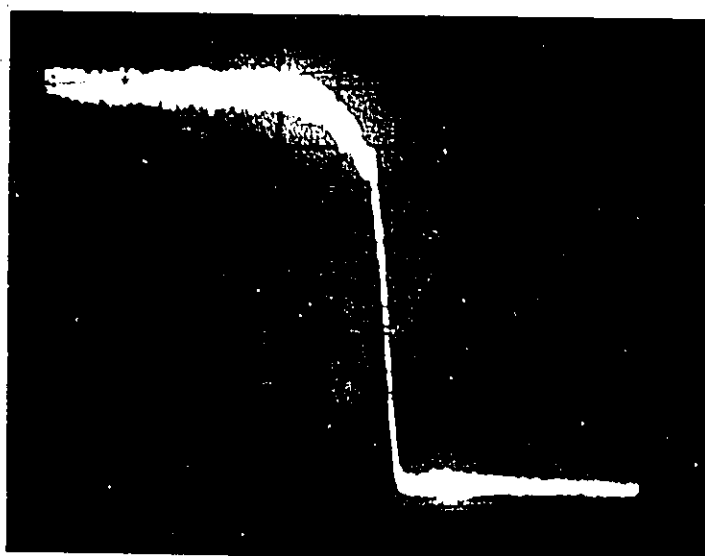


Horiz. 50 KHz/div.
Vert. 10 dB/div.

FIGURE A.4: Measured eye and spectrum diagrams of the wideband 4-PAM signal generated by the circuit of Fig. A.2. The signal rate is 206.66 kBaud.



Horiz. 890ns/div.
Vert. 200mV/div.



Horiz. 20 KHz/div.
Vert. 10 dB/div.

FIGURE A.5 . Measured eye and spectrum diagrams of the 4-PAM signal generated by the circuit of Figure A.2. Nyquist filters with $\alpha = 0.2$ were used. The signal rate is 206.66 kBaud.

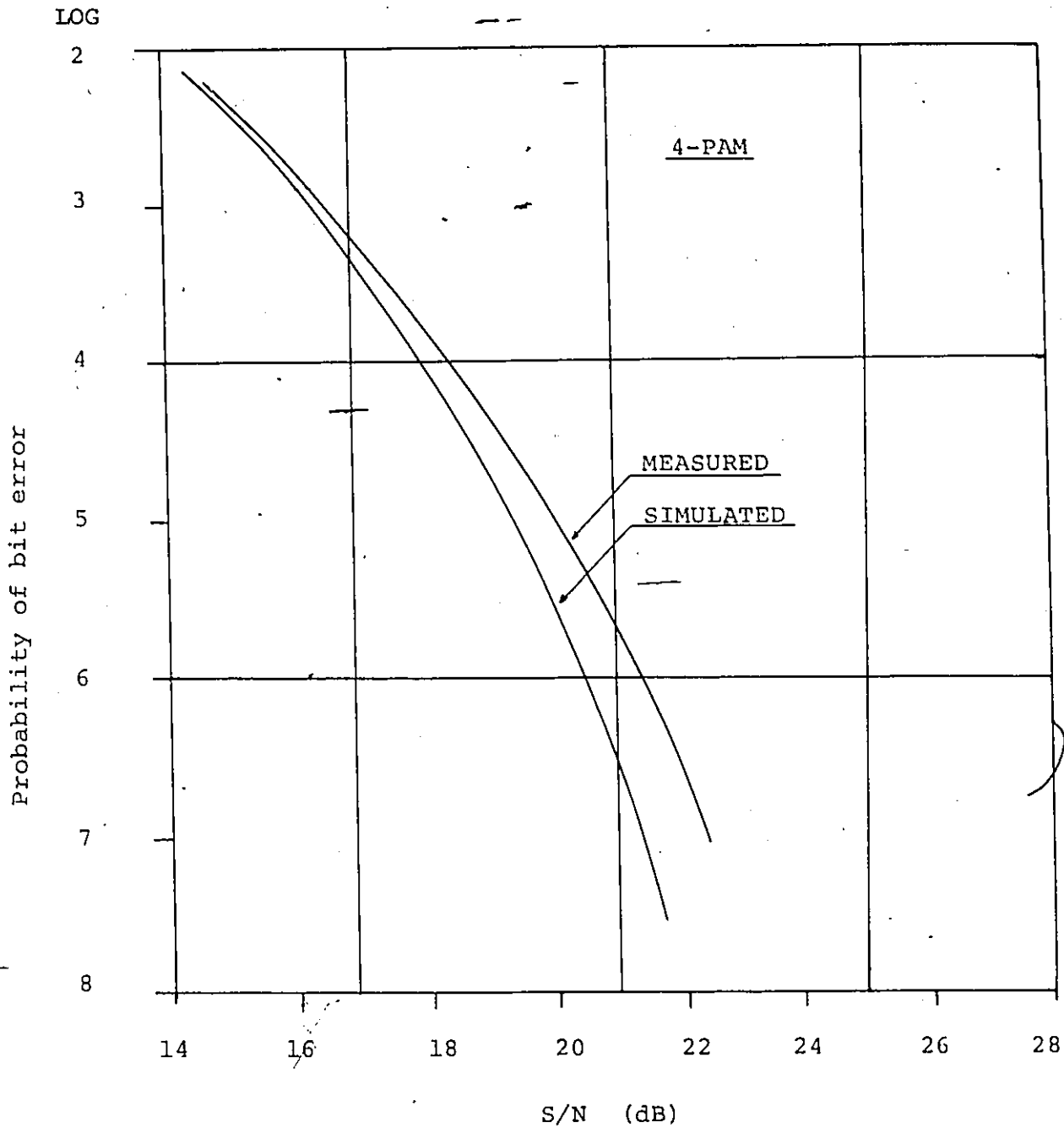


FIGURE A.6. Error performance of the 4-PAM signal generated by the implemented circuit. Nyquist filters with $\alpha = 0.2$ were used.

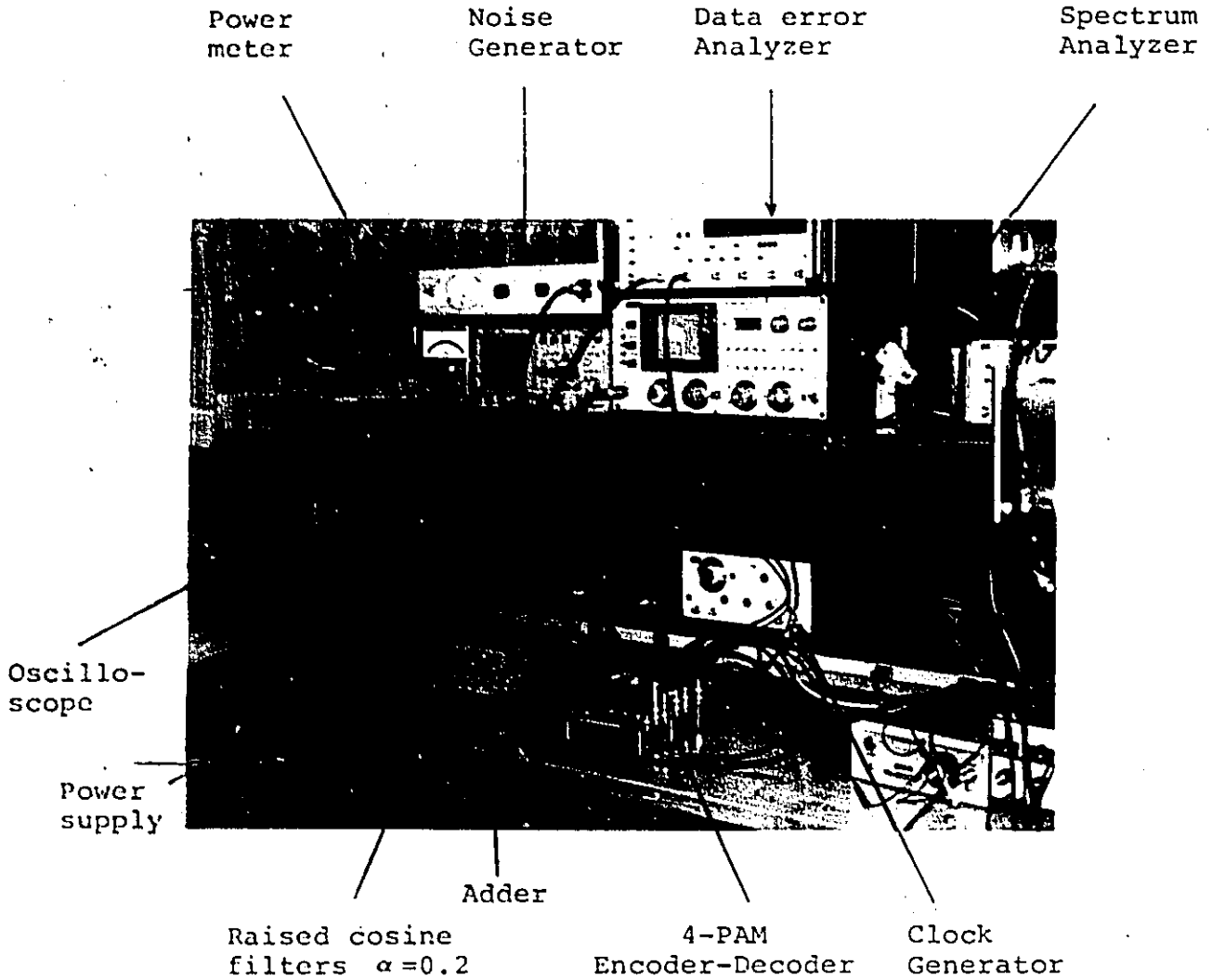


FIGURE A.7. Photograph of the experimental set-up in the Digital Communications Laboratory, Department of Electrical Engineering, University of Ottawa.

Appendix B

AMPLIFICATION STAGE CIRCUIT DESCRIPTION

The circuit of the amplification stage is shown in Figure B.1. It consists of the following parts.

In the input an operational amplifier (TL-084) is used for input impedance matching and buffering. The input impedance of the amplification stage is 50 Ohm in order to match with the signal sources (sinusoidal generator or Nyquist transmit filter).

The LM-380 audio power amplifier amplifies the incoming signal. In order to cause nonlinear distortions to the signal, it is operated in full input range from low input power levels to saturation. The output of the amplifier is set automatically at one-half of the supply voltage.

The second operational amplifier is used for the DC offset of the amplifier output and for output impedance matching which is 50 Ohm.

The amplitude response of the stage (AM-AM characteristic) was measured using a single tone input and is given in section 2.1. The power bandwidth of the amplification stage was also measured and it is shown in Figure B.2. We note that the gain is constant over sufficient range for the used bandlimited 4-PAM signal which has a bandwidth of 124 KHz. In the same Figure, the phase of the LM-380 amplifier (as it is given by the designer) is also drawn. As we see in Figure B.3 the

phase contributes to additional degradation in the error performance of the 4-PAM signal.

In this point we must mention that in the computer simulation model the LM-380 amplifier is assumed phase equalized. For the simulated results of chapters III and V only distortions due to the LM-380 AM-AM characteristic are considered.

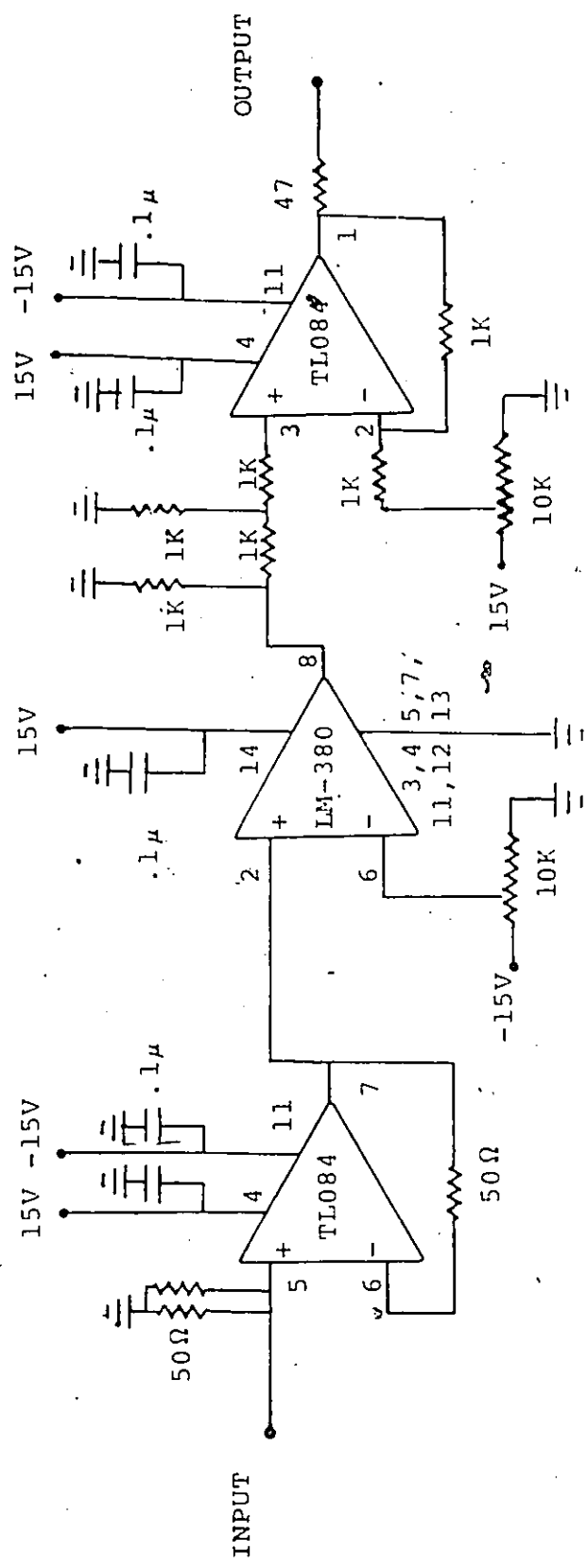


Figure B.1. Amplification stage circuit diagram.

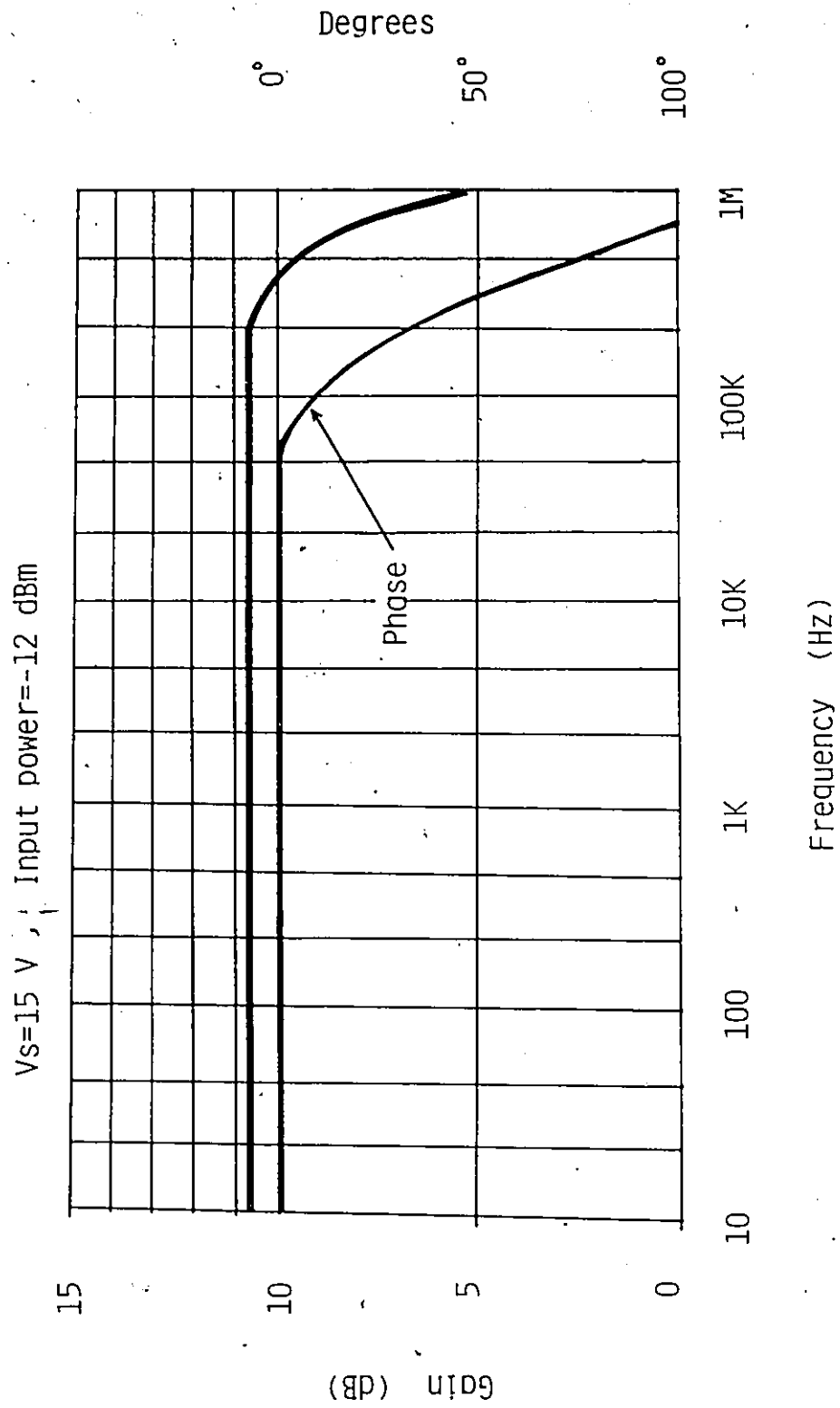


Figure B.2. Output power gain versus frequency of the LM-380 amplification stage .

LOG

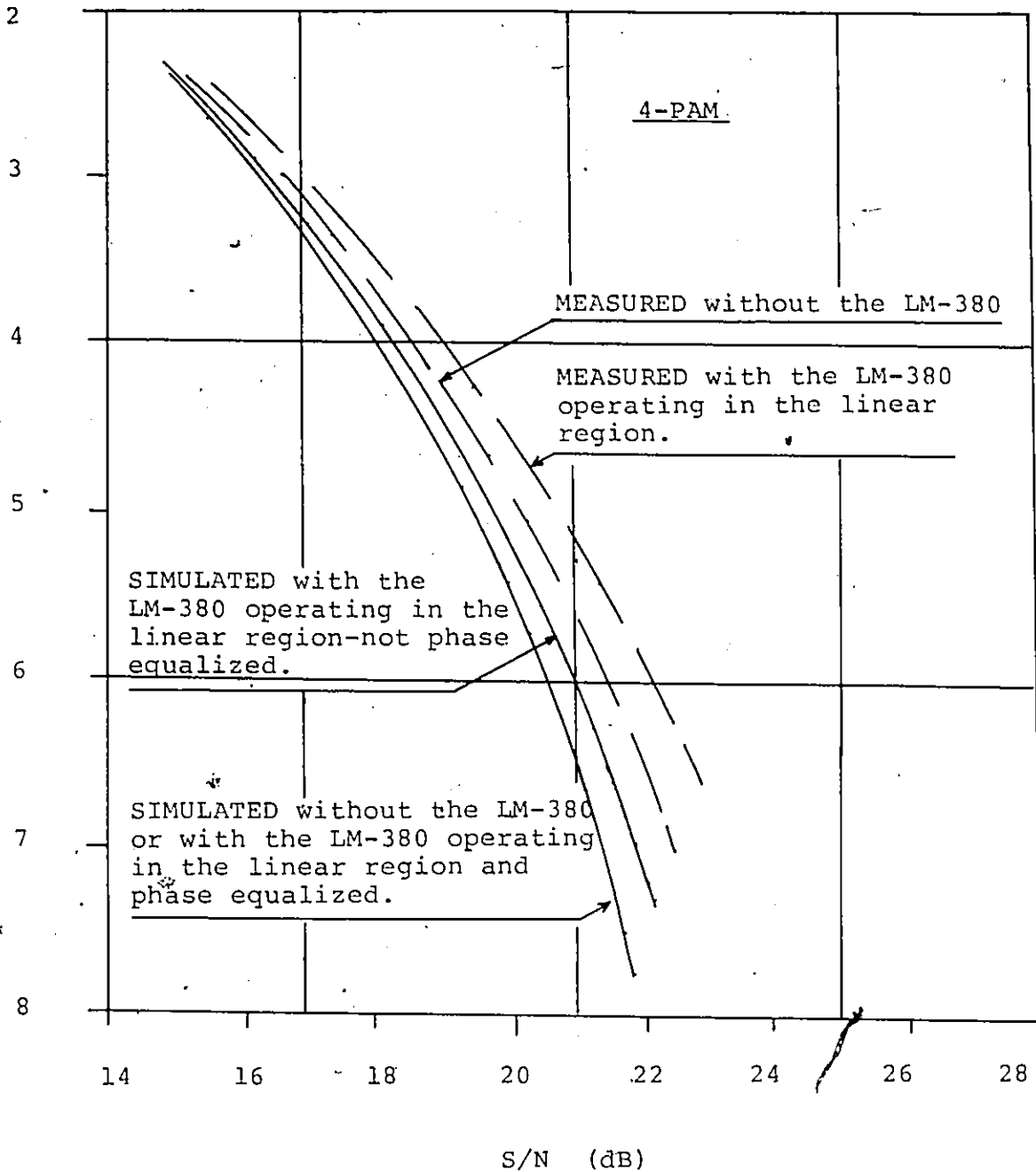


FIGURE B.3 . Error performance of the 4-PAM signal of Appendix A with the LM-380 amplification stage. Nyquist filters with $\alpha=0.2$ were used.

Appendix C

IMPLEMENTATION AND PERFORMANCE EVALUATION OF A PREDISTORTER LINEARIZER FOR THE LM-380 AMPLIFICATION STAGE.

C.1 DESCRIPTION OF THE CIRCUIT.

A photograph of the implemented predistorter is shown in Figure C.1. The following description refers to the circuit of Figure C.2. As we see the predistorter is a diode based circuit. Although semiconductor diodes available today are close to "ideal" devices they have severe limitations in low level applications. Thus, due to the low level of the required signals (see Figure 4.4) the input to the predistorter is first amplified (1A). The degree of amplification is such that we operate in the "linear" region of the diodes. Two half wave rectifiers with dc balancing adjustment (1B), separate the negative and positive parts of the signal. This is necessary because of the two quadrant type (one polarity signals) of the following waveshaping stages (1C) [20].

The diodes D1-D4 of the waveshaping stages have a threshold which depends on the value of the voltages V1-V4. When the outputs of the operational amplifiers overcome the diodes thresholds, the corresponding branches are conducting and the resistances R1 to R4 are placed in parallel with the resistance R. This changes the gain of the operational amplifier resulting in a piece wise linear response [20].

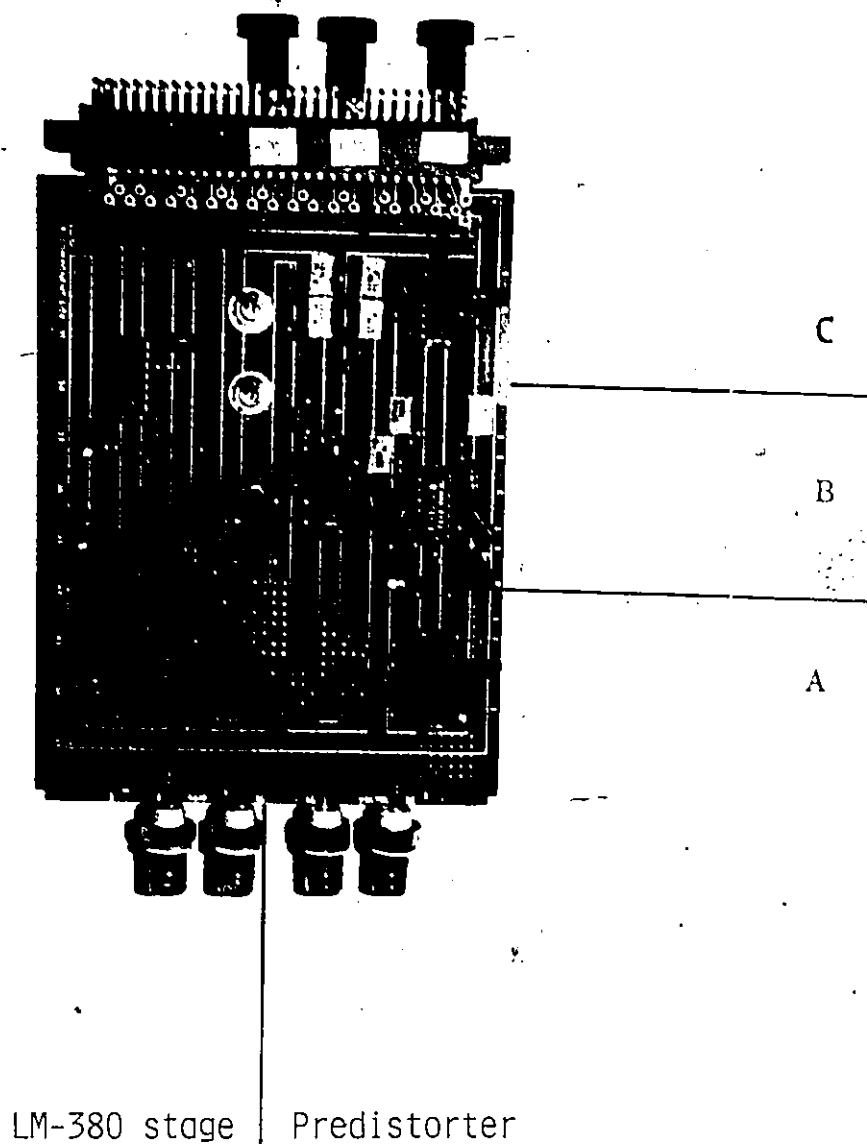


Figure C.1: Photograph of the implemented predistorter linearizer for the LM-380 amplification stage.

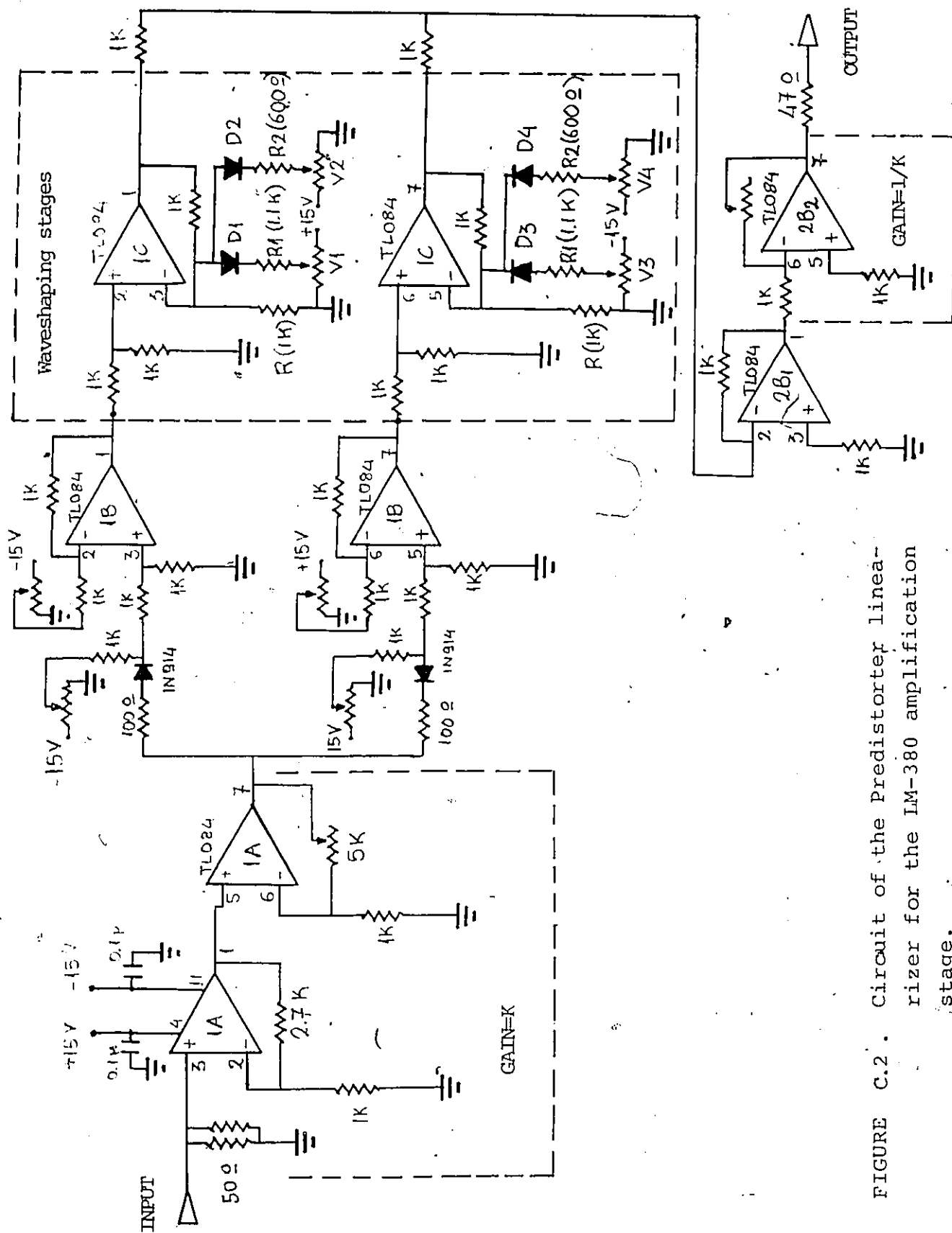


FIGURE C.2. Circuit of the Predistorter linearizer for the LM-380 amplifier stage.

Finally the two signal parts are added (2B1) and the resulting signal is amplified (2B2) so that the overall predistorter gain becomes one. The input and output impedance of the predistorter are 50 Ohm.

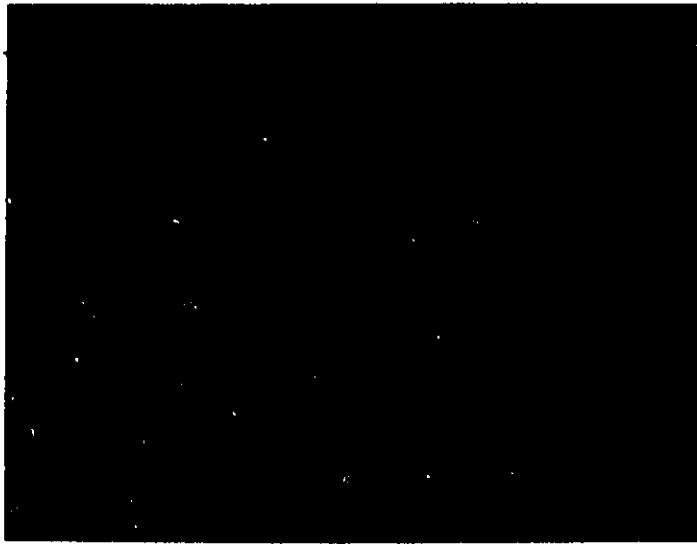
C.2 PERFORMANCE OF THE PREDISTORTER.

The single tone measured piece-wise linear transfer characteristic of the predistorter was given in Figure 4.4. As we see the slope of the characteristic is changing as it is shown in Table C.1:

Input range	Gain
$ R \leq 0.12$	1.0
$0.12 \leq R \leq 0.1825$	1.45
$0.1825 \leq R $	2.3

Table C.1. Gain of the predistorter.

The effect of the predistorter on the 4-PAM signal generated by the encoder of Appendix B, is shown in Figure C.3. Considering the saturation power of the LM-380 amplification stage the operating point is 4 dB Output Backoff. Only the transmit raised cosine filter is used. We note that the higher levels of the signal are amplified more than the lower ones. The effect is the inverse of that of the LM-380 nonlinearity. Thus the overall response of the cascaded combination of the predistorter and the LM-380 stage becomes more linear (Figure 4.4, section 5.1).



(a)

Horiz. 1 μ s/div.

Vert. 50 mV/div.

4 dB Out.Backoff.



(b)

Horiz. 1 μ s/div.

Vert. 50 mV/div.

4 dB Out.Backoff.

FIGURE C.3. Measured eye diagrams of a 4-PAM signal at the (a) input, (b) output of the LM-380 predistorter. Only the transmit raised cosine filter with $\alpha=0.2$ is used.

Appendix D

COMPUTER SIMULATION PROGRAMS.

The simulation programs listed in the first part of this appendix were used to simulate various performances of PAM systems, such as the performance in nonlinear channels and the performance in the linearized channels, with or without threshold adjustment. The programs listed in the second part, were used to fit the various AM-AM and AM-PM characteristics with suitable models and to optimize the coefficients of the equations which we used in the linearization process.

The author of this thesis used, modified and extended numerous subroutines and programs which were developed by the Digital Communications Research Group, Department of Electrical Engineering, University of Ottawa.

FILE: PAM FORTRAN A UNIV D' /OF OTTAWA

```

C*****
C PROGRAM FOR SIMULATION OF PAM SCHEMES IN NONLINEAR CHANNEL.
C FILE NAME: PAM
C*****
COMPLEX DATA(262144),TF(262144)
DIMENSION PL1(64),EBNO(64),NI(16384),NQ(16384),PE(64)
DIMENSION XARRAY(68),YARRAY(68),P(64)
REAL SS(262144),P
C
C INITIALIZE PROGRAM.
C
COMMON /NUMB1/ FBW,ALPHA,LDIM,IOFF,LSAMPL
COMMON /NUMB2/ NSNR,NSYMB,BAUD
C
ALPHA=0.20
ALPHA=0.50
CF=4.
LDIM=262144
IOFF=0
LSAMPL=16
OFF=FLOAT(IOFF)/FLOAT(LSAMPL)
NSNR=64
NSYMB=16384
BAUD=200
FBW=100
FFB=FBW*(1.+ALPHA)
WRITE(6,23) FBW,ALPHA,OFF
23 FORMAT(5X,11H 16QAM FBW=,F10.6,5X,7H ALPHA=,F6.3,5X,5H OFF=,F6.3)
ISIN=1
NFILTR=2
NRUNS=4
LMAX=31
ID=1.
C
C END OF INITIALIZATIONS.
C-----
C
C START OF COMPUTATIONS.
DO 100 NR=1,NRUNS
DSEED=135791.D0
CALL RAND (NI,NSYMB,DSEED)
DSEED=780956.D0
CALL RAND (NQ,NSYMB,DSEED)
CALL SIGNAL(DATA,NI,NQ)
CALL RCOSTX(1F)
CALL FILTER(DATA,TF)
CALL POWER(DATA,MP,PF)
GO TO (1,2,3,4,5,6,7,8),NR
1 GO TO 20
2 BAKOFF=15.4
GO TO 21
3 BAKOFF=13.4
GO TO 31
4 BAKOFF=12.4
GO TO 11

```

```

PAM00010
PAM00020
PAM00030
PAM00040
PAM00050
PAM00060
PAM00070
PAM00080
PAM00090
PAM00100
PAM00110
PAM00120
PAM00130
PAM00140
PAM00150
PAM00160
PAM00170
PAM00180
PAM00190
PAM00200
PAM00210
PAM00220
PAM00230
PAM00240
PAM00250
PAM00260
PAM00270
PAM00280
PAM00290
PAM00300
PAM00310
PAM00320
PAM00330
PAM00340
PAM00350
PAM00360
PAM00370
PAM00380
PAM00390
PAM00400
PAM00410
PAM00420
PAM00430
PAM00440
PAM00450
PAM00460
PAM00470
PAM00480
PAM00490
PAM00500
PAM00510
PAM00520
PAM00530
PAM00540
PAM00550

```

FILE: PAM FORTRAN A UNIV D'/OF OTTAWA

5	BAKOFF=11.4	PAM00560
	GO TO 51	PAM00570
6	BAKOFF=0.0	PAM00580
	GO TO 21	PAM00590
7	BAKOFF=4.9	PAM00600
	GO TO 21	PAM00610
8	BAKOFF=3.2	PAM00620
	GO TO 21	PAM00630
71	CALL TWT(DATA, BAKOFF, PSHIFT)	PAM00640
	CALL AMPH(TF)	PAM00650
	CALL FILTER(DATA, TF)	PAM00660
	GO TO 20	PAM00670
11	CALL TWT(DATA, BAKOFF, PSHIFT)	PAM00680
	GO TO 20	PAM00690
21	CALL TWT1(DATA, BAKOFF, PSHIFT)	PAM00700
	GO TO 20	PAM00710
41	CALL TWT2(DATA, BAKOFF, PSHIFT)	PAM00720
	GO TO 20	PAM00730
31	CALL TWT3(DATA, BAKOFF, PSHIFT)	PAM00740
	GO TO 20	PAM00750
51	CALL TWT4(DATA, BAKOFF, PSHIFT)	PAM00760
	GO TO 20	PAM00770
61	CALL TWT5(DATA, BAKOFF, PSHIFT)	PAM00780
20	CALL ENERGY(DATA, ES)	PAM00790
C		PAM00800
C	END OF TRANSMITTER	PAM00810
C		PAM00820
C	CALL SPECT(DATA, PO, NR)	PAM00830
	CALL PFOBP(PO, NR, NRUNS)	PAM00840
	CALL RCOSRX(TF)	PAM00850
	CALL HHGG(TF, PNOISE)	PAM00860
	CALL FILTER(DATA, TF)	PAM00870
	CALL SYNCRO(DATA, PNOISE, NI, NQ, MI, MQ, ES, LMAX)	PAM00880
C	CALL PSPACE(DATA, NR, NRUNS, MI)	PAM00890
	CALL DETECT(NERROR, DATA, PNOISE, MI, MQ, NI, NQ, EBNO, PE, ES, LMAX)	PAM00900
	CALL DECOD1(NERROR, DATA, PNOISE, MI, NI, EBNO, P, PE, ES, BAKOFF, NR)	PAM00910
C		PAM00920
C	CALL THE DRAWING ROUTINE	PAM00930
C		PAM00940
	DO 99 I=1, NSNR	PAM00950
	XARRAY(I)=EBNO(I)	PAM00960
99	YARRAY(I)=PE(I)	PAM00970
	CALL DRAWCN(I, XARRAY, YARRAY, NR, NRUNS)	PAM00980
C	CALL THE EYE DIAGRAM ROUTINE	PAM00990
C	CALL EYEQ(DATA, NR, NRUNS)	PAM01000
100	CONTINUE	PAM01010
	STOP	PAM01020
	END	PAM01030
		PAM01040
C	*****	PAM01050
C	THIS SUBROUTINE GENERATES RANDOM NUMBERS FOR PRODUCING RANDOM DATA.	PAM01060
C	*****	PAM01070
	SUBROUTINE RAND(IR, N, DSEED)	PAM01080
	INTEGER IR(1)	PAM01090
	DOUBLE PRECISION DSEED	PAM01100

FILE: PAM FORTRAN A1 UNIV D'OF OTTAWA

```

DO 3000 I=1,N
R=GGUBIS(DSEED)
IR(I)=IFIX(R)
IF(R.LE.0.031) IR(I)=-31
IF((R.GT.0.031).AND.(R.LE.0.062))IR(I)=-29
IF((R.GT.0.062).AND.(R.LE.0.093))IR(I)=-27
IF((R.GT.0.093).AND.(R.LE.0.124))IR(I)=-25
IF((R.GT.0.124).AND.(R.LE.0.155))IR(I)=-23
IF((R.GT.0.155).AND.(R.LE.0.186))IR(I)=-21
IF((R.GT.0.186).AND.(R.LE.0.217))IR(I)=-19
IF((R.GT.0.217).AND.(R.LE.0.248))IR(I)=-17
IF((R.GT.0.248).AND.(R.LE.0.279))IR(I)=-15
IF((R.GT.0.279).AND.(R.LE.0.31))IR(I)=-13
IF((R.GT.0.31).AND.(R.LE.0.341))IR(I)=-11
IF((R.GT.0.341).AND.(R.LE.0.372))IR(I)=-9
IF((R.GT.0.372).AND.(R.LE.0.403))IR(I)=-7
IF((R.GT.0.403).AND.(R.LE.0.434))IR(I)=-5
IF((R.GT.0.434).AND.(R.LE.0.465))IR(I)=-3
IF((R.GT.0.465).AND.(R.LE.0.496))IR(I)=-1
IF((R.GT.0.496).AND.(R.LE.0.527))IR(I)=1
IF((R.GT.0.527).AND.(R.LE.0.558))IR(I)=3
IF((R.GT.0.558).AND.(R.LE.0.589))IR(I)=5
IF((R.GT.0.589).AND.(R.LE.0.62))IR(I)=7
IF((R.GT.0.62).AND.(R.LE.0.651))IR(I)=9
IF((R.GT.0.651).AND.(R.LE.0.682))IR(I)=11
IF((R.GT.0.682).AND.(R.LE.0.713))IR(I)=13
IF((R.GT.0.713).AND.(R.LE.0.744))IR(I)=15
IF((R.GT.0.744).AND.(R.LE.0.775))IR(I)=17
IF((R.GT.0.775).AND.(R.LE.0.806))IR(I)=19
IF((R.GT.0.806).AND.(R.LE.0.837))IR(I)=21
IF((R.GT.0.837).AND.(R.LE.0.868))IR(I)=23
IF((R.GT.0.868).AND.(R.LE.0.899))IR(I)=25
IF((R.GT.0.899).AND.(R.LE.0.930))IR(I)=27
IF((R.GT.0.930).AND.(R.LE.0.961))IR(I)=29
IF((R.GT.0.961).AND.(R.LE.0.996))IR(I)=31
IF(R.GT.0.996)IR(I)=-31
3000 CONTINUE
RETURN
END
.....
C THIS FORMS COMPLEX BASEBAND SIGNAL
C NI : I-CHANNEL SEQ
C NI : Q-CHANNEL SEQ
C DATA : OUTPUT SIGNAL
.....
SUBROUTINE SIGNAL (DATA,NI,NQ)
COMPLEX DATA(1)
DIMENSION NI(1), NQ(1)
COMMON /NUMB1/ FBW,ALPHA,LDIM,LOFF,LSAMPL
COMMON /NUMB2/ NSNR,NSYMB,BAND
DO 2 I=1,NSYMB
C DO 3 INTO SAMPLE ARRAY, LSAMPLES PER SYMBOL
J1=(I-1)*LSAMPL+1
J2=I*LSAMPL
DO 3 J3=J1,J2

```

PAM01110
PAM01120
PAM01130
PAM01140
PAM01150
PAM01160
PAM01170
PAM01180
PAM01190
PAM01200
PAM01210
PAM01220
PAM01230
PAM01240
PAM01250
PAM01260
PAM01270
PAM01280
PAM01290
PAM01300
PAM01310
PAM01320
PAM01330
PAM01340
PAM01350
PAM01360
PAM01370
PAM01380
PAM01390
PAM01400
PAM01410
PAM01420
PAM01430
PAM01440
PAM01450
PAM01460
PAM01470
PAM01480
PAM01490
PAM01500
PAM01510
PAM01520
PAM01530
PAM01540
PAM01550
PAM01560
PAM01570
PAM01580
PAM01590
PAM01600
PAM01610
PAM01620
PAM01630
PAM01640
PAM01650

FILE: PAM FORTRAN A1 UNIV D'OF OTTAWA

```

3 DATA(J3)=CMPLX(FLOAT(N1(1)),0.0)
2 CONTINUE
RETURN
END
C*****
C RAISED COSINE FILTER WITH ARBITRARY ALPHA AND X/SINX
C*****
SUBROUTINE RCOSTX(TF)
COMPLEX TF(1)
COMMON /NUMB1/ FBW,ALPHA,LDIM,LOFF,1SAMPL
COMMON /NUMB2/ NSNR,NSYMB,BAUD
SBANDW=BAUD*1SAMPL
NO=LDIM/2
NO1=NO+1
IF (ALPHA.EQ.0) ALPHA=0.0001
FN=LDIM*(FBW/SBANDW)
F1=(1.-ALPHA)*FN
F2=(1.+ALPHA)*FN
IFN=IFIX(FN)
IF1=IFIX(F1)+1
IF2=IFIX(F2)+1
C
C THE AMPLITUDE CHARACTERISTICS
C
A1=3.1415926/(2.*FLOAT(IFN))
DO 8 I=2,IF1
TF(I)=CMPLX(1.0,0.0)
I=I-1
C
C X/SIN(X) EQUALIZATION
C
A2=(FLOAT(J)*A1)/(SIN(FLOAT(J)*A1))
TF(I)=CMPLX(A2,0.0)
8 CONTINUE
JK=IF1+1
DO 9 J=JK,IF2
I=J-1
C
C ROOT OF RAISED COSINE
C
A3=(FLOAT(I)*A1)/(SIN(FLOAT(I)*A1))
A=(3.1415926/(2.0*ALPHA))*(FLOAT(I)/FLOAT(IFN))-1.0
TF(J)=CMPLX(SQRT(0.5*(1.0-SIN(A))),0.0)
TF(J)=TF(J)*CMPLX(A3,0.0)
9 CONTINUE
JH=IF2+1
DO 10 I=JH,NO1
TF(I)=CMPLX(0.05,0.0)
10 CONTINUE
NO2=NO1+1
DO 5 I=NO2,LDIM
TF(I)=CONJG(TF(LDIM+2-I))
5 CONTINUE

```

PAM01660
PAM01670
PAM01680
PAM01690
PAM01700
PAM01710
PAM01720
PAM01730
PAM01740
PAM01750
PAM01760
PAM01770
PAM01780
PAM01790
PAM01800
PAM01810
PAM01820
PAM01830
PAM01840
PAM01850
PAM01860
PAM01870
PAM01880
PAM01890
PAM01900
PAM01910
PAM01920
PAM01930
PAM01940
PAM01950
PAM01960
PAM01970
PAM01980
PAM01990
PAM02000
PAM02010
PAM02020
PAM02030
PAM02040
PAM02050
PAM02060
PAM02070
PAM02080
PAM02090
PAM02100
PAM02110
PAM02120
PAM02130
PAM02140
PAM02150
PAM02160
PAM02170
PAM02180
PAM02190
PAM02200

FILE: PAM FORTRAN AT UNIV D'OF OTTAWA

```

      RETURN
      END
C*****
C  RAISED COSINE FILTER WITH ARBITRARY ALPHA
C*****
      SUBROUTINE RCOSRX(FF)
      COMPLEX FF(1)
      COMMON /NUMB1/ FBW,ALPHA,LDIM,IOFF,LSAMPL
      COMMON /NUMB2/ NSNR,NSYMB,BAUD
      SBANDW=BAUD*LSAMPL
      NO=LDIM/2
      NO1=NO+1
      IF (ALPHA.EQ.0) ALPHA=0.0001
      FN=LDIM*(FBW/SBANDW)
      F1=(1.-ALPHA)*FN
      F2=(1.+ALPHA)*FN
      IFN=IFIX(FN)
      IF1=IFIX(F1)+1
      IF2=IFIX(F2)+1
C
C  AMPLITUDE CHARACTERISTIC
C
      A1=3.141592/(2.*FLOAT(IFN))
      DO 8 I=2,IF1
      TF(I)=CMPLX(1.0,0.0)
      J=I-1
      TF(I)=CMPLX(1.,0.0)
      8 CONTINUE
      JK=IF1+1
      DO 9 J=JK,IF2
      I=J-1
C
C  ROOT OF RAISED COSINE
C
      A (3.141592/(2.0*ALPHA))*(FLOAT(I)/FLOAT(IFN))-1.)
      TF(J)=CMPLX(SQRT(0.5*(1.0-SIN(A))),0.0)
      9 CONTINUE
      JH=IF2+1
      DO 10 I=JH,NO1
      TF(I)=CMPLX(0.0,0.0)
      10 CONTINUE
      NO2=NO1+1
      DO 5 I=NO2,LDIM
      TF(I)=CONJG(TF(LDIM+2-I))
      5 CONTINUE
      RETURN
      END
C*****
C  THE FOLLOWING SUBROUTINE PERFORMS THE FILTERING
C  PROCESS ON THE DATA SEQUENCE.
C*****
C  SUBROUTINE FILTER(DATA,FF)

```

PAM02210
PAM02220
PAM02230
PAM02240
PAM02250
PAM02260
PAM02270
PAM02280
PAM02290
PAM02300
PAM02310
PAM02320
PAM02330
PAM02340
PAM02350
PAM02360
PAM02370
PAM02380
PAM02390
PAM02400
PAM02410
PAM02420
PAM02430
PAM02440
PAM02450
PAM02460
PAM02470
PAM02480
PAM02490
PAM02500
PAM02510
PAM02520
PAM02530
PAM02540
PAM02550
PAM02560
PAM02570
PAM02580
PAM02590
PAM02600
PAM02610
PAM02620
PAM02630
PAM02640
PAM02650
PAM02660
PAM02670
PAM02680
PAM02690
PAM02700
PAM02710
PAM02720
PAM02730
PAM02740
PAM02750

FILE: PAM , FORTRAN A1 UNIV D' /OF OTTAWA

```

COMPLEX DATA(1),TF(1)
DIMENSION IWK(19)
COMMON /NUMB1/ FBW,ALPHA,LDIM,IOFF,LSAMPL
COMMON /NUMB2/ NSNR,NSYMB,BAUD
CALL FFT2C(DATA,18,IWK)
DO 1 I=1,LDIM
1 DATA(I)=CONJG(DATA(I)*TF(I))
CALL FFT2C(DATA,18,IWK)
DO 2 I=1,LDIM
2 DATA(I)=CONJG(DATA(I))/FLOAT(LDIM)
RETURN
END
C*****
C THIS SUBROUTINE COMPUTES THE EFFECTIVE NOISE (PNOISE)
C AT THE OUTPUT OF THE RECEIVE FILTER
C*****
C
SUBROUTINE HHGG(TF,PNOISE)
COMPLEX TF(1)
COMMON /NUMB1/ FBW,ALPHA,LDIM,IOFF,LSAMPL
COMMON /NUMB2/ NSNR,NSYMB,BAUD
SUM=0.0
SBANDW=BAUD*LSAMPL
DO 1 L=1,LDIM
HH=(CABS(TF(L)))**2
1 SUM=SUM+HH
PNOISE=SUM*SBANDW/FLOAT(LDIM)/2.
WRITE (6,2) PNOISE
2 FORMAT(5X,'PNOISE=',F7.3,/)
RETURN
END
C*****
C CALCULATE ENERGY (ES)
C *****
SUBROUTINE ENERGY(DATA,ES)
COMPLEX DATA(1)
COMMON /NUMB2/ NSNR,NSYMB,BAUD
COMMON /NUMB1/ FBW,ALPHA,LDIM,IOFF,LSAMPL
WATTS=0.
DO 1 I=1,LDIM
WATTS=WATTS+((CABS(DATA(I)))**2.)
1 CONTINUE
WATTS=WATTS/FLOAT(LDIM)
ES=WATTS/BAUD
WRITE (6,40) WATTS,ES
40 FORMAT(5X,E15.8,5X,E15.8)
RETURN
END
C*****
C THIS SUBROUTINE DRAWS PROBABILITY OF ERROR CURVES
C*****
SUBROUTINE DRAWCN(ID,XARRAY,YARRAY,JCURV,JI,AST)
DIMENSION XARRAY(68),YARRAY(68),X(64),Y(64)
PAM02760
PAM02770
PAM02780
PAM02790
PAM02800
PAM02810
PAM02820
PAM02830
PAM02840
PAM02850
PAM02860
PAM02870
PAM02880
PAM02890
PAM02900
PAM02910
PAM02920
PAM02930
PAM02940
PAM02950
PAM02960
PAM02970
PAM02980
PAM02990
PAM03000
PAM03010
PAM03020
PAM03030
PAM03040
PAM03050
PAM03060
PAM03070
PAM03080
PAM03090
PAM03100
PAM03110
PAM03120
PAM03130
PAM03140
PAM03150
PAM03160
PAM03170
PAM03180
PAM03190
PAM03200
PAM03210
PAM03220
PAM03230
PAM03240
PAM03250
PAM03260
PAM03270
PAM03280
PAM03290
PAM03300

```

FILE: PAM FORTRAN A1 UNIV D'/OF OTTAWA

```

COMMON /NUMB1/ FBW,ALPHA,LDIM,IOFF,LSAMPL.
COMMON /NUMB2/ NSNR,NSYMB,BAUD
CF=2.0
M=NSNR
NNSNR=NSNR
DO 1 K=1,NNSNR
XARRAY(K) =XARRAY(K)+10. *A1 DG10(CF)
I1(YARRAY(K),CL,1.0) YAPRAY(K)-1.0
I1(YARRAY(K),LE,1.0E-9) GOTO 3
GOTO 1
3 M=M+1
GOTO 4
1 CONTINUE
4 CONTINUE
I=M+1
I1=I+1
XARRAY(I)=4.0
XARRAY(I1)=3.0
YARRAY(I)=1.E-9
YARRAY(I1)=0.4
I1(JCURV.GT.1) GOTO 2
C
C ESTABLISH THE SURFACE AREA.
C
C CALL PLOTS(30.0,27.5)
C CALL FACTOR(0.85)
C
C ESTABLISH THE ORIGIN.
C
C CALL PLOT(3.0,1.5,-3)
C
C DRAW THE LOGARITHMIC Y-AXIS.
C
C CALL LGAXS(0.0,0.0,0.29HPROBABILITY OF A SYMBOL ERROR,29.25.,
+90.,1.0E-9,.4)
C
C DRAW THE LINEAR X-AXIS.
C
C CALL AXIS(0.0,0.0,11H C/N IN DB,-11,
+27.0,0.0,4.0,3.0)
C CALL IGLIN(XARRAY,YARRAY,M,1,2,JCURV,1)
C IF(JCURV.EQ.JLAST) CALL PLOT(0.0,0.0,999)
C RETURN
C END
C*****
C THIS SUBROUTINE DRAWS THE EYE DIAGRAM FOR TWO
C SYMBOL DURATION.
C*****
SUBROUTINE EYEQ(DATA,NR,NRUNS)
DIMENSION DATA2(66),DATA3(66)
COMPLEX DATA(1)
REAL XLEN,YLEN
INTEGER NR,NRUNS

```

PAM03310
PAM03320
PAM03330
PAM03340
PAM03350
PAM03360
PAM03370
PAM03380
PAM03390
PAM03400
PAM03410
PAM03420
PAM03430
PAM03440
PAM03450
PAM03460
PAM03470
PAM03480
PAM03490
PAM03500
PAM03510
PAM03520
PAM03530
PAM03540
PAM03550
PAM03560
PAM03570
PAM03580
PAM03590
PAM03600
PAM03610
PAM03620
PAM03630
PAM03640
PAM03650
PAM03660
PAM03670
PAM03680
PAM03690
PAM03700
PAM03710
PAM03720
PAM03730
PAM03740
PAM03750
PAM03760
PAM03770
PAM03780
PAM03790
PAM03800
PAM03810
PAM03820
PAM03830
PAM03840
PAM03850

FILE: PAM -FORTRAN A1 UNIV D'OF OTTAWA

```

COMMON /NUMB1/ FBW,ALPHA,LDIM,LOFF,LSAMPL
COMMON /NUMB2/ NSNR,NSYMB,BAUD
C ESTABLISH THE SURFACE AREA.
IF (NR.NE.1) GO TO 15
XLEN=40.0*FLOAT(NRUNS)
YLEN=27.5
CALL PLOTS(XLEN,YLEN)
C ESTABLISH THE ORIGIN.
CALL PLOT(3.0,13.0,-3)
GO TO 110
15 CALL PLOT(40.0,0.0,-3)
C WRITE THE TITLE OF THE GRAPH.
110 CALL SYMBOL(10.0,12.0,0.49,17HL-PAM EYE DIAGRAM,0.0,17)
C DRAW THE TIME AXIS.
CALL AXIS(0.0,0.0,1H,-1.32,0.0,1.0,1.0)
C DRAW THE AMPLITUDE AXIS.
CALL AXIS(0.0,-8.00,1H,1.16,0.90,0,-32.,4.0)
C PLOT THE DATA.
JJ=2*LSAMPL
DATA2(JJ+1)=0.0
DATA2(JJ+2)=4.0
DATA3(JJ+1)=1.0
DATA3(JJ+2)=1.0
M2=750
DO 40 KK=1,M2
DO 20 I=1,JJ
II=(KK-1)*LSAMPL+I
IF (II.GT.LDIM) II=II-LDIM
DATA2(I)=REAL(DATA(II))
20 DATA3(I)=FLOAT(I)
CALL LINE(DATA3,DATA2,JJ,1.0,0)
40 CONTINUE
IF (NR.NE.NRUNS) GO TO 10
CALL PLOT(0.0,0.0,999)
10 RETURN
END

C*****
C THIS SUBROUTINE SIMULATES THE BASEBAND AM-AM
C NONLINEARITY OF THE LM-380 AMPLIFIER
C*****
SUBROUTINE IWT(DATA,BAFOFF,PSHIFT)
COMMON /NUMB1/ FBW,ALPHA,LDIM,LOFF,LSAMPL
COMMON /NUMB2/ NSNR,NSYMB,BAUD
COMPLEX DATA(1)
REAL MP,C(80),D(80),G(80),E(80)
DATA ZPMAX,ZQMAX,VMAX,VO/1.414,0.000,1.350,1.414/
DATA A1,A3,A5,A7,A9,A11,A13,A15,A17/1.4621619,-0.0998297,0.59917,
&-0.8914303,-0.817838,2.0430622,-1.2413568,0.2490589,0.0/
DATA B1,B3,B5,B7,B9,B11,B13,B15,B17/0.0,0.0,0.0,0.0,0.0,0.0,0.0,0.0,
#0.0,0.0/
P(X)={((((((A17**2+A15)*X**2+A13)*X**2+A11)*X**2+A9)*
#X**2+A7)*X**2+A5)*X**2+A3)*X**2+A1
ZP(X)=P(X)*X

```

FILE: PAM FORTRAN A1 UNIV O' OF OTTAWA

```

      Q(X)=((((((B17*X**2+B15)*X**2+B13)*X**2+B11)*X**2+B9)*
#X**2+B7)*X**2+B5)*X**2+B3)*X**2+B1
      ZQ(X)=Q(X)*X
      Z(X)=SQRT(ZP(X)**2+ZQ(X)**2)
      TWTIN=VO*10.**(-BAKOFF/20.)
      PPP=ZQ(TWTIN)/ZP(TWTIN)
      PSHIFT=ATAN(PPP)
      WRITE (6,2) BAKOFF,PSHIFT,TWTIN
2  FORMAT(5X,'TWTIN INPUT BACKOFF:',F4.1,' DB',
# ' OUTPUT PHASE SHIFT:',F7.3,1X,'TWTIN:',F5.3./)
      MP=0.0
      DO 15 K=1,LDIM
      MP=MP+((CABS(DA(A(K)))**2.)
15  CONTINUE
      MP=MP/LDIM
      WRITE(6,20) MP
20  FORMAT(5X,'MEAN POWER:',F8.4)
      FNORMI=TWTIN/SQRT(MP)
      WRITE (6,22) FNORMI
22  FORMAT(5X,'FNORMI:',F8.4)
      DO 11 I=1,LDIM
      DATA(I)=DATA(I)*FNORMI
11  CONTINUE
      DO 10 I=1,LDIM
      X=REAL(DATA(I))
      Y=0.0
      R=SQRT(X**2+Y**2)
      IF(R.GT.VMAX) GO TO 12
      DATA(I)=CMPLX(P(R)*X-Q(R)*Y,P(R)*Y+Q(R)*X)
      GO TO 10
12  DATA(I)=CMPLX(ZPMAX*X-ZQMAX*Y,ZQMAX*X+ZPMAX*Y)/R
10  CONTINUE
      DO 16 I=1,LDIM
      DATA(I)=DATA(I)/FNORMI/A1
16  CONTINUE
      RETURN
      END

C *****
C THIS SUBROUTINE DRAWS SPACE DIAGRAM
C *****
C SUBROUTINE PSPACE (DATA,NR,NRUNS,MI)
      COMPLEX DATA(1)
      REAL XLEN,YLEN
      REAL X(2000),Y(2000)
      INTEGER NR,NRUNS
      COMMON /NUMB1/ FBW,ALPHA,LDIM,IOFF,LSAMPL
      COMMON /NUMB2/ NSNR,NSYMB,BAUD
C ESTABLISH THE SURFACE AREA.
      IF(NR.NE.1) GO TO 2
      XLEN=40.0*FLOAT(NRUNS)
      YLEN=27.5
      CALL PLOTS(XLEN,YLEN)
C ESTABLISH THE ORIGIN.

```

PAM04410
PAM04420
PAM04430
PAM04440
PAM04450
PAM04460
PAM04470
PAM04480
PAM04490
PAM04500
PAM04510
PAM04520
PAM04530
PAM04540
PAM04550
PAM04560
PAM04570
PAM04580
PAM04590
PAM04600
PAM04610
PAM04620
PAM04630
PAM04640
PAM04650
PAM04660
PAM04670
PAM04680
PAM04690
PAM04700
PAM04710
PAM04720
PAM04730
PAM04740
PAM04750
PAM04760
PAM04770
PAM04780
PAM04790
PAM04800
PAM04810
PAM04820
PAM04830
PAM04840
PAM04850
PAM04860
PAM04870
PAM04880
PAM04890
PAM04900
PAM04910
PAM04920
PAM04930
PAM04940
PAM04950

FILE: PAM FORTRAN A1 UNIV D'/OF OTTAWA

```

CALL PLOT(20.0,12.5,-3)
GO TO 3
2 CALL PLOT(40.0,0.0,-3)
C TITLE
3 CALL SYMBOL(-6.0,12.5,0.49,13HSPACE DIAGRAM,0.0,13)
C DRAW AXES
CALL AXIS(-16.0,0.0,1H,1,32.0,0.0,-32.0,2,0)
CALL AXIS(0.0,-8.0,1H,1,16.0,90.0,-16.0,2,0)
C PLOT THE DATA.
X(1999)=0.0
X(2000)=2.0
Y(2000)=0.0
Y(2000)=2.0
L=M1
DO 4 I=1,1997
K=LSAMPL*I+L
IF (K.GT.LDIM) K=K-LDIM
Y(I)=(AIMAG(DATA(K))+AIMAG(DATA(K+1)))/2.
X(I)=(REAL(DATA(K))+REAL(DATA(K+1)))/2.
4 CONTINUE
X(1998)=X(I)
Y(1998)=Y(I)--
CALL LINE (X,Y,1998,1,-1,11)
IF(NR.EQ.NRUNS) CALL PLOT(0.0,0.0,999)
WRITE(6,61)
61 FORMAT(5X,'---SPACE DIAGRAM IS REQUESTED ---')
RETURN
END
C*****
C COMPUTATION OF MEAN POWER
C*****
SUBROUTINE POWER(DATA,MP,PF)
COMMON /NUMB1/ FBW,ALPHA,LDIM,IOFF,LSAMPL
COMMON /NUMB2/ NSNR,NSYMB,BAUD
COMPLEX DATA(1)
REAL MP,PF,XX(65536),NP
MP=0.0
PF=0.0
DO 10 I=1,LDIM
MP=MP+((CABS(DATA(I)))**2.)
IF(PF.LT.CABS(DATA(I))) PF=CABS(DATA(I))
10 CONTINUE
WRITE(6,11) PF
11 FORMAT(5X,'PEAK VALUE:',F5.2)
NP=MP/FLOAT(LDIM)
PF=PF**2./NP
GO TO 15
15 PF=10.*ALOG10(PF)
WRITE(6,20) PF,NP
20 FORMAT(5X,'PEAK FACTOR:',F8.4,' DB ',1X,'MEAN POWER:',F9.3,/)
RETURN
END
C *****

```

PAM04960
PAM04970
PAM04980
PAM04990
PAM05000
PAM05010
PAM05020
PAM05030
PAM05040
PAM05050
PAM05060
PAM05070
PAM05080
PAM05090
PAM05100
PAM05110
PAM05120
PAM05130
PAM05140
PAM05150
PAM05160
PAM05170
PAM05180
PAM05190
PAM05200
PAM05210
PAM05220
PAM05230
PAM05240
PAM05250
PAM05260
PAM05270
PAM05280
PAM05290
PAM05300
PAM05310
PAM05320
PAM05330
PAM05340
PAM05350
PAM05360
PAM05370
PAM05380
PAM05390
PAM05400
PAM05410
PAM05420
PAM05430
PAM05440
PAM05450
PAM05460
PAM05470
PAM05480
PAM05490
PAM05500

FILE: PAM FORTRAN A1 UNIV D'/OF OTTAWA

```

4 PE(M)=PE(M)+PEI
2 CONTINUE
DO 6 I=1,NSNR
6 PE(I)=PE(I)/FLOAT(NSYMB)
DO 7 I=1,NSNR
P(I)=PE(I)
7 CONTINUE
101 DO 8 I=1,NSNR
8 EBNO(I)=FLOAT(I)
PRINT 150
150 FORMAT(5X,'ES/NO',10X,'PROB. OF ERROR',/)
WRITE(6,151) (EBNO(I),P(I),I=1,NSNR)
151 FORMAT(5X,F5.2,10X,E15.6)
GO TO 155
153 PRINT 154
154 FORMAT(10X,'SYMBOL WAS IN ERROR, RUN WAS TERMINATED',/)
155 CONTINUE
RETURN
END

```

PAM06060
PAM06070
PAM06080
PAM06090
PAM06100
PAM06110
PAM06120
PAM06130
PAM06140
PAM06150
PAM06160
PAM06170
PAM06180
PAM06190
PAM06200
PAM06210
PAM06220
PAM06230
PAM06240
PAM06250
PAM06260
PAM06270
PAM06280
PAM06290
PAM06300
PAM06310
PAM06320
PAM06330
PAM06340
PAM06350
PAM06360
PAM06370
PAM06380
PAM06390
PAM06400
PAM06410
PAM06420
PAM06430
PAM06440
PAM06450
PAM06460
PAM06470
PAM06480
PAM06490
PAM06500
PAM06510
PAM06520
PAM06530
PAM06540
PAM06550
PAM06560
PAM06570
PAM06580
PAM06590
PAM06600

```

C *****
C THIS SUBROUTINE SIMULATES THE LINEARIZED
C LM-380 CHARACTERISTIC.
C *****
SUBROUTINE TWT1(DATA,BAKOFF,PSHIFT)
COMMON/NUMB1/FBW,ALPHA,LDIM,IOFF,LSAMPL
COMMON/NUMP2/NSNR,NSYMB,BAUD
COMPLEX DATA(1)
REAL MP,R,Q,OI,ZP
DATA A1,A2,A3/0.98102,3.80665,104.1995/
P(X)=A1*X+A2*X**3+A3*X**5
MP=0.0
DO 15 K=1,LDIM
MP=MP+((CABS(DATA(K)))**2.)
15 CONTINUE
MP=MP/LDIM
WRITE(6,20) MP,BAKOFF
20 FORMAT(5X,'MEAN POWER:',F8.4,3X,'OPER. POINT:',F8.4,'V',/)
FNORM=BAKOFF/SQRT(MP)
DO 11 I=1,LDIM
DATA(I)=DATA(I)*FNORM
11 CONTINUE
DO 10 I=1,LDIM
R=REAL(DATA(I))
Y=AIMAG(DATA(I))
S=ABS(R)
IF(S.LT.0.1) GO TO 35
Q=7.462*(P(R)**2)
OI=1.0+0.25*Q**2+0.015625*Q**4+0.000434*Q**6
ZP=3.590262*P(R)*EXP(-Q)*OI
GO TO 45
35 ZP=3.311*R
45 DATA(I)=CMPLX(ZP,Y)
DATA(I)=DATA(I)/FNORM/3.311

```

FILE: PAM FORTRAN A1 UNIV D'OF OTTAWA

```

10 CONTINUE
RETURN
END
C *****
C THIS SUBROUTINE SIMULATES THE COMPENSATION OF THE
C AM-AM(LM-380), AM-PM(HUNGES-261) NONLINEARITIES
C *****
SUBROUTINE IWT3(DATA,BAKOFF,PSHIFT)
COMMON /NUMB1/ FBW,ALPHA,LDIM,IOFF,LSAMPL
COMMON /NUMB2/ NSNR,NSYMB,BAUD
COMPLEX DATA(1)
REAL MP
DATA ZPMAX,ZQMAX,VMAX,VO/1.3,0.55,1.400,1.414/
DATA A1,A3,A5,A7,A9,A11,A13,A15,A17/1.463,-0.1424,0.65738,
#-2.5463552,3.2320452,-1.9768057,0.5927067,-0.0695537,0.0/
DATA B3,B5,B7,B9,B11,B13,B15,B17/1.1649265,
&0.053574,-4.4133043,7.7314234,-6.0660324,2.294553,-0.3385,0.0/
ZP(X)=((((((A17*X**2+A15)*X**2+A13)*X**2+A11)*X**2+A9)*
#X**2+A7)*X**2+A5)*X**2+A3)*X**2+A1)*X
ZQ(X)=((((((B17*X**2+B15)*X**2+B13)*X**2+B11)*X**2+B9)*
#X**2+B7)*X**2+B5)*X**2+B3)*X
TWTN=VO*10.**(-BAKOFF/20.)
MP=0.0
DO 15 K=1,LDIM
MP=MP+((CABS(DATA(K)))**2.)
15 CONTINUE
MP=MP/LDIM
WRITE(6,20) MP
20 FORMAT(5X,'MEAN POWER:',F8.4)
FNORM1=TWTN/SQRT(MP)
WRITE(6,22) FNORM1
22 FORMAT(5X,'FNORM1:',F8.4)
DO 11 I=1,LDIM
DATA(I)=DATA(I)*FNORM1
11 CONTINUE
DO 10 I=1,LDIM
R=REAL(DATA(I))
GP=1.024364*R-0.215228*R**3+0.287643*R**5
GQ=-0.52577*R**3+0.151374*R**5-0.038831*R**7
B=SQRT(GP**2+GQ**2)
IF(B.GT.1.414)GO TO 12
ZZ=SQRT((ZP(B)**2)+(ZQ(B)**2))
IF(R.LT.0.0) ZZ=-ZZ
PPP=ATAN(GQ/GP)+ATAN(ZQ(B)/ZP(B))
DATA(I)=CMPLX(ZZ*COS(PPP),ZZ*SIN(PPP))
GO TO 10
12 ZZ=SQRT(1.3**2+0.55**2)
IF(R.LT.0.0) ZZ=-ZZ
PPP=ATAN(GQ/GP)+ATAN(0.55/1.3)
DATA(I)=CMPLX(ZZ*COS(PPP),ZZ*SIN(PPP))
10 CONTINUE
WRITE(6,2) BAKOFF,PSHIFT,TWTN
2 FORMAT(5X,'TWTA INPUT BACKOFF:',F4.1,' DB',

```

PAM06610
PAM06620
PAM06630
PAM06640
PAM06650
PAM06660
PAM06670
PAM06680
PAM06690
PAM06700
PAM06710
PAM06720
PAM06730
PAM06740
PAM06750
PAM06760
PAM06770
PAM06780
PAM06790
PAM06800
PAM06810
PAM06820
PAM06830
PAM06840
PAM06850
PAM06860
PAM06870
PAM06880
PAM06890
PAM06900
PAM06910
PAM06920
PAM06930
PAM06940
PAM06950
PAM06960
PAM06970
PAM06980
PAM06990
PAM07000
PAM07010
PAM07020
PAM07030
PAM07040
PAM07050
PAM07060
PAM07070
PAM07080
PAM07090
PAM07100
PAM07110
PAM07120
PAM07130
PAM07140
PAM07150

FILE: PAM FORTRAN A1 UNIV D'OF OTTAWA

```

#1 OUTPUT PHASE SHIFT:'.F9.4,IX.'TWTIN:'.F5.3./)
DO 16 I=1,LDIM
DATA(1)=DATA(1)/FNORM1/A1
16 CONTINUE
RETURN
END
PAM07160
PAM07170
PAM07180
PAM07190
PAM07200
PAM07210
PAM07220
PAM07230
PAM07240
C *****
C THIS SUBROUTINE SIMULATES THE AM-AM COMPENSATION OF THE
C AM-AM(LM-380),AM-PM(HUNGLES-261) CHARACTERISTICS.
C *****
SUBROUTINE TW14(DATA,BAKOFF,PSHIFT)
COMMON /NUMB1/ FBW,ALPHA,LDIM,IOFF,LSAMPL
COMMON /NUMB2/ NSNR,NSYMB,BAUD
COMPLEX DATA(1)
REAL MP
DATA ZPMAX,ZQMAX,VMAX,VO/1.3,0.55,1.414,1.414/
DATA A1,A3,A5,A7,A9,A11,A13,A15,A17/1.463,-0.1424,0.65738,
#-2.5463552,3.2320452,-1.9768057,0.5927067,-0.0695537,0.0/
DATA B3,B5,B7,B9,B11,B13,B15,B17/1.1649265,
&0.053574,-4.4133043,7.7314234,-6.0660324,2.294553,-0.3385,0.0/
ZP(X)={((((((A17*X**2+A15)*X**2+A13)*X**2+A11)*X**2+A9)*
#X**2+A7)*X**2+A5)*X**2+A3)*X**2+A1)*X
ZQ(X)={((((((B17*X**2+B15)*X**2+B13)*X**2+B11)*X**2+B9)*
#X**2+B7)*X**2+B5)*X**2+B3)*X
TWTIN=VO*10.**(-BAKOFF/20.)
MP=0.0
DO 15 K=1,LDIM
MP=MP+((CABS(DATA(K)))**2.)
15 CONTINUE
MP=MP/LDIM
WRITE(6,20) MP
20 FORMAT(5X,'MEAN POWER:'.F8.4)
FNORM1=TWTIN/SQRT(MP)
WRITE(6,22) FNORM1
22 FORMAT(5X,'FNORM1:'.F8.4)
DO 11 I=1,LDIM
DATA(1)=DATA(1)*FNORM1
11 CONTINUE
DO 10 I=1,LDIM
R=REAL(DATA(1))
GP=0.693974*R-0.0659*R**3+0.06755*R**5
GQ=0.0
B=SQRT(GP**2+GQ**2)
IF(B.GT.1.414)GO TO 12
ZZ=SQRT((ZP(B)**2)+(ZQ(B)**2))
IF(R.LT.0.0) ZZ=-ZZ
PPP=ATAN(GQ/GP)+ATAN(ZQ(B)/ZP(B))
DATA(1)=CMPLX(ZZ*COS(PPP),ZZ*SIN(PPP))
GO TO 10
12 ZZ=SQRT(1.3**2+0.55**2)
IF(R.LT.0.0) ZZ=-ZZ
PPP=ATAN(GQ/GP)+ATAN(0.55/1.3)
DATA(1)=CMPLX(ZZ*COS(PPP),ZZ*SIN(PPP))
PAM07250
PAM07260
PAM07270
PAM07280
PAM07290
PAM07300
PAM07310
PAM07320
PAM07330
PAM07340
PAM07350
PAM07360
PAM07370
PAM07380
PAM07390
PAM07400
PAM07410
PAM07420
PAM07430
PAM07440
PAM07450
PAM07460
PAM07470
PAM07480
PAM07490
PAM07500
PAM07510
PAM07520
PAM07530
PAM07540
PAM07550
PAM07560
PAM07570
PAM07580
PAM07590
PAM07600
PAM07610
PAM07620
PAM07630
PAM07640
PAM07650
PAM07660
PAM07670
PAM07680
PAM07690
PAM07700

```

FILE: PAM FORTRAN A1 UNIV D'/OF OTTAWA

```

10 CONTINUE
WRITE (6,2) BAKOFF, PSHIFT, TWTIN
2  FORMAT(5X, 'TWA INPUT BACKOFF:', F4.1, ' DB',
# ' OUTPUT PHASE SHIFT:', F9.4, 'X, 'TWTIN:', F5.3, '/')
DO 16 I=1, LDIM
DATA(I) = DATA(I) / FNORM1
16 CONTINUE
RETURN
END
PAM07710
PAM07720
PAM07730
PAM07740
PAM07750
PAM07760
PAM07770
PAM07780
PAM07790
PAM07800
PAM07810
PAM07820
PAM07830
PAM07840
PAM07850
PAM07860
PAM07870
PAM07880
PAM07890
PAM07900
PAM07910
PAM07920
PAM07930
PAM07940
PAM07950
PAM07960
PAM07970
PAM07980
PAM07990
PAM08000
PAM08010
PAM08020
PAM08030
PAM08040
PAM08050
PAM08060
PAM08070
PAM08080
PAM08090
PAM08100
PAM08110
PAM08120
PAM08130
PAM08140
PAM08150
PAM08160
PAM08170
PAM08180
PAM08190
PAM08200
PAM08210
PAM08220
PAM08230
PAM08240
PAM08250
C *****
C THIS SUBROUTINE SIMULATES THE CHARACTERISTICS OF THE
C AM-AM (LM-380), AM-PM (HUNGES-261) OR THE
C AM-AM (LM-380), AM-PM (INTELSAT-V) NONLINEARITIES
C *****
SUBROUTINE TWT5(DATA, BAKOFF, PSHIFT)
COMMON /NUMB1/ FBW, ALPHA, LDIM, IOFF, LSAMP
COMMON /NUMB2/ NSNR, NSYMB, BAUD
COMPLEX DATA(1)
REAL MP, C(80), D(80), G(80), E(80)
DATA ZPMAX, ZQMAX, VMAX, VO/1.300, 0.550, 1.400, 1.414/
DATA A1, A3, A5, A7, A9, A11, A13, A15, A17/1.463, -0.1424, 0.65738,
# -2.5463552, 3.2320452, -1.9768057, 0.5927067, -0.0695537, 0.0/
DATA B3, B5, B7, B9, B11, B13, B15, B17/1.1649265,
& 0.053574, -4.4133043, 7.7314234, -6.0660324, 2.294553, -0.3385, 0.0/
C DATA A1, A3, A5, A7, A9, A11, A13, A15, A17/1.461936, -0.0975490, 0.413473,
C & -2.333527, 2.9813547, -1.7313, 0.4804, -0.0510523, 0.0/
C DATA B3, B5, B7, B9, B11, B13, B15/0.1769764, 6.0393476, -16.5881, 20.556,
C & -13.41762, 4.4521, -0.591, 0.0/
P(X) = ((((((A17*X**2+A15)*X**2+A13)*X**2+A11)*X**2+A9)*
#X**2+A7)*X**2+A5)*X**2+A3)*X**2+A1
ZP(X) = P(X)**X
Q(X) = ((((((B17*X**2+B15)*X**2+B13)*X**2+B11)*X**2+B9)**
#X**2+B7)*X**2+B5)*X**2+B3
ZQ(X) = Q(X)**X
Z(X) = SQRT(ZP(X)**2 + ZQ(X)**2)
TWTIN = VO*10.**(-BAKOFF/20.)
PPP = ZQ(TWTIN)/ZP(TWTIN)
PSHIFT = ATAN(PPP)
WRITE (6,2) BAKOFF, PSHIFT, TWTIN
2  FORMAT(5X, 'TWA INPUT BACKOFF:', F4.1, ' DB',
# ' OUTPUT PHASE SHIFT:', F9.4, 'X, 'TWTIN:', F5.3, '/')
MP = 0.0
DO 15 K=1, LDIM
MP = MP + ((CABS(DATA(K)))**2.)
15 CONTINUE
MP = MP / LDIM
WRITE (6,20) MP
20  FORMAT(5X, 'MEAN POWER:', F8.4)
FNORM1 = TWTIN / SQRT(MP)
WRITE (6,22) FNORM1
22  FORMAT(5X, 'FNORM1:', F8.4)
DO 11 I=1, LDIM
DATA(I) = DATA(I) * FNORM1

```

FILE: PAM FORTRAN A1 UNIV D'OF OTTAWA

```

11 CONTINUE
C DO 31 M=1,80
C D(M)=REAL(DATA(M))
C 31 CONTINUE
DO 10 I=1,LDIM
X=REAL(DATA(I))
Y=0.0
C Y=AIMAG(DATA(I))
R=SQRT(X**2+Y**2)
IF(R.GT.VMAX) GOTO 12
DATA(I)=CMPLX(P(R)*X-Q(R)*Y,P(R)*Y+Q(R)*X)
GO 10 10
12 DATA(I)=CMPLX(ZPMAX*X-ZOMAX*Y,ZOMAX*X+ZPMAX*Y)/R
10 CONTINUE
C DO 32 K=1,80
C G(K)=REAL(DATA(K))
C 32 CONTINUE
DO 16 I=1,LDIM
DATA(I)=DATA(I)/FNORM1/A1
16 CONTINUE
RETURN
END
C *****
C THIS SUBROUTINE SIMULATE THE EQUIVALENT BASEBAND CHARACTERISTIC
C OF THE AM-PM (HUNGES-261) NONLINEARITY
C *****
SUBROUTINE TWT2(DATA,BAKOFF,PSHIFT)
COMMON /NUMB1/ FBW,ALPHA,LDIM,IOFF,LSAMPL
COMMON /NUMB2/ NSNR,NSYMB,BAUD
COMPLEX EPS,DATA(1)
REAL MP
DATA A2,A4,A6,A8,A10,A12,A14,A16/1.032361,-1.202852,0.164144,
#1.191,-1.267618,0.503055,-0.59495,-0.0048490/
P(X)={(((A16*X**2+A14)*X**2+A12)*X**2+A10)*X**2+A8}*
#X**2+A6)*X**2+A4)*X**2+A2
TWTIN=VO*10.**(-BAKOFF/20.)
WRITE(6,2) BAKOFF,TWTIN
2 FORMAT(5X,'TWT INPUT BACKOFF:',F4.1,' DB',
#1X,'TWTIN:',F5.3,/)
MP=0.0
DO 15 K=1,LDIM
MP=MP+({CABS(DATA(K))})**2.)
15 CONTINUE
MP=MP/LDIM
WRITE(6,20) MP
20 FORMAT(5X,'MEAN POWER:',F8.4)
FNORM1=TWTIN/SQRT(MP)
WRITE(6,22) FNORM1
22 FORMAT(5X,'FNORM1:',F8.4)
DO 11 I=1,LDIM
DATA(I)=DATA(I)*FNORM1
11 CONTINUE
DO 10 I=1,LDIM

```

PAM08260
PAM08270
PAM08280
PAM08290
PAM08300
PAM08310
PAM08320
PAM08330
PAM08340
PAM08350
PAM08360
PAM08370
PAM08380
PAM08390
PAM08400
PAM08410
PAM08420
PAM08430
PAM08440
PAM08450
PAM08460
PAM08470
PAM08480
PAM08490
PAM08500
PAM08510
PAM08520
PAM08530
PAM08540
PAM08550
PAM08560
PAM08570
PAM08580
PAM08590
PAM08600
PAM08610
PAM08620
PAM08630
PAM08640
PAM08650
PAM08660
PAM08670
PAM08680
PAM08690
PAM08700
PAM08710
PAM08720
PAM08730
PAM08740
PAM08750
PAM08760
PAM08770
PAM08780
PAM08790
PAM08800

FILE: PAM FORTRAN A1 UNIV D'OF OTTAWA

```

      EPS=CMPLX(COS(P(X)), -SIN(P(X)))
      DATA(1)=DATA(1)*EPS
10   CONTINUE
      DO 16 I=1,LDIM
      DATA(1)=DATA(1)/INORMI
16   CONTINUE
      RETURN
      END

C *****
C   THE FOLLOWING SUBROUTINE SYNCHRONIZES THE RECEIVED DATA.
C *****
C
      SUBROUTINE SYNCRO(DATA,PNOISE,NI,NQ,MI,MQ,EB,LMAX)
      INTEGER Q7FLAG
      COMPLEX DATA(1),AMP
      DIMENSION NI(1),NQ(1)
      COMMON /NUMB1/ FBW,ALPHA,LDIM,IOFF,LSAMPL
      COMMON /NUMB2/ NSNR,NSYMB,BAUD
      NERROR=0
      AMAX=0.0
      S=FLOAT(LSAMPL)/2.
      DO 1,J=1,NSYMB
      J1=(J-1)*LSAMPL+S
      XX1=(REAL(DATA(J1))+REAL(DATA(J1+1)))/2.
      XX1=ABS(XX1)
      IF(AMAX.LT.XX1) AMAX=XX1
1   CONTINUE
      YY=AMAX/FLOAT(LMAX)
      IF (IOFF.EQ.0) GO TO 111
      DO 6 K=1,IOFF
      XX=AIMAG(DATA(LDIM))
      LL=LDIM-1
      DO 7 KK=1,LL
      LDKK=LDIM+1-KK
7     DATA(LDKK)=CMPLX(REAL(DATA(LDKK)),AIMAG(DATA(LDKK-1)))
6     DATA(1)=CMPLX(REAL(DATA(1)),XX)
C
C   SYNCHRONIZE THE RECEIVED DATA
C
111  NOI=0
      NOF=0
      K=1
300  CONTINUE
      NEW=0
      DO 200 J=1,NSYMB
      J1=K+(J-1)*LSAMPL
      IF(J1.GT.LDIM) J1=J1-LDIM
      AXBAR=(REAL(DATA(J1))+REAL(DATA(J1+1)))/2.
      AYBAR=(AIMAG(DATA(J1))+AIMAG(DATA(J1+1)))/2.
      SS=AXBAR*NI(J)
      IF (SS.GT.0.) NEW=NEW+1
      SS=AYBAR*NQ(J)
      IF (SS.GT.0.) NEW=NEW+1
200  CONTINUE
      K=K+1
      IF (K.GT.100) GO TO 300
      END

```

PAM08810
 PAM08820
 PAM08830
 PAM08840
 PAM08850
 PAM08860
 PAM08870
 PAM08880
 PAM08890
 PAM08900
 PAM08910
 PAM08920
 PAM08930
 PAM08940
 PAM08950
 PAM08960
 PAM08970
 PAM08980
 PAM08990
 PAM09000
 PAM09010
 PAM09020
 PAM09030
 PAM09040
 PAM09050
 PAM09060
 PAM09070
 PAM09080
 PAM09090
 PAM09100
 PAM09110
 PAM09120
 PAM09130
 PAM09140
 PAM09150
 PAM09160
 PAM09170
 PAM09180
 PAM09190
 PAM09200
 PAM09210
 PAM09220
 PAM09230
 PAM09240
 PAM09250
 PAM09260
 PAM09270
 PAM09280
 PAM09290
 PAM09300
 PAM09310
 PAM09320
 PAM09330
 PAM09340
 PAM09350

FILE: PAM FORTRAN A1 UNIV D' / OF OTTAWA

```

200 CONTINUE
    IF (NOLD.GE.NEW) GO TO 399
    NOLD=NEW
    NOF=K
399  K=K+1
    LFD=2*NSYMB
C
C   SHEET RECEIVED DATA LEFT UNTIL ALL SYMBOLS ARE LISTED UP
C
C-----
    NSFI=LSAMPL*3
    IF (NOLD.LT.LFD.AND.K.LE.NSFI) GO TO 300
    NOF=NOF-1
    WRITE(6,56) NOLD,K
56  FORMAT(1X,'NO OF CORRECT SYMBOLS = ',16.1X,'NO OF
    *SHEET = ',16.1X)
    IF (NOF.EQ.0) GO TO 230
    LD=LDIM-1
    DO 250 I=1,NOF
    AMP=DATA(I)
    DO 240 J=1,LD
    DATA(J)=DATA(J+1)
240  CONTINUE
    DATA(LDIM)=AMP
250  CONTINUE
C
C   OPTIMIZE THE SAMPLING INSTANT
C
230  MI=1
    MQ=1
    EQ1=FLOAT(NSYMB) + 1.
    EQ2=FLOAT(NSYMB) + 1.
    M=22
    VARIAN=PNOSIS*(EB*(10.**(-0.1*FLOAT(M))))
    SIGMA=SQRT(VARIAN)
    DO 80 J=1,LSAMPL
    EI 0.
    EQ=0.
    DO 70 K=1,NSYMB
C   VERIFY THAT NO SAMPLED SYMBOL IS IN ERROR
    J1=(K-1)*LSAMPL+J
    AXBAR=(REAL(DATA(J1))+REAL(DATA(J1+1)))/2.
    AYBAR=(AIMAG(DATA(J1))+AIMAG(DATA(J1+1)))/2.
    INDEX1=0
    SS=FLOAT(N1(K))*AXBAR
    IF (SS.LT.0.) INDEX1=1
    AMPX=ABS(AXBAR)
    AMPI=ABS(FLOAT(N1(K)))
    THR11=AMPI - 1.0
    THR21=AMPI + 1.0
    THR11=THR11**YY
    THR21=THR21**YY
    I7FLAG=0
    IF (AMPI.EQ.31.) GO TO 30
    IF ((AMPX.GE.THR21).OR.(AMPX.LE.THR11)) INDEX1=1

```

PAM09360
PAM09370
PAM09380
PAM09390
PAM09400
PAM09410
PAM09420
PAM09430
PAM09440
PAM09450
PAM09460
PAM09470
PAM09480
PAM09490
PAM09500
PAM09510
PAM09520
PAM09530
PAM09540
PAM09550
PAM09560
PAM09570
PAM09580
PAM09590
PAM09600
PAM09610
PAM09620
PAM09630
PAM09640
PAM09650
PAM09660
PAM09670
PAM09680
PAM09690
PAM09700
PAM09710
PAM09720
PAM09730
PAM09740
PAM09750
PAM09760
PAM09770
PAM09780
PAM09790
PAM09800
PAM09810
PAM09820
PAM09830
PAM09840
PAM09850
PAM09860
PAM09870
PAM09880
PAM09890
PAM09900

FILE: PAM FORTRAN A1 UNIV D'OF OTTAWA

```

      GO TO 40
30  IF(AMPX.LE.THR1) INDEX1=1
      I7FLAG=1
40  CONTINUE
      INDEXQ=0
      SS=FLOAT(NQ(K))*AYBAR
      IF(SS.LT.0.) INDEXQ=1
      AMPY=ABS(AYBAR)
      AMPQ=ABS(FLOAT(NQ(K)))
      THR1Q=AMPQ - 1.0
      THR2Q=AMPQ + 1.0
      THR1Q=THR1Q*YY
      THR2Q=THR2Q*YY
      Q7FLAG=0
      IF (AMPQ.EQ. 3.) GO TO 50
      IF (( AMPY.GE.THR2Q).OR.(AMPY.LE.THR1Q)) INDEXQ=1
      GO TO 60
50  IF(AMPY.LE.THR1Q) INDEXQ=1
      Q7FLAG=1
60  CONTINUE
      IF(INDEX1.EQ.1) EI=EI + 1.
      IF(INDEXQ.EQ.1) EQ=EQ + 1.
C
C   COMPUTE THE PROBABILITY OF ERROR FOR THIS SYMBOL AT EB/NO=22dB.
C
      D1=ABS(AMPX-THR1)
      ARG=D1/(SIGMA*SQRT(2.))
C   CHECK IF ARG IS LARGE IN WHICH CASE PE IS INSIGNIFICANT
C
      IF (ARG.GT.12.) ARG=12.
      F1=EI + ERFC(ARG)/2.
      IF (I7FLAG.EQ. 1) GO TO 65
      D2=ABS(THR21-AMPX)
      ARG=D2/(SIGMA*SQRT(2.))
      IF (ARG.GT.12.) ARG=12.
      F2=F1 + ERFC(ARG)/2.
65  D1=ABS(AMPY-THR1Q)
      ARG=D1/(SIGMA*SQRT(2.))
      IF (ARG.GT.12.) ARG=12.
      EQ=EQ + ERFC(ARG)/2.
      IF (Q7FLAG.EQ. 1) GO TO 70
      D2=ABS(THR2Q-AMPY)
      ARG=D2/(SIGMA*SQRT(2.))
      IF (ARG.GT.12.) ARG=12.
      EQ=EQ + ERFC(ARG)/2.
70  CONTINUE
      IF(EQ1.LE.EI) GO TO 75
      EQ1=E1
      MI=J
75  CONTINUE
      IF (EQ.LE.EQ) GO TO 80
      EQ=EQ
      MQ=J
80  MOFF=IABS(MI-MQ)
      IF(MOFF.NE.0) WRITE(6,90) MOFF

```

PAM09910
 PAM09920
 PAM09930
 PAM09940
 PAM09950
 PAM09960
 PAM09970
 PAM09980
 PAM09990
 PAM10000
 PAM10010
 PAM10020
 PAM10030
 PAM10040
 PAM10050
 PAM10060
 PAM10070
 PAM10080
 PAM10090
 PAM10100
 PAM10110
 PAM10120
 PAM10130
 PAM10140
 PAM10150
 PAM10160
 PAM10170
 PAM10180
 PAM10190
 PAM10200
 PAM10210
 PAM10220
 PAM10230
 PAM10240
 PAM10250
 PAM10260
 PAM10270
 PAM10280
 PAM10290
 PAM10300
 PAM10310
 PAM10320
 PAM10330
 PAM10340
 PAM10350
 PAM10360
 PAM10370
 PAM10380
 PAM10390
 PAM10400
 PAM10410
 PAM10420
 PAM10430
 PAM10440
 PAM10450

FILE: PAM FORTRAN AT UNIV D'OF OTTAWA

```

OFF=(FLOAT(MI) + FLOAT(NOF))/FLOAT(LSAMPL)
90 FORMAT(5X, 'SAMPLING POINTS FOR I AND Q CHANNELS DIFFER BY',
#12, ' SIXTEENTHS OF THE SYMBOL INTERVAL',/)
WRITE(6,95) OFF
95 FORMAT(5X, 'RECEIVED DATA IS DELAYED BY ',F7.3, ' SYMBOLS',/)
RETURN
END

```

PAM10460
PAM10470
PAM10480
PAM10490
PAM10500
PAM10510
PAM10520
PAM10530
PAM10540
PAM10550
PAM10560
PAM10570
PAM10580
PAM10590
PAM10600
PAM10610
PAM10620
PAM10630
PAM10640
PAM10650
PAM10660
PAM10670
PAM10680
PAM10690
PAM10700
PAM10710
PAM10720
PAM10730
PAM10740
PAM10750
PAM10760
PAM10770
PAM10780
PAM10790
PAM10800
PAM10810
PAM10820
PAM10830
PAM10840
PAM10850
PAM10860
PAM10870
PAM10880
PAM10890
PAM10900
PAM10910
PAM10920
PAM10930
PAM10940
PAM10950
PAM10960
PAM10970
PAM10980
PAM10990
PAM11000

```

C*****
C   THE FOLLOWING SUBROUTINE DECODES THE RECEIVED DATA
C   BY ADJUSTING THE CONVENTIONAL DECODING THRESHOLDS.
C*****
C
SUBROUTINE DETECT(NERROR, DATA, PROISE, MI, MQ, NI, NQ, EBNO, PE, FB, LMAX)
COMPLEX DATA(1),AMP
INTEGER JJ
DIMENSION EBNO(1),PE(1),NI(1),NQ(1)
DIMENSION REG(31,2),THR1(31),THRQ(31),IS1IC(31),AA(31),BB(31)
COMMON /NUMB1/ FBW,ALPHA,LDIM,IOFF,LSAMPL
COMMON /NUMB2/ NSNR,NSYMB,BAUD
NERROR=0
DO 1 I=1,NSNR
1 PE(I)=0.
C   OBTAIN THE OPTIMUM THRESHOLDS
AMAX1=0.0
AMAX2=0.0
C   NUMBER OF POSITIVE THRESHOLDS IS NI (FOR LMAX-1)
NI=(LMAX-1)/2
DO 7 J=1,NSYMB
J1=(J-1)*LSAMPL+MI
XX1=(REAL(DATA(J1))+REAL(DATA(J1+1)))/2.
XX1=ABS(XX1)
IF(AMAX1.LT. XX1) AMAX1=XX1
XX2=(AMAX1-1)/NI
7 CONTINUE
WRITE(6,555) XX2
555 FORMAT(5X, 'XX2=',F6.3)
CC=XX2
C   FIX CRUDE THRESHOLDS INITIALLY
DO 10 K=1,LMAX,2
THR1(K)=(FLOAT(K-1)/2.)*XX2
10 CONTINUE
C   NOW REFINE THE THRESHOLDS
REG(1,1)=1.01
REG(1,2)=0.99
DO 21 J=3,LMAX,2
REG(J,1)=REG(1,1)+(FLOAT(J-1))*AMAX1/FLOAT(LMAX)
REG(J,2)=REG(1,2)+(FLOAT(J-1))*AMAX1/FLOAT(LMAX)
21 CONTINUE
DO 2 K=1,NSYMB
J1=(K-1)*LSAMPL+MI
XX1=(REAL(DATA(J1))+REAL(DATA(J1+1)))/2.
INDEX1=0
SS=FLOAT(NI(K))*XX1

```

FILE: PAM FORTRAN A1 UNIV D'OF OTTAWA

```

IF(SS.LT.0.) INDEX1=1
XX1=ABS(XX1)
DO 11 J=1,LMAX,2
IF((XX1.GT. THRI(J)).AND.(XX1.LE.(THRI(J)+XX2))) GO TO 15
11 CONTINUE
15 IF ((REG(J,1).GT.XX1).AND.(REG(J,2).GT.XX1)) REG(J,2)-XX1
IF ((REG(J,1).LE.XX1).AND.(REG(J,2).LE.XX1)) REG(J,1)=XX1
IF(J.EQ.1) GO TO 100
THRI(J)=(REG((J-2),1)+REG(J,2))/2.
GO TO 63
100 THRI(1)=0.
63 CONTINUE
IF (INDEX1.EQ.1.) NERROR=NERROR+1
2 CONTINUE
IF (NERROR.GT.1) GO TO 400
WRITE(6,3) (THRI(I),I=1,31,2)
3 FORMAT(5X,'THRI=' ,F6.3)
C
C COMPUTE THE PROBABILITY OF ERROR FOR EACH SYMBOL.
C THE VARIABLES ARE AS FOLLOWS: M IS EB/NO IN dB; PNOISE IS
C 1/2*INTEGRAL ( H(F)**2 DF); AND VARIAN = NO*PNOISE.
C FOR THE END POINTS THE PE=1/2*ERFC(D1/(SIGMA*SQRT(2)))
C AND FOR THE INNER POINTS THE PE=1/2*ERFC(D1/(SIGMA*SQRT(2))) +
C 1/2*ERFC(D2/(SIGMA*SQRT(2))).
C
DO 202 K=1,NSYMB
J1=(K-1)*LSAMPL+M1
XX1=(REAL(DATA(J1))+REAL(DATA(J1+1)))/2.
XX1=ABS(XX1)
DO 22 J=1,LMAX,2
IF((XX1.GT. THRI(J)).AND.(XX1.LE.(THRI(J)+CC))) GO TO 34
22 CONTINUE
34 AA(J)=THRI(J)
DO 4 M=1,NSNR
VARIAN=PNOISE*LB*(10.**(-0.1*FLOAT(M))).
SIGMA=SQRT(VARIAN)
D1=ABS(XX1-AA(J))
ARG=D1/(SIGMA*SQRT(2.))
C CHECK IF ARG IS LARGE IN WHICH CASE PE IS INSIGNIFICANT
C
IF (ARG.GT.12.) ARG=12.
PE1=ERFC(ARG)/2.
IF (J.EQ.1MAX) GO TO 54
D2=ABS(AA(J+2)-XX1)
ARG=D2/(SIGMA*SQRT(2.))
IF (ARG.GT.12.) ARG=12.
PE1=PE1 + ERFC(ARG)/2.
54 IF(PE1.LT.1.E-15) PE1=0.
4 PE(M)=PE(M)+PE1
202 CONTINUE
DO 5 I=1,NSNR
PF(I)=PF(I)/FLOAT(NSYMB)
5 EBNO(I)=FLOAT(I)
GO TO 220
400 WRITE(6,420) NERROR

```

PAM11010
PAM11020
PAM11030
PAM11040
PAM11050
PAM11060
PAM11070
PAM11080
PAM11090
PAM11100
PAM11110
PAM11120
PAM11130
PAM11140
PAM11150
PAM11160
PAM11170
PAM11180
PAM11190
PAM11200
PAM11210
PAM11220
PAM11230
PAM11240
PAM11250
PAM11260
PAM11270
PAM11280
PAM11290
PAM11300
PAM11310
PAM11320
PAM11330
PAM11340
PAM11350
PAM11360
PAM11370
PAM11380
PAM11390
PAM11400
PAM11410
PAM11420
PAM11430
PAM11440
PAM11450
PAM11460
PAM11470
PAM11480
PAM11490
PAM11500
PAM11510
PAM11520
PAM11530
PAM11540
PAM11550

FILE: PAM FORTRAN A UNIV D' / OF OTTAWA

```

420  FORMAT(5X, 'ERRORS=', I5)
      PRINT 440
440  FORMAT(5X, 'SYMBOL WAS IN ERROR, RUN WAS TERMINATED', /)
220  CONTINUE
      PRINT 150
150  FORMAT(5X, 'ES/NO', 10X, 'PROB. OF ERROR', /)
      WRITE(6, 151) (EBNO(I), PE(I), I=1, NSNR)
151  FORMAT(5X, F5.2, 10X, E15.6)
      RETURN
      END
C*****
C   THIS SUBROUTINE SIMULATES THE PHASE OF THE
C   LM-380 AMPLIFIER
C*****
      SUBROUTINE AMPH(TF)
      COMPLEX TF(1)
      COMMON /NUMB1/ FBW, ALPHA, LDIM, IOFF, LSAMPL
      COMMON /NUMB2/ NSNR, NSYMB, BAUD
      SBANDW=BAUD*LSAMPL
      NO=LDIM/2
      NO1=NO+1
      FN=LDIM*(FBW/SBANDW)
      F1=0.7*FN
      IF1=IFIX(F1)+1
      DO 8 I=2, IF1
      TF(I)=CMPLX(1.0, 0.0)
      TF(I)=CMPLX(1., 0.0)
8  CONTINUE
      JK=IF1+1
      DO 9 J=JK, NO1
      PHI=-0.8167+0.00114*J
      TF(J)=CMPLX(COS(PHI), SIN(PHI))
9  CONTINUE
      NO2=NO1+1
      DO 5 I=NO2, LDIM
      TF(I)=CONJG(TF(LDIM+2-I))
5  CONTINUE
      RETURN
      END

```

PAM11560
PAM11570
PAM11580
PAM11590
PAM11600
PAM11610
PAM11620
PAM11630
PAM11640
PAM11650
PAM11660
PAM11670
PAM11680
PAM11690
PAM11700
PAM11710
PAM11720
PAM11730
PAM11740
PAM11750
PAM11760
PAM11770
PAM11780
PAM11790
PAM11800
PAM11810
PAM11820
PAM11830
PAM11840
PAM11850
PAM11860
PAM11870
PAM11880
PAM11890
PAM11900
PAM11910
PAM11920
PAM11930
PAM11940

FILE: FITOPT FORTRAN A1 UNIV D'/OF OTTAWA

```

C*****
C THIS PROGRAM IS USED TO SOLVE A MATRIX EQUATION.
C USED FOR FINDING THE COEFFICIENTS OF AM/AM
C OR AM-PM CHARACTERISTICS
C*****
      INTEGER IJOB,N,IA,IER
      N=6
      REAL C(6,6),D1,D2,WKAREA(12),B(6),A(6)
      DATA A(1),A(2),A(3),A(4),A(5),A(6)/
&0.16,0.17,0.18,0.19,0.195,0.205/
      DO 55 J=1,N
      DO 56 I=1,N
      L=(2*J)-1
56 C(L,J)=(A(I))**L
55 CONTINUE
      DATA B(1),B(2),B(3),B(4),B(5),B(6)/
&0.52976,0.555,0.575,0.59,0.595,0.6025/
      IA=6
      IJOB=3
      D1=-1.0
      CALL LINV3F (C,B,IJOB,N,IA,D1,D2,WKAREA,IER)
20 WRITE(6,20) B
   FORMAT(5X,F18.7)
   WRITE(6,30) IER
30 FORMAT(5X,I4)
      X=0.0
      DO 44 I=1,35
      X=X+0.01
      F=B(1)*X+B(2)*X**3+B(3)*X**5+B(4)*X**7+B(5)*X**9+B(6)*X**11
      WRITE(6,45) X,F
45 FORMAT(5X,F4.2,5X,F18.7)
44 CONTINUE
      END
C *****
C EVALUATION OF A,B PARAMETERS FOR CURVE FITTING WITH SALEM MODEL.
C *****
      DIMENSION R(14),Z(14)
      REAL A,B,RA1,SQ,R2,R4,W,WR2
      DATA R(1),R(2),R(3),R(4),R(5),R(6),R(7),R(8),R(9),R(10),R(11),
&R(12),R(13),R(14)/
&0.2,0.3,0.4,0.5,0.6,0.7,0.8,0.9,1.0,1.1,1.2,1.3,1.4,1.5/
      DATA Z(1),Z(2),Z(3),Z(4),Z(5),Z(6),Z(7),Z(8),Z(9),Z(10),Z(11),
&Z(12),Z(13),Z(14)/
&0.0408057,0.0734502,0.1305782,0.179551,0.668512,0.2693176,0.302,
&0.330526,0.351,0.36725,0.3754124,0.3835735,0.3917347,0.4/
      M=13
      F=1.0
      R2=0.0
      R4=0.0
      W=0.0
      WR2=0.0
      N=M
      DO 1 I=1,N
      SQ=R(I)**2.
      R2=R2+SQ
FIT00010
FIT00020
FIT00030
FIT00040
FIT00050
FIT00060
FIT00070
FIT00080
FIT00090
FIT00100
FIT00110
FIT00120
FIT00130
FIT00140
FIT00150
FIT00160
FIT00170
FIT00180
FIT00190
FIT00200
FIT00210
FIT00220
FIT00230
FIT00240
FIT00250
FIT00260
FIT00270
FIT00280
FIT00290
FIT00300
FIT00310
FIT00320
FIT00330
FIT00340
FIT00350
FIT00360
FIT00370
FIT00380
FIT00390
FIT00400
FIT00410
FIT00420
FIT00430
FIT00440
FIT00450
FIT00460
FIT00470
FIT00480
FIT00490
FIT00500
FIT00510
FIT00520
FIT00530
FIT00540
FIT00550

```

FILE: FITOPT FORTRAN A1 UNIV D' /OF OTTAWA

```

R4=R4+(SQ**2.)
RAF=(R(1)**2)/Z(1)
W=W+RAF
WR2=WR2+RAF*SQ
1 CONTINUE
ARA=R2**2.-M*R4
PARA=R2*WR2-R4*W
ARB=R2*W-M*WR2
PARB=R2*WR2-R4*W
C=ARA/PARA
A=C**F
B=ARB/PARB
WRITE(6,2) A,B
2 FORMAT(5X,'A=',F10.6,6X,'B=',F10.6)
STOP
END
C *****
C THIS PROGRAMME OPTIMIZES N UNKNOWN PARAMETERS OF A
C GIVEN FUNCTION (FOR THE LM-380,H-261 PREDISTORTER)
C *****
EXTERNAL FUNCT
INTEGER N,NSIG,MAXFN,IOPT
REAL X(6),H(21),G(6),W(18),F
N=6
NSIG=3
MAXFN=500
IOPT=0
X(1)=3.3
X(2)=1.0
X(3)=-1.0
X(4)=1.5
X(5)=-2.0
X(6)=3.0
CALL ZXMIN(FUNCT,N,NSIG,MAXFN,IOPT,X,H,G,F,W,IER)
WRITE(6,5)(X(N),N=1,6)
5 FORMAT(3X,F11.6)
WRITE(6,9) F
9 FORMAT(3X,F13.8)
STOP
END
C ***** SUBROUTINE FUNCT *****
SUBROUTINE FUNCT(N,X,F)
INTEGER N
REAL X(N),F,SUM
ZP(Y)=1.60138*Y*EXP(-0.325713*(Y**2))*(1.0+0.25*((0.325713*Y**2)
**2)+0.045625*((0.325713*Y**2)**4)+0.000434*((0.325713*Y**2)**6))
ZQ(Y)=1.887482*(Y**3)/((1.+1.063857*(Y**2))**2)
SUM=0.
R=0.0
DO 20 I=1,150
R=R+0.01
GF=X(1)*R+X(2)*R**3+X(3)*R**5
GQ=X(4)*R**3+X(5)*R**5+X(6)*R**7
E=GF**2+GQ**2
B=SQRT(E)
FIT00560
FIT00570
FIT00580
FIT00590
FIT00600
FIT00610
FIT00620
FIT00630
FIT00640
FIT00650
FIT00660
FIT00670
FIT00680
FIT00690
FIT00700
FIT00710
FIT00720
FIT00730
FIT00740
FIT00750
FIT00760
FIT00770
FIT00780
FIT00790
FIT00800
FIT00810
FIT00820
FIT00830
FIT00840
FIT00850
FIT00860
FIT00870
FIT00880
FIT00890
FIT00900
FIT00910
FIT00920
FIT00930
FIT00940
FIT00950
FIT00960
FIT00970
FIT00980
FIT00990
FIT01000
FIT01010
FIT01020
FIT01030
FIT01040
FIT01050
FIT01060
FIT01070
FIT01080
FIT01090
FIT01100

```

FILE: FITOPT FORTRAN A UNIV D'OF OTTAWA

```

      IF(B.GT.1.35) GO TO 23
      Q=ZQ(B)
      U=ZP(B)
      IF(Q.LT.1.0E-09) Q=0.0
      IF(U.LT.1.0E-09) U=0.0
      C=(GP**2)*((U**2+Q**2)/(U**2))
      GO TO 22
23  C=(GP**2)*((0.56**2+1.3**2)/1.3**2)
22  CONTINUE
      D=SQRT(C)
      IF(D.GT.1.35) GO TO 33
      Q=ZP(D)
      U=ZQ(D)
      IF(U.LT.1.0E-09) U=0.0
      IF(Q.LT.1.0E-09) Q=0.0
      ZZ=Q**2+U**2
      GO TO 32
33  ZZ=0.56**2+1.3**2
32  CONTINUE
      PZ=SQRT(ZZ)
      IF(R.GT.0.968) GO TO 10
      SUM=SUM+(U-1.463*R)**2
      GO TO 20
10  SUM=SUM+(PZ-1.414)**2
20  CONTINUE
      F=SUM
      RETURN
      END

C *****
C   THIS PROGRAMME OPTIMIZES N UNKNOWN PARAMETERS OF A
C   GIVEN FUNCTION (LINEARIZATION OF THE LM-380 CHARACTERISTIC).
C *****
      EXTERNAL FUNCT
      INTEGER N, NSIG, MAXFN, IOPT
      REAL X(3), H(6), G(3), W(9), F
      N=3
      NSIG=3
      MAXFN=500
      IOPT=0
      X(1)=3.3
      X(2)=1.0
      X(3)=-1.0
      CALL ZXMIN(FUNCT, N, NSIG, MAXFN, IOPT, X, H, G, F, W, IER)
      WRITE(6, 5)(X(N), N=1, 3)
5   FORMAT(3X, F11.6)
      WRITE(6, 9) F
9   FORMAT(3X, F13.8)
C*****SUBROUTINE FUNCTION*****
      SUBROUTINE FUNCT(N, X, F)
      INTEGER N
      REAL X(N), F, SUM
      ZP(Y)=3.5902620*EXP(7.462*(Y**2))*(1.0+0.25*((-7.462*Y**2)
&**2)+0.015625*((-7.462*Y**2)**4)+0.000434*((-7.462*Y**2)**6))

```

FIT01110
 FIT01120
 FIT01130
 FIT01140
 FIT01150
 FIT01160
 FIT01170
 FIT01180
 FIT01190
 FIT01200
 FIT01210
 FIT01220
 FIT01230
 FIT01240
 FIT01250
 FIT01260
 FIT01270
 FIT01280
 FIT01290
 FIT01300
 FIT01310
 FIT01320
 FIT01330
 FIT01340
 FIT01350
 FIT01360
 FIT01370
 FIT01380
 FIT01390
 FIT01400
 FIT01410
 FIT01420
 FIT01430
 FIT01440
 FIT01450
 FIT01460
 FIT01470
 FIT01480
 FIT01490
 FIT01500
 FIT01510
 FIT01520
 FIT01530
 FIT01540
 FIT01550
 FIT01560
 FIT01570
 FIT01580
 FIT01590
 FIT01600
 FIT01610
 FIT01620
 FIT01630
 FIT01640
 FIT01650

FILE: FITOPT FORTRAN A1 UNIV D'/OF OTTAWA

```
SUM=0.
R=0.0
DO 20 I=1,150
R=R+0.01
GP=X(1)*Q+X(2)*Q**3+X(3)*Q**5
IF(GP.GT.1.414) GO TO 23
U=ZZ(GP)
GO TO 22
23 U=1.414
22 CONTINUE
IF(R.GT.0.968) GO TO 10
SUM=SUM+(ZZ-1.463*R)**2
GO TO 20
10 SUM=SUM+(ZZ-1.4140)**2
20 CONTINUE
F=SUM
RETURN
END
```

F1101660
F1101670
F1101680
F1101690
F1101700
F1101710
F1101720
F1101730
F1101740
F1101750
F1101760
F1101770
F1101780
F1101790
F1101800
F1101810
F1101820
F1101830